Development and Clinical Application of a Novel Left Ventricular Diastolic Stress Test

by

Thomas Jake Samuel

BSc at Cardiff Metropolitan University, United Kingdom, 2014

MSc at Cardiff Metropolitan University, United Kingdom, 2016

A Thesis Submitted in Partial Fulfillment

of the Requirements for the Degree of

Doctor of Philosophy

In Integrative and Applied Physiology

Department of Kinesiology

College of Nursing and Health Innovation

University of Texas at Arlington

May 2020

Supervisory Committee:

Dr. Michael D. Nelson, Supervising Professor

Dr. Mark Haykowsky

Dr. Satyam Sarma

Dr. Rhonda Prisby

Dr. Daisha Cipher

Dr. Barry Borlaug (external member)

Supervisory Committee

Michael D. Nelson, PhD	Department of Kinesiology
Supervisor	University of Texas at Arlington
Mark J. Haykowsky, PhD	Faculty of Nursing
Committee Member	University of Alberta
Satyam Sarma, MD	Department of Internal Medicine (Cardiology)
Committee Member	University of Texas Southwestern Medical Center
Rhonda Prisby, PhD	Department of Kinesiology
Committee Member	University of Texas at Arlington
Daisha Cipher, PhD	College of Nursing and Health Innovation
Committee Member	University of Texas at Arlington
Barry A. Borlaug, MD	Department of Cardiovascular Medicine
External Committee Member	Mayo Clinic, Rochester, MN

Abstract

Development and Clinical Application of a Novel Left Ventricular Diastolic Stress Test

Thomas Jake Samuel

The University of Texas at Arlington, 2020

Supervising Professor: Dr. Michael D. Nelson, PhD

Cardiology has long focused on the hearts ability to generate forward pressure and ejection of blood from the left ventricle to supply the systemic circulation with oxygen and nutrients. The ability and capacity of the left ventricle to fill with blood prior to systolic ejection is equally important and, until recently, has been largely under studied. The coordination of passive elastic recoil and active relaxation allows the left ventricle to fill with blood in early diastole through generation of the transmitral pressure gradient. Therefore, dysregulation of the molecular and cellular mechanisms governing these two processes could lead to diastolic dysfunction. While invasive assessment of left ventricular isovolumic pressure decay remains the gold-standard approach for measuring diastolic function, echocardiography and magnetic resonance imaging (MRI) are often used in place of this invasive approach, as non-invasive surrogates. Despite the relative successes of both techniques however, the majority of work in this area has been limited to evaluation of diastolic function under resting conditions, challenging the interpretation of results, particularly in subclinical disease. To address this limitation, diastolic

stress testing— often with a cycle ergometer— has emerged as a complementary approach, unmasking diastolic dysfunction otherwise hidden at rest. However, cycle-based stress testing is limited by both movement and respiratory artifact, orthopedic limitations, and resource availability. Accordingly, this dissertation, focused on the development and application of an alternative diastolic stress testing approach, using isometric handgrip exercise, which addresses each of the aforementioned limitations. First, we showed that isometric handgrip echocardiography could discriminate between normal and abnormal diastolic function. Then, given the popularity of using cycle exercise to perform diastolic stress testing, we directly compared isometric handgrip with cycle exercise, demonstrating good agreement between both approaches. With these positive results, we then incorporated isometric handgrip into a single-center prospective clinical trial to define specific mechanisms of diastolic dysfunction in women with ischemia but no coronary artery disease; a population at increased risk of developing heart failure with preserved ejection fraction. Together, the work performed herein, supports the use of isometric handgrip as a robust diastolic discriminator. Unlike cycle exercise, which is currently advocated by the American Society of Echocardiogaphy and European Association of Cardiovascular Imaging, isometric handgrip is easy to perform, requires fewer resources, and can easily be adopted into both echocardiography and MRI-based exams/studies.

Table of Contents

Acknowledgments

There are many individuals that deserve recognition for their contribution to my time in graduate school, without whom this dissertation would not have been possible.

I would like to express my deepest gratitude to my family and friends for their unwavering support throughout my PhD studies. Particular thanks to my parents, Huw and Jill; and my siblings, Nathan and Menna-Clare for encouraging me to pursue my dream in the United States.

Thank you to my PhD supervisor, Dr. Michael D. Nelson for continuously encouraging me to think critically and for providing me with the best opportunities to develop as a young scientist. Dr. Nelson takes his “open door policy” quite seriously and is always willing to help. This, along with his infectious enthusiasm for scientific discovery has made working and learning under his mentorship a true pleasure.

I would also like to thank the other members of my dissertation committee for their invaluable advice and guidance throughout this process. I would particularly like to thank Dr. Mark Haykowsky for our daily discussions about cardiac mechanics. Similarly, thanks to Dr. Satyam Sarma for providing a unique clinical and scientific perspective to our discussions.

To the numerous friends and colleagues I have had the pleasure to work with at UT Arlington, I thank you for the countless stimulating conversations we’ve shared over the past 4 years. Finally, I would like to thank the American Heart Association and the Harry S. Moss Heart Trust for helping fund my predoctoral training (18PRE33960358), and of course to the countless members of the Dallas-Fort Worth community who volunteered their time to participate in the studies presented herein

Chapter 1

Introduction

Blood flows through the human circulation due to a hydrostatic pressure gradient, determined largely by the forward pressure created by the rhythmically contracting heart muscle. Cardiology has long focused on the hearts ability to generate this pressure gradient, and supply the systemic circulation with oxygen and nutrients. Historically less appreciated— but equally important— is the hearts ability and capacity to fill with blood; a critical prerequisite to systolic ejection. Given this knowledge gap, this dissertation sought to extend our understanding of diastolic function.

Diastole is characterized by three main phases: early diastole, diastasis, and late diastole. In early diastole, elastic recoil and active relaxation of cardiac myocytes gives rise to a reduction in left ventricular pressure, which once drops below that of left atrium, causes the mitral valve to open, and blood enters the ventricle along the transmitral pressure gradient. A period of pressure equilibrium then ensues, termed diastasis, followed by atrial contraction in late diastole which provides the final contribution to left ventricular end-diastolic volume. Systolic deformation leads to compression of the large sarcomere protein titin, generating potential energy which is released in early diastole, analogous to the elastic recoil of a compressed spring, as the myocardium aims to return to its resting shape (1,2). While elastic recoil is a mainly passive process, in contrast, active relaxation is highly energy dependent, requiring ATP for three fundamental processes: (a) the uncoupling of actin-myosin cross-bridges, (b) sequestration of calcium into the sarcoplasmic reticulum, and (c) uncoupling of calcium from troponin-C (3). Therefore, dysregulation of any of these processes could lead to increased left ventricular filling pressures and thus diastolic dysfunction.

Diastolic dysfunction is associated with poor clinical prognosis and is a major cause of pulmonary edema and exertional dyspnea (4). Diagnosis of diastolic dysfunction is often confirmed through gold-standard invasive assessment of left ventricular or pulmonary capillary wedge pressures using a pressure tipped catheter inserted through a peripheral artery or vein (4,5). However, recent technological advancements have allowed for accurate assessment of diastolic function using non-invasive echocardiography and magnetic resonance imaging (MRI) methodologies. High-temporal resolution and relative accessibility has led to Doppler ultrasound being the most common clinically used tool for assessing diastolic function. Indeed, the ratio between Doppler-derived early diastolic mitral inflow velocity and early diastolic tissue velocity (E/e' ratio) correlates strongly with invasively measured filling pressures (6-8). However, while diagnosis of resting diastolic dysfunction in overt decompensated heart failure is relatively straightforward using echocardiography, diagnosis is less clear in subclinical disease (9,10) and/or when the diagnosis remains equivocal in well-compensated heart failure (11,12). In such cases, exercise based diastolic stress testing has emerged as an important clinical tool to unmask diastolic dysfunction not otherwise seen at rest. Exercise stress increases the hemodynamic load on the left ventricle and increases myocardial oxygen demand, which in turn can unmask diastolic dysfunction by challenging the relationship between myocardial oxygen supply and demand. Several groups of investigators have added to *Ha and colleagues* pioneering work (12) which has led to cycle exercise now being recommended by both the American Society of Echocardiography and the European Association of Cardiovascular Imaging for clinical diagnosis of diastolic dysfunction (7,13). Chapter 2 (and Appendix A) provides a comprehensive review of the current

invasive and non-invasive diastolic stress testing approaches, along with their success and limitations.

While conventional cycle exercise has emerged as the most common diastolic stress test modality over the past two decades (11,12), this technique is not without limitation. Indeed, dynamic cycle exercise is associated respiratory and motion artifact which compromises echocardiographic image quality. These limitations are exacerbated in clinical populations who have increased body adiposity and limited acoustic windows for echocardiography image acquisition and often have orthopedic restrictions limiting the ability to perform cycle exercise (14-16). This has led to our group advocating for the use of isometric handgrip exercise, which reproducibly elicits an increase in left ventricular afterload and myocardial oxygen demand, while also avoiding respiratory and movement artifacts associated with dynamic exercise (17,18). In Chapter 3, we showed, for the first time, that isometric handgrip echocardiography can indeed be used as a diastolic discriminator, differentiating between normal and abnormal diastolic response to physiologic stress. Recognizing that cycle exercise is the most common, and currently advocated, diastolic stress testing modality, Chapter 4 described the results of a head-to-head comparison between isometric handgrip and cycle exercise. Remarkably, the data show that isometric handgrip is equally discriminatory as cycle exercise.

With these promising proof-of-concept data, we performed isometric handgrip in women with ischemia but no obstructive coronary artery disease (INOCA) to identify individuals with stress induced diastolic dysfunction. Indeed, women with INOCA often have coronary vascular dysfunction (19-27), and my mentor has consistently shown these individuals also have diastolic dysfunction, at least at rest (28-30). Moreover, women with INOCA are at increased risk of

developing heart failure with preserved ejection fraction (HFpEF), leading to the hypothesis that INOCA precedes HFpEF, and is mechanistically associated with ischemia-mediated diastolic impairment. Chapter 5 describes the results of an MRI-based study designed specifically to test this hypothesis, for which isometric handgrip was used to challenge the oxygen supply-demand relationship, and therefore exacerbate stress-induced diastolic dysfunction.

Together, the work performed herein, supports the use of isometric handgrip as a diastolic discriminator. Unlike cycle exercise, which is currently advocated by the American Society of Echocardiogaphy and European Association of Cardiovascular Imaging, isometric handgrip is easy to perform, requires fewer resources, and as shown in Chapter 5, can easily be adopted into MRI-based exams/studies.

Reference List

1. Notomi Y, Martin-Miklovic MG, Oryszak SJ et al. Enhanced ventricular untwisting during exercise: a mechanistic manifestation of elastic recoil described by Doppler tissue imaging. Circulation 2006;113:2524-33.
2. Opdahl A, Remme EW, Helle-Valle T, Edvardsen T, Smiseth OA. Myocardial relaxation, restoring forces, and early-diastolic load are independent determinants of left ventricular untwisting rate. Circulation 2012;126:1441-51.
3. Gorski PA, Ceholski DK, Hajjar RJ. Altered myocardial calcium cycling and energetics in heart failure--a rational approach for disease treatment. Cell Metab 2015;21:183-94.
4. Kitzman DW, Higginbotham MB, Cobb FR, Sheikh KH, Sullivan MJ. Exercise intolerance in patients with heart failure and preserved left ventricular systolic function: failure of the Frank-Starling mechanism. J Am Coll Cardiol 1991;17:1065-72.
5. Zile MR, Baicu CF, Gaasch WH. Diastolic heart failure--abnormalities in active relaxation and passive stiffness of the left ventricle. N Engl J Med 2004;350:1953-9.
6. Burgess MI, Jenkins C, Sharman JE, Marwick TH. Diastolic stress echocardiography: hemodynamic validation and clinical significance of estimation of ventricular filling pressure with exercise. J Am Coll Cardiol 2006;47:1891-900.
7. Nagueh SF, Smiseth OA, Appleton CP et al. Recommendations for the Evaluation of Left Ventricular Diastolic Function by Echocardiography: An Update from the American Society of Echocardiography and the European Association of Cardiovascular Imaging. Eur Heart J Cardiovasc Imaging 2016;17:1321-1360.
8. Obokata M, Kane GC, Reddy YN, Olson TP, Melenovsky V, Borlaug BA. Role of Diastolic Stress Testing in the Evaluation for Heart Failure With Preserved Ejection Fraction: A Simultaneous Invasive-Echocardiographic Study. Circulation 2017;135:825-838.
9. Ha JW, Lee HC, Kang ES et al. Abnormal left ventricular longitudinal functional reserve in patients with diabetes mellitus: implication for detecting subclinical myocardial dysfunction using exercise tissue Doppler echocardiography. Heart 2007;93:1571-6.
10. Choi EY, Ha JW, Yoon SJ et al. Increased plasma aldosterone-to-renin ratio is associated with impaired left ventricular longitudinal functional reserve in patients with uncomplicated hypertension. J Am Soc Echocardiogr 2008;21:251-6.
11. Borlaug BA, Nishimura RA, Sorajja P, Lam CS, Redfield MM. Exercise hemodynamics enhance diagnosis of early heart failure with preserved ejection fraction. Circ Heart Fail 2010;3:588-95.
12. Ha JW, Oh JK, Pellikka PA et al. Diastolic stress echocardiography: a novel noninvasive diagnostic test for diastolic dysfunction using supine bicycle exercise Doppler echocardiography. J Am Soc Echocardiogr 2005;18:63-8.
13. Nagueh SF, Smiseth OA, Appleton CP et al. Recommendations for the Evaluation of Left Ventricular Diastolic Function by Echocardiography: An Update from the American Society of Echocardiography and the European Association of Cardiovascular Imaging. J Am Soc Echocardiogr 2016;29:277-314.
14. Haykowsky MJ, Brubaker PH, Morgan TM, Kritchevsky S, Eggebeen J, Kitzman DW. Impaired aerobic capacity and physical functional performance in older heart failure

patients with preserved ejection fraction: role of lean body mass. J Gerontol A Biol Sci Med Sci 2013;68:968-75.
15. Upadhya B, Haykowsky MJ, Eggebeen J, Kitzman DW. Exercise intolerance in heart failure with preserved ejection fraction: more than a heart problem. J Geriatr Cardiol 2015;12:294-304.
16. Upadhya B, Haykowsky MJ, Eggebeen J, Kitzman DW. Sarcopenic obesity and the pathogenesis of exercise intolerance in heart failure with preserved ejection fraction. Curr Heart Fail Rep 2015;12:205-14.
17. Mark AL, Victor RG, Nerhed C, Wallin BG. Microneurographic studies of the mechanisms of sympathetic nerve responses to static exercise in humans. Circ Res 1985;57:461-9.
18. Victor RG, Secher NH, Lyson T, Mitchell JH. Central command increases muscle sympathetic nerve activity during intense intermittent isometric exercise in humans. Circ Res 1995;76:127-31.
19. AlBadri A, Bairey Merz CN, Johnson BD et al. Impact of Abnormal Coronary Reactivity on Long-Term Clinical Outcomes in Women. J Am Coll Cardiol 2019;73:684-693.
20. AlBadri A, Leong D, Bairey Merz CN et al. Typical angina is associated with greater coronary endothelial dysfunction but not abnormal vasodilatory reserve. Clin Cardiol 2017.
21. Bairey Merz CN, Shaw LJ, Reis SE et al. Insights from the NHLBI-Sponsored Women's Ischemia Syndrome Evaluation (WISE) Study: Part II: gender differences in presentation, diagnosis, and outcome with regard to gender-based pathophysiology of atherosclerosis and macrovascular and microvascular coronary disease. J Am Coll Cardiol 2006;47:S21-9.
22. Gulati M, Cooper-DeHoff RM, McClure C et al. Adverse cardiovascular outcomes in women with nonobstructive coronary artery disease: a report from the Women's Ischemia Syndrome Evaluation Study and the St James Women Take Heart Project. Arch Intern Med 2009;169:843-50.
23. Pepine CJ, Anderson RD, Sharaf BL et al. Coronary microvascular reactivity to adenosine predicts adverse outcome in women evaluated for suspected ischemia results from the National Heart, Lung and Blood Institute WISE (Women's Ischemia Syndrome Evaluation) study. J Am Coll Cardiol 2010;55:2825-32.
24. Petersen JW, Mehta PK, Kenkre TS et al. Comparison of low and high dose intracoronary adenosine and acetylcholine in women undergoing coronary reactivity testing: results from the NHLBI-sponsored Women's Ischemia Syndrome Evaluation (WISE). Int J Cardiol 2014;172:e114-5.
25. Shufelt CL, Thomson LE, Goykhman P et al. Cardiac magnetic resonance imaging myocardial perfusion reserve index assessment in women with microvascular coronary dysfunction and reference controls. Cardiovasc Diagn Ther 2013;3:153-60.
26. Thomson LE, Wei J, Agarwal M et al. Cardiac magnetic resonance myocardial perfusion reserve index is reduced in women with coronary microvascular dysfunction. A National Heart, Lung, and Blood Institute-sponsored study from the Women's Ischemia Syndrome Evaluation. Circ Cardiovasc Imaging 2015;8.
27. von Mering GO, Arant CB, Wessel TR et al. Abnormal coronary vasomotion as a prognostic indicator of cardiovascular events in women: results from the National Heart,

Lung, and Blood Institute-Sponsored Women's Ischemia Syndrome Evaluation (WISE). Circulation 2004;109:722-5.
28. Nelson MD, Sharif B, Shaw JL et al. Myocardial tissue deformation is reduced in subjects with coronary microvascular dysfunction but not rescued by treatment with ranolazine. Clin Cardiol 2017;40:300-306.
29. Nelson MD, Szczepaniak LS, Wei J et al. Diastolic dysfunction in women with signs and symptoms of ischemia in the absence of obstructive coronary artery disease: a hypothesis-generating study. Circulation Cardiovascular imaging 2014;7:510-6.
30. Wei J, Mehta PK, Shufelt C et al. Diastolic dysfunction measured by cardiac magnetic resonance imaging in women with signs and symptoms of ischemia but no obstructive coronary artery disease. Int J Cardiol 2016;220:775-80.

Chapter 2

Diastolic Stress Testing Along the Heart Failure Continuum*

T. Jake Samuel, Rhys Beaudry, Satyam Sarma, Vlad Zaha, Mark J. Haykowsky, and Michael D. Nelson (2018). Diastolic Stress Testing Along the Heart Failure Continuum. *Curr Heart Fail Rep*, 15 (6): 332-339. DOI: 10.1007/s11897-018-0409-5.

Introduction

Normal left ventricular (LV) diastole requires the coordination of several physiological processes which allow the heart to fill sufficiently under low filling pressures. As systole ends, LV elastic recoil and active relaxation gives rise to an abrupt decline in LV pressure until the mitral valve opens, and blood flows along a pressure gradient toward the apex. Upon pressure equilibration between the left atrium and the LV (i.e. diastasis), the final component of ventricular filling occurs when the atrium contracts and systole resumes. Impairment of any one of these processes can result in a rise in LV filling pressure that is transmitted to the left atrium and pulmonary veins, and can be associated with pulmonary edema and dyspnea (1). Progression along the American College of Cardiology/American Heart Association (ACC/AHA) heart failure continuum from Stage A (presence of cardiovascular risk factors with no structural adaptations) to Stage C (structural adaptation and symptoms of heart failure) is associated with graded levels of diastolic dysfunction.

Conventional resting measures of diastolic function, particularly Doppler derived mitral inflow and annular tissue velocities, are both prognostic and predictive of events in overt heart disease (e.g. Stage C) (2-4). However, when disease is less advanced (e.g. Stage A) and/or when the diagnosis remains equivocal, diastolic stress testing may be indicated to differentiate cardiac *vs*. non-cardiac pathology. Indeed, over the past decade, assessment of diastolic function during physiological stress, termed “diastolic stress testing”, has emerged as a powerful tool to enhance detection of diastolic dysfunction as the etiological feature of exertional dyspnea (5). As a result, diastolic stress testing is now recommended by both the American Society of Echocardiography and the European Association of Cardiovascular Imaging (2,3,6).

This article reviews the evolution of diastolic stress testing, current practices and procedures, and discusses the potential for diastolic stress testing across the heart failure continuum.

Pathophysiology of Diastolic Dysfunction

Diastole is a complex process governed by multiple factors that regulate active LV pressure decay and passive LV diastolic stiffness (***Figure 1***). Determinants of active LV pressure decay include oxygen delivery, and intracellular calcium handling. Indeed, diastole is a highly energy dependent process, requiring sufficient delivery of oxygen for the generation of adenosine triphosphate (ATP). Unlike systole, which only requires ATP for the removal of troponin-C from actin, diastole requires ATP for the: 1) reuptake of calcium into the sarcoplasmic reticulum via the sarco-endoplasmic reticulum calcium ATP-ase (SERCA), 2) dissociation of actin and myosin, and 3) uncoupling of calcium from troponin-C (7). In addition to these direct consequences, oxygen deprivation also contributes to diastolic dysfunction by shifting substrate utilization away from fatty acid metabolism towards glucose metabolism (8-10).

Impaired intracellular calcium handling has also been implicated as a primary mechanism driving diastolic dysfunction. For example, excess calcium entry through L-type calcium channels, over activity of calcium-release-activated calcium channels (such as Orai-1), impaired sodium-calcium exchanger pumps, and reuptake and leaky ryanodine receptors, have each been implicated in a variety of conditions associated with diastolic dysfunction, including heart failure

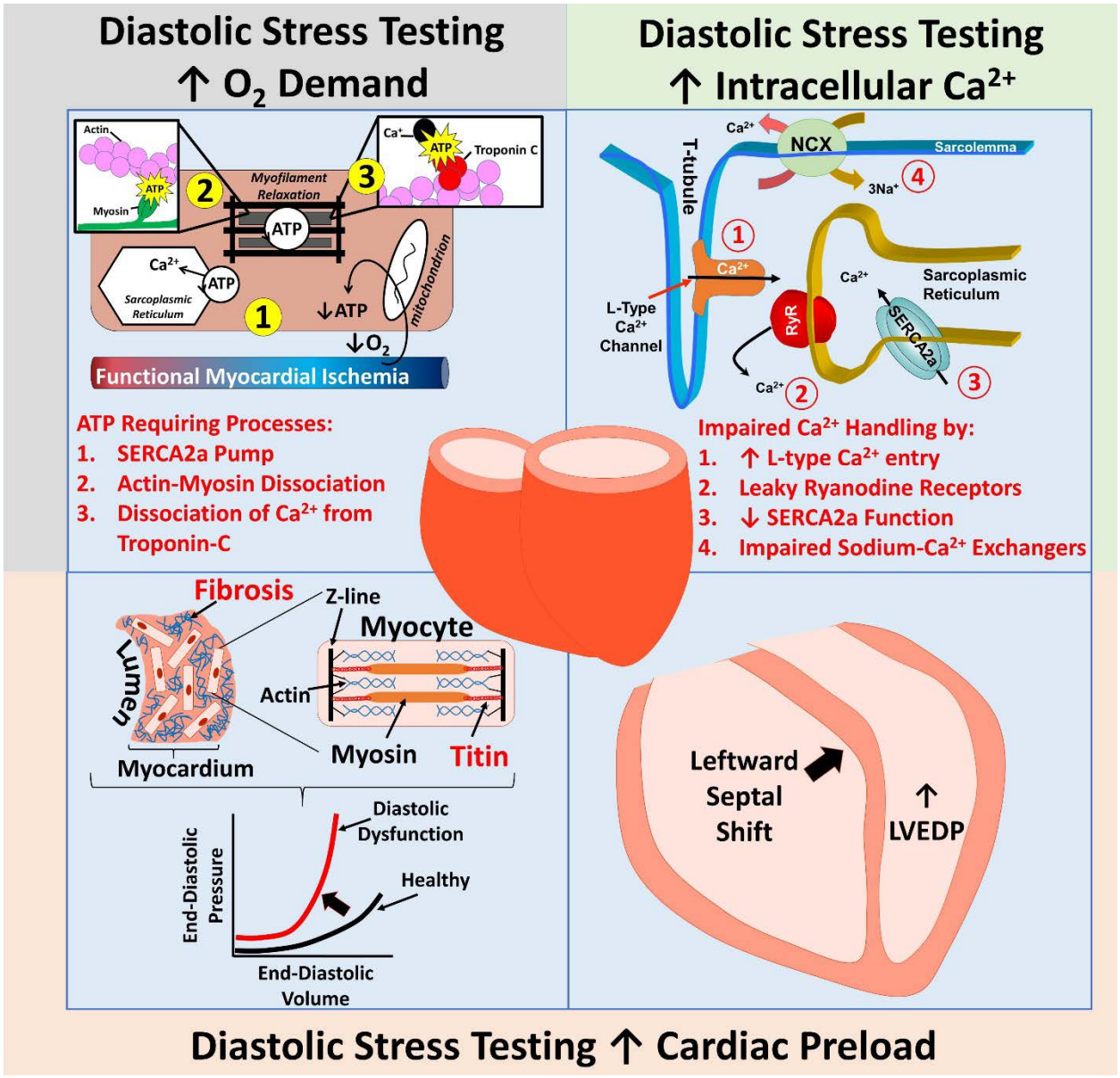

Figure 1. Key pathological mechanisms invloved in the development of diastolic dysfunction and the role of diastolic stress testing in exaccerbating each mechanistic pathway. *Clockwise from top-left*: functional myocardial ischemia caused by an increased myocardial oxygen (O_2) demand can lead to insufficient production of myocardial adensosine triphosphate (ATP); impaired calcium (Ca^{2+}) handling due to elevated intracellular Ca^{2+} concertrations can lead to prolonged and delayed myocardial relaxation; pericardial constraint can be exaccerbated by increases in preload and lead to an increased right ventricular pressure, causing a leftward shift of the interventricular septum, and ultimately leading to increased left ventricular end-diastolic (LVEDP) pressures; increased diffuse fibrosis and impaired titin function can be exaccerbated by increases in preload and lead to a shift in the end-diastolic pressure volume relationship upwards and to the left. SERCA2a – sarco/endoplasmic reticulum Ca^{2+} ATP-ase; RyR – ryanodine receptor; NCX – sodium-Ca^{2+} exchanger.

with preserved ejection fraction (HFpEF) (11-15). These detrimental molecular processes ultimately impair actin-myosin cross-bridge cycling and lead to a stiff ventricle.

In addition to the contributions from active LV pressure decay, diastolic dysfunction is also associated with increased passive LV stiffness. Expansion of the extracellular matrix (increased myocardial fibrosis), left ventricular hypertrophy, and dysregulation of structural proteins like titin, can each reduce passive ventricular compliance both independently, and in concert (16-20). Moreover, factors external to the myocardium can also negatively affect passive LV stiffness. For example, pericardial fat deposition, in combination with pericardial constraint, has recently been implicated as a major source of diastolic dysfunction (21-23). Under this paradigm, with the LV constrained by the pericardium, right ventricular filling causes a leftward septal shift and an elevation in LV end-diastolic pressure (23).

While in extreme cases, each of the above mechanisms can independently contribute to overt diastolic dysfunction, less extreme cases often fail to present under resting conditions. Diastolic stress testing is therefore necessary to exacerbate these underlying mechanisms and unmask diastolic dysfunction (***Figure 1***). For example, increasing myocardial oxygen demand can disrupt myocardial energetics and the processes governing calcium handling (24-28). Increasing cardiac afterload floods the myocardium with calcium to support increased force production, but places greater stress on the processes governing intracellular calcium homeostasis. Finally, increasing cardiac preload (e.g. saline infusion, leg lifts, dynamic exercise) can exacerbate LV passive stiffness, augment LV/RV interaction, and adversely increase cardiac filling pressures (23).

Diastolic Stress Testing along the Heart Failure Continuum

The term "diastolic stress testing" was first coined by *Ha and colleagues* (29), describing an abnormal rise in left ventricular filling pressures during exercise. However, in practice, "diastolic stress testing" has been utilized for several decades (30,31). For example, more than 60 years ago, *Lewis and colleagues* demonstrated an abnormal rise in pulmonary capillary wedge pressure (PCWP) in response to recumbent cycle exercise in some, but not all, patients with cardiovascular disease despite normal PCWP at rest (30). More recently, *Levine and coworkers* have used acute volume loading/unloading to characterize LV compliance in health and disease (24,31-38). Today, diastolic stress testing is recognized as the most robust method for discriminating between cardiac and non-cardiac involvement in exercise-induced dyspnea (39-42). Some of the most compelling and influential examples of this have recently come from *Borlaug and colleagues* at the Mayo Clinic in Rochester, MN, using invasive assessment of left ventricular filling pressures during submaximal cycle exercise to differentiate patients with HFpEF from those without cardiac involvement (5,10,25,39-41,43-63). Importantly, while the majority of these studies have focused on direct, gold-standard, invasive measures of LV filling pressure, *Borlaug and colleagues* have also shown strong agreement between PCWP and its noninvasive, Doppler derived, surrogate (early mitral inflow velocity to early annual tissue velocity ratio, E/e') (63). Indeed, this helps further validate the noninvasive work of *Ha and colleagues*, who have consistently used E/e' during cycle exercise to differentiate cardiac from non-cardiac pathology (29,64). Specifically, in 2005, this group was able to identify individuals who had seemingly normal resting diastolic function (i.e. normal E/e'), but upon exercise, shared an exaggerated E/e'

response (i.e. abnormal rise in cardiac filling pressure) (29). Across each of these studies, the common threshold defining an abnormal rise in cardiac filling pressure was a change in E/e' > 1.5.

Cycle echocardiography is susceptible to several limitations however, including respiratory and movement artifacts that are exaggerated in clinical populations at risk for diastolic dysfunction (obese, elderly, etc). Moreover, while *Borlaug and colleagues* have convincingly demonstrated that only a mild-level of exercise is needed to elicit an abnormal diastolic response (~20-40W), this approach hinges upon the ability of patients to perform dynamic leg exercise. In an effort to overcome these limitations, our group has advocated replacing cycle exercise with isometric handgrip (27,28). Indeed, isometric handgrip causes a robust, and highly reproducible pressor-mediated increase in heart rate and blood pressure (65), without causing dramatic increases in respiration or chest wall movement. Importantly, isometric handgrip also elicits marked increases in invasively measured LV filling pressures (42,66-68). In our hands, isometric handgrip echocardiography is capable of differentiating normal from abnormal diastolic function (defined as a rise in E/e' >1.5) (28), with comparable hemodynamic changes to conventional cycle exercise (27).

While isometric handgrip produces a similar hemodynamic challenge compared to low level cycle exercise (27), these two stressors likely exacerbate diastolic dysfunction through somewhat different mechanisms. Independent of increased myocardial oxygen demand, the primary mechanism driving diastolic dysfunction during cycle exercise is likely related to the demand for increased cardiac output and reduced LV relaxation time. In this scenario, a stiff ventricle combined with increased venous return leads to an increase in LV filling pressure. In contrast, isometric handgrip uniquely increases LV afterload secondary to a neurally mediated

exercise pressor reflex (69-73). To support the ejection of blood during systole, this increase in afterload is met by a concomitant increase in intracellular calcium; which must either be sequestrated back in to the sarcoplasmic reticulum or extruded from the myocyte during ventricular relaxation (74-76). Dysregulation of this processes will lead to prolonged actin-myosin cross-bridge formation and impaired active relaxation (77,78); and thus increased LV stiffness and elevated LV filling pressure (24). The potential for varying mechanistic pathways ought to be considered when designing diastolic stress tests, and warrants future investigation.

Regardless of the mechanism driving diastolic dysfunction during physiological stress, or the method by which diastolic dysfunction is measured, there is increasing body of literature supporting the use of diastolic stress testing across the heart failure continuum (**Table 1**). Indeed, diastolic stress testing can successfully unmask diastolic dysfunction in asymptomatic patients with hypertension with no structural remodeling (i.e. Stage A, (10,79,80)), asymptomatic patients with mild aortic stenosis (i.e. Stage B, (81,82)) and compensated HFpEF patients (i.e. Stage C, (10,39,42,49,50,63,68,83-88). While cycle exercise has been the predominant method of diastolic stress testing (10,39,85), isometric handgrip echocardiography has been shown to be a robust alternative (27,28,42,68), with comparable end-results (27).

Table 1. Diastolic stress testing along the heart failure continuum, data from seminal investigations and those conducted in the 5 years.

	First Author and Date	Population	Measurement Modality	Stress Modality	Main Outcomes
ACC/AHA Stage A					
	Shim, 2013 (79)	Hypertensives with no increase in LV mass – 72 with abnormal ventricular-vascular interaction and 72 normal ventricular-vascular interaction	Echo	Cycle	Patients with abnormal ventricular-vascular interaction during exercise - ΔE/e' 2.1 during 50W cycle exercise. Patients with normal ventricular-vascular interaction - ΔE/e' 1.3 (below established diastolic cutoff).
	van Empel, 2014 (10)	7 hypertensives with no increase in LV mass and 12 healthy controls	Invasive	Cycle	Hypertensives - ΔPCWP of 8 mmHg at max exercise (~87W). Healthy controls - ΔPCWP of 8 mmHg at max exercise (~114W).
	Samuel, 2017 (28)	17 asymptomatic elderly and 19 young healthy controls	Echo	IHG	65% of the elderly individuals showed ΔE/e' > 1.5. 0% of healthy controls showed ΔE/e' > 1.5.
	Samuel, 2018 (27)	12 asymptomatic elderly individuals	Echo	IHG, cycle	75% of individuals had a ΔE/e' > 1.5 during IHG. 67% of individuals had a ΔE/e' > 1.5 during cycle.
	Gibby, 2013 (80)	559 hypertensives with diabetes and no structural remodeling	Echo	Cycle	20% of participants showed post-exercise E/e' > 13 (max exercise ~7.7 METs).
ACC/AHA Stage B					
	Tan, 2010 (89)	30 hypertensives with a history of dyspnea and 22 healthy controls	Echo	Cycle	Hypertensives showed reduced longitudinal strain, delayed untwisting rate, reduced LV suction.
	Sonaglioni, 2015 (81)	90 asymptomatic patients with aortic stenosis	Echo	Cycle	ΔE/e' of 6.5 at peak exercise (only 16.7% of patients reached >75W).
	Christensen, 2016 (82)	25 asymptomatic patients with aortic stenosis and LA volume index >35 mL/m^2 and 14 asymptomatic patients with aortic stenosis and LA volume index <35 mL/m^2	Invasive	Cycle	Group with LA volume index <35 mL/m^2 - ΔPCWP of 15 mmHg at 75W. Group with LA volume index >35 mL/m^2 - ΔPCWP of 16 mmHg at 75W.
ACC/AHA Stage C					
	Borlaug, 2010 (39)	32 HFpEF patients and 23 patients with non-cardiac dyspnea	Invasive	Cycle, leg lift	HFpEF - ΔPCWP 17 mmHg at 20W cycle and ΔPCWP 7 with leg lift. Non-cardiac dyspnea - ΔPCWP 2 mmHg at 20W cycle and ΔPCWP 2 with leg lift.
	Penicka, 2010 (42)	20 HFpEF patients and 10 non-cardiac dyspnea	Invasive	IHG, leg lift	HFpEF - ΔEDP 7 mmHg with IHG and ΔEDP 3 mmHg with leg lift. Non-cardiac dyspnea - ΔEDP 2 mmHg with IHG and ΔEDP 3 mmHg with leg lift.
	van Empel, 2014 (10)	9 HFpEF patients and 12 healthy controls	Invasive	Cycle	HFpEF - ΔPCWP 18 mmHg at max exercise (~43W). Healthy controls - ΔPCWP of 8 mmHg at max exercise (~114W).

	Borlaug, 2015 (49)	28 HFpEF patients	Invasive	Cycle	ΔPCWP of 13 mmHg at 20W.
	Borlaug, 2016 (50)	26 HFpEF patients	Invasive	Cycle	ΔPCWP of 13 mmHg at 20W.
	Obokata, 2016 (63)	50 HFpEF patients and 24 patients with non-cardiac dyspnea.	Invasive, echo	Cycle	HFpEF - ΔPCWP of 14 mmHg and ΔE/e' of 3 at 20W. Non-cardiac dyspnea - ΔPCWP of 7 mmHg and ΔE/e' of 1 at 20W.
	Obokata, 2017 (86)	37 HFpEF patients and 43 HFrEF patients	Echo	Cycle	HFpEF - ΔE/e' 1.7 at 10W. HFrEF - ΔE/e' 1.6 at 10W.
	Rommel, 2018 (68)	24 HFpEF patients and 9 patients with non-cardiac dyspnea	Invasive	IHG	HFpEF - ΔPCWP of 11.1 mmHg. Non-cardiac dyspnea - ΔPCWP of 6.2 mmHg.
	Kosmala, 2018 (87)	171 patients with unexplained dyspnea and suspected HFpEF	Echo	Treadmill	60% abnormal exercise response (post-exercise E/e' > 14).
	Gorter, 2018 (83)	21 HFpEF patients with no pulmonary hypertension, 95 HFpEF patients with post-capillary pulmonary hypertension and 45 HFpEF patients with pre- and post-capillary pulmonary hypertension	Invasive	Cycle	No pulmonary hypertension - ΔPCWP 12 mmHg at max exercise (~42W). Post-capillary pulmonary hypertension - ΔPCWP 13 mmHg at max exercise (~32W). Pre- and post-capillary pulmonary hypertension - ΔPCWP 12 mmHg at peak exercise (~31W).
	Obokata, 2018 (85)	38 HFpEF patients and 20 patients with non-cardiac dyspnea	Invasive	Cycle	HFpEF - ΔPCWP of 14 mmHg at 20W. Non-cardiac dyspnea - ΔPCWP of 7 mmHg at 20W.
	Obokata, 2018 (84)	50 HFpEF patients and 24 patients with non-cardiac dyspnea	Invasive	Cycle	HFpEF - ΔPCWP 14 mmHg at 20W. Non-cardiac dyspnea - ΔPCWP 7 mmHg at 20W.
	Hieda, 2018 (88)	10 HFpEF patients and 12 healthy controls.	Invasive	LBNP and saline	Up- and leftward shift of the end-diastolic pressure volume relationship (i.e. increased LV stiffness).

ACC/AHA – American College of Cardiology/American Heart Association; LV – left ventricular; Echo – echocardiography; E/e' – ratio between Doppler derived early diastolic mitral inflow velocity and early diastolic tissue velocity; W – Watts; PCWP – pulmonary capillary wedge pressure; IHG – isometric handgrip exercise; MET's – metabolic equivolents; LA – left atrial; HFpEF – heart failure with preserved ejection fraction; EDP – end-daistolic pressure; HFrEF – heart failure with reduced ejection fraction; LBNP – lower body negative pressure.

The Future of Diastolic Stress Testing

The demonstration of clinical benefit for early diagnosis and management of diastolic dysfunction advocates for the widespread clinical adoption of diastolic stress testing. Indeed, cardiac stress testing (particularly recumbent cycle exercise) is already integrated and practiced in echocardiography laboratories worldwide. Inclusion of simple Doppler derived estimates of LV filling pressures can be easily added to standard of care measures, providing relevant diagnostic and prognostic information (2-4,63). That non-invasive diastolic stress testing can also be done by simply performing handgrip exercise (27,28) holds even greater promise for widespread clinical adoption. In an ideal world, every echocardiography machine would come equipped with a stress ball or handgrip dynamometer so that diastolic stress testing may be included as part of every routine cardiac scan. While diastolic stress testing has strong prognostic and diagnostic utility in patients with unexplained dyspnea and/or heart failure symptoms, it remains unclear what the predictive capacity is for asymptomatic patients (e.g. ACC/AHA Stage A). Longitudinal studies are therefore needed to define the predictive value of diastolic stress testing across the heart failure continuum.

Conclusions

Diastolic stress testing provides diagnostic and prognostic value in those at risk for heart failure and those with symptoms of unexplained dyspnea. The ability of non-invasive diastolic stress testing to successfully discriminate between cardiac and non-cardiac limitation to exercise and unmask diastolic dysfunction in both clinical and sub-clinical patients, highlights its potential

application in the cardiology clinic. That noninvasive diastolic stress testing, either with cycle echocardiography or isometric handgrip echocardiography, is both simple and relatively low cost, holds great promise. Future work is needed to use this approach to better understand specific pathophysiological mechanisms and the predictive capacity of this novel approach.

Reference List

1. Borlaug BA, Paulus WJ. Heart failure with preserved ejection fraction: pathophysiology, diagnosis, and treatment. Eur Heart J 2011;32:670-9.
2. Nagueh SF, Smiseth OA, Appleton CP et al. Recommendations for the Evaluation of Left Ventricular Diastolic Function by Echocardiography: An Update from the American Society of Echocardiography and the European Association of Cardiovascular Imaging. Eur Heart J Cardiovasc Imaging 2016;17:1321-1360.
3. Nagueh SF, Smiseth OA, Appleton CP et al. Recommendations for the Evaluation of Left Ventricular Diastolic Function by Echocardiography: An Update from the American Society of Echocardiography and the European Association of Cardiovascular Imaging. J Am Soc Echocardiogr 2016;29:277-314.
4. Burgess MI, Jenkins C, Sharman JE, Marwick TH. Diastolic stress echocardiography: hemodynamic validation and clinical significance of estimation of ventricular filling pressure with exercise. J Am Coll Cardiol 2006;47:1891-900.
5. Borlaug BA. Exercise haemodynamics and outcome in patients with dyspnoea. Eur Heart J 2014;35:3085-7.
6. Mitter SS, Shah SJ, Thomas JD. A Test in Context: E/A and E/e' to Assess Diastolic Dysfunction and LV Filling Pressure. J Am Coll Cardiol 2017;69:1451-1464.
7. Gorski PA, Ceholski DK, Hajjar RJ. Altered myocardial calcium cycling and energetics in heart failure--a rational approach for disease treatment. Cell Metab 2015;21:183-94.
8. Lopaschuk GD, Stanley WC. Glucose metabolism in the ischemic heart. Circulation 1997;95:313-5.
9. Zile MR, Baicu CF, Gaasch WH. Diastolic heart failure--abnormalities in active relaxation and passive stiffness of the left ventricle. N Engl J Med 2004;350:1953-9.
10. van Empel VP, Mariani J, Borlaug BA, Kaye DM. Impaired myocardial oxygen availability contributes to abnormal exercise hemodynamics in heart failure with preserved ejection fraction. J Am Heart Assoc 2014;3:e001293.
11. Schroder F, Handrock R, Beuckelmann DJ et al. Increased availability and open probability of single L-type calcium channels from failing compared with nonfailing human ventricle. Circulation 1998;98:969-76.
12. Luo X, Hojayev B, Jiang N et al. STIM1-dependent store-operated Ca(2)(+) entry is required for pathological cardiac hypertrophy. J Mol Cell Cardiol 2012;52:136-47.
13. Goonasekera SA, Hammer K, Auger-Messier M et al. Decreased cardiac L-type Ca(2)(+) channel activity induces hypertrophy and heart failure in mice. J Clin Invest 2012;122:280-90.
14. Hasenfuss G, Reinecke H, Studer R et al. Relation between myocardial function and expression of sarcoplasmic reticulum Ca(2+)-ATPase in failing and nonfailing human myocardium. Circ Res 1994;75:434-42.
15. Sipido KR, Volders PG, Vos MA, Verdonck F. Altered Na/Ca exchange activity in cardiac hypertrophy and heart failure: a new target for therapy? Cardiovasc Res 2002;53:782-805.
16. Ahmed SH, Clark LL, Pennington WR et al. Matrix metalloproteinases/tissue inhibitors of metalloproteinases: relationship between changes in proteolytic determinants of matrix

composition and structural, functional, and clinical manifestations of hypertensive heart disease. Circulation 2006;113:2089-96.
17. Gonzalez A, Lopez B, Querejeta R, Zubillaga E, Echeverria T, Diez J. Filling pressures and collagen metabolism in hypertensive patients with heart failure and normal ejection fraction. Hypertension 2010;55:1418-24.
18. Mohammed SF, Hussain S, Mirzoyev SA, Edwards WD, Maleszewski JJ, Redfield MM. Coronary microvascular rarefaction and myocardial fibrosis in heart failure with preserved ejection fraction. Circulation 2015;131:550-9.
19. Hidalgo C, Hudson B, Bogomolovas J et al. PKC phosphorylation of titin's PEVK element: a novel and conserved pathway for modulating myocardial stiffness. Circ Res 2009;105:631-8, 17 p following 638.
20. Hidalgo C, Granzier H. Tuning the molecular giant titin through phosphorylation: role in health and disease. Trends Cardiovasc Med 2013;23:165-71.
21. Motoki H, Alraies MC, Dahiya A et al. Changes in left atrial mechanics following pericardiectomy for pericardial constriction. J Am Soc Echocardiogr 2013;26:640-8.
22. Yamamoto K, Masuyama T, Tanouchi J et al. Decreased and abnormal left ventricular filling in acute heart failure: role of pericardial constraint and its mechanism. J Am Soc Echocardiogr 1992;5:504-14.
23. Borlaug BA, Carter RE, Melenovsky V et al. Percutaneous Pericardial Resection: A Novel Potential Treatment for Heart Failure With Preserved Ejection Fraction. Circ Heart Fail 2017;10:e003612.
24. Arbab-Zadeh A, Dijk E, Prasad A et al. Effect of aging and physical activity on left ventricular compliance. Circulation 2004;110:1799-805.
25. van Empel VP, Kaye DM, Borlaug BA. Effects of healthy aging on the cardiopulmonary hemodynamic response to exercise. Am J Cardiol 2014;114:131-5.
26. Hollingsworth KG, Blamire AM, Keavney BD, Macgowan GA. Left ventricular torsion, energetics, and diastolic function in normal human aging. Am J Physiol Heart Circ Physiol 2012;302:H885-92.
27. Samuel TJ, Beaudry R, Haykowsky MJ, Sarma S, Nelson MD. Diastolic Stress Testing: Similarities and Differences between Isometric Handgrip and Cycle Echocardiography. J Appl Physiol (1985) 2018.
28. Samuel TJ, Beaudry R, Haykowsky MJ et al. Isometric handgrip echocardiography: A noninvasive stress test to assess left ventricular diastolic function. Clin Cardiol 2017;40:1247-1255.
29. Ha JW, Oh JK, Pellikka PA et al. Diastolic stress echocardiography: a novel noninvasive diagnostic test for diastolic dysfunction using supine bicycle exercise Doppler echocardiography. J Am Soc Echocardiogr 2005;18:63-8.
30. Lewis BM, Houssay HE, Haynes FW, Dexter L. The dynamics of both right and left ventricles at rest and during exercise in patients with heart failure. Circ Res 1953;1:312-20.
31. Levine BD, Lane LD, Buckey JC, Friedman DB, Blomqvist CG. Left ventricular pressure-volume and Frank-Starling relations in endurance athletes. Implications for orthostatic tolerance and exercise performance. Circulation 1991;84:1016-23.

32. Drazner MH, Prasad A, Ayers C et al. The relationship of right- and left-sided filling pressures in patients with heart failure and a preserved ejection fraction. Circ Heart Fail 2010;3:202-6.
33. Levine BD. Regulation of central blood volume and cardiac filling in endurance athletes: the Frank-Starling mechanism as a determinant of orthostatic tolerance. Med Sci Sports Exerc 1993;25:727-32.
34. Popovic ZB, Prasad A, Garcia MJ et al. Relationship among diastolic intraventricular pressure gradients, relaxation, and preload: impact of age and fitness. Am J Physiol Heart Circ Physiol 2006;290:H1454-9.
35. Shibata S, Hastings JL, Prasad A et al. Congestive heart failure with preserved ejection fraction is associated with severely impaired dynamic Starling mechanism. J Appl Physiol (1985) 2011;110:964-71.
36. Steppan J, Tran H, Benjo AM et al. Alagebrium in combination with exercise ameliorates age-associated ventricular and vascular stiffness. Exp Gerontol 2012;47:565-72.
37. Fujimoto N, Borlaug BA, Lewis GD et al. Hemodynamic responses to rapid saline loading: the impact of age, sex, and heart failure. Circulation 2013;127:55-62.
38. Fujimoto N, Shibata S, Hastings JL et al. Effects of pericardial constraint and ventricular interaction on left ventricular hemodynamics in the unloaded heart. Am J Physiol Heart Circ Physiol 2011;300:H1688-95.
39. Borlaug BA, Nishimura RA, Sorajja P, Lam CS, Redfield MM. Exercise hemodynamics enhance diagnosis of early heart failure with preserved ejection fraction. Circ Heart Fail 2010;3:588-95.
40. Borlaug BA, Jaber WA, Ommen SR, Lam CS, Redfield MM, Nishimura RA. Diastolic relaxation and compliance reserve during dynamic exercise in heart failure with preserved ejection fraction. Heart 2011;97:964-9.
41. Andersen MJ, Ersboll M, Bro-Jeppesen J et al. Exercise hemodynamics in patients with and without diastolic dysfunction and preserved ejection fraction after myocardial infarction. Circ Heart Fail 2012;5:444-51.
42. Penicka M, Bartunek J, Trakalova H et al. Heart failure with preserved ejection fraction in outpatients with unexplained dyspnea: a pressure-volume loop analysis. J Am Coll Cardiol 2010;55:1701-10.
43. Abudiab MM, Redfield MM, Melenovsky V et al. Cardiac output response to exercise in relation to metabolic demand in heart failure with preserved ejection fraction. Eur J Heart Fail 2013;15:776-85.
44. Andersen MJ, Borlaug BA. Invasive hemodynamic characterization of heart failure with preserved ejection fraction. Heart Fail Clin 2014;10:435-44.
45. Andersen MJ, Ersboll M, Bro-Jeppesen J et al. Relationships between biomarkers and left ventricular filling pressures at rest and during exercise in patients after myocardial infarction. J Card Fail 2014;20:959-67.
46. Andersen MJ, Olson TP, Melenovsky V, Kane GC, Borlaug BA. Differential hemodynamic effects of exercise and volume expansion in people with and without heart failure. Circ Heart Fail 2015;8:41-8.
47. Borlaug BA. Mechanisms of exercise intolerance in heart failure with preserved ejection fraction. Circ J 2014;78:20-32.

48. Borlaug BA, Kane GC, Melenovsky V, Olson TP. Abnormal right ventricular-pulmonary artery coupling with exercise in heart failure with preserved ejection fraction. Eur Heart J 2016;37:3293-3302.
49. Borlaug BA, Koepp KE, Melenovsky V. Sodium Nitrite Improves Exercise Hemodynamics and Ventricular Performance in Heart Failure With Preserved Ejection Fraction. J Am Coll Cardiol 2015;66:1672-82.
50. Borlaug BA, Melenovsky V, Koepp KE. Inhaled Sodium Nitrite Improves Rest and Exercise Hemodynamics in Heart Failure With Preserved Ejection Fraction. Circ Res 2016;119:880-6.
51. Borlaug BA, Melenovsky V, Russell SD et al. Impaired chronotropic and vasodilator reserves limit exercise capacity in patients with heart failure and a preserved ejection fraction. Circulation 2006;114:2138-47.
52. Borlaug BA, Reddy YN. Determinants and Correlates of Exercise Capacity in Heart Failure. JACC Heart Fail 2015;3:815-7.
53. Gharacholou SM, Scott CG, Borlaug BA et al. Relationship between diastolic function and heart rate recovery after symptom-limited exercise. J Card Fail 2012;18:34-40.
54. Hussain I, Mohammed SF, Forfia PR et al. Impaired Right Ventricular-Pulmonary Arterial Coupling and Effect of Sildenafil in Heart Failure With Preserved Ejection Fraction: An Ancillary Analysis From the Phosphodiesterase-5 Inhibition to Improve Clinical Status And Exercise Capacity in Diastolic Heart Failure (RELAX) Trial. Circ Heart Fail 2016;9:e002729.
55. Kaye D, Shah SJ, Borlaug BA et al. Effects of an interatrial shunt on rest and exercise hemodynamics: results of a computer simulation in heart failure. J Card Fail 2014;20:212-21.
56. Lam CS, Grewal J, Borlaug BA et al. Size, shape, and stamina: the impact of left ventricular geometry on exercise capacity. Hypertension 2010;55:1143-9.
57. Little WC, Borlaug BA. Exercise intolerance in heart failure with preserved ejection fraction: what does the heart have to do with it? Circ Heart Fail 2015;8:233-5.
58. Mohammed SF, Borlaug BA, McNulty S et al. Resting ventricular-vascular function and exercise capacity in heart failure with preserved ejection fraction: a RELAX trial ancillary study. Circ Heart Fail 2014;7:580-9.
59. Redfield MM, Borlaug BA, Lewis GD et al. PhosphdiesteRasE-5 Inhibition to Improve CLinical Status and EXercise Capacity in Diastolic Heart Failure (RELAX) trial: rationale and design. Circ Heart Fail 2012;5:653-9.
60. Redfield MM, Chen HH, Borlaug BA et al. Effect of phosphodiesterase-5 inhibition on exercise capacity and clinical status in heart failure with preserved ejection fraction: a randomized clinical trial. JAMA 2013;309:1268-77.
61. Wolsk E, Kaye D, Borlaug BA et al. Resting and exercise haemodynamics in relation to six-minute walk test in patients with heart failure and preserved ejection fraction. Eur J Heart Fail 2017.
62. Zakeri R, Borlaug BA, McNulty SE et al. Impact of atrial fibrillation on exercise capacity in heart failure with preserved ejection fraction: a RELAX trial ancillary study. Circ Heart Fail 2014;7:123-30.

63. Obokata M, Kane GC, Reddy YN, Olson TP, Melenovsky V, Borlaug BA. The Role of Diastolic Stress Testing in the Evaluation for HFpEF:A Simultaneous Invasive-Echocardiographic Study. Circulation 2016.
64. Ha JW, Choi EY, Choi D et al. Time course of recovery of left ventricular filling pressure after exercise in healthy subjects. Circ J 2008;72:186-8.
65. Alam M, Smirk FH. Observations in man upon a blood pressure raising reflex arising from the voluntary muscles. J Physiol 1937;89:372-83.
66. Westermann D, Kasner M, Steendijk P et al. Role of left ventricular stiffness in heart failure with normal ejection fraction. Circulation 2008;117:2051-60.
67. Kawaguchi M, Hay I, Fetics B, Kass DA. Combined ventricular systolic and arterial stiffening in patients with heart failure and preserved ejection fraction: implications for systolic and diastolic reserve limitations. Circulation 2003;107:714-20.
68. Rommel KP, von Roeder M, Oberueck C et al. Load-Independent Systolic and Diastolic Right Ventricular Function in Heart Failure With Preserved Ejection Fraction as Assessed by Resting and Handgrip Exercise Pressure-Volume Loops. Circ Heart Fail 2018;11:e004121.
69. Mark AL, Victor RG, Nerhed C, Wallin BG. Microneurographic studies of the mechanisms of sympathetic nerve responses to static exercise in humans. Circ Res 1985;57:461-9.
70. Victor RG, Secher NH, Lyson T, Mitchell JH. Central command increases muscle sympathetic nerve activity during intense intermittent isometric exercise in humans. Circ Res 1995;76:127-31.
71. Victor RG, Vissing SF, Urias L, Scherrer U. Central Motor Command Activates Sympathetic Outflow to Skin during Static Exercise in Humans. Clin Res 1989;37:A524-A524.
72. Delaney EP, Greaney JL, Edwards DG, Rose WC, Fadel PJ, Farquhar WB. Exaggerated sympathetic and pressor responses to handgrip exercise in older hypertensive humans: role of the muscle metaboreflex. Am J Physiol Heart Circ Physiol 2010;299:H1318-27.
73. Ogoh S, Wasmund WL, Keller DM et al. Role of central command in carotid baroreflex resetting in humans during static exercise. J Physiol-London 2002;543:349-364.
74. Kawase Y, Ly HQ, Prunier F et al. Reversal of cardiac dysfunction after long-term expression of SERCA2a by gene transfer in a pre-clinical model of heart failure. J Am Coll Cardiol 2008;51:1112-9.
75. Balderas-Villalobos J, Molina-Munoz T, Mailloux-Salinas P, Bravo G, Carvajal K, Gomez-Viquez NL. Oxidative stress in cardiomyocytes contributes to decreased SERCA2a activity in rats with metabolic syndrome. Am J Physiol Heart Circ Physiol 2013;305:H1344-53.
76. Berridge MJ, Bootman MD, Roderick HL. Calcium signalling: dynamics, homeostasis and remodelling. Nat Rev Mol Cell Biol 2003;4:517-29.
77. Gwathmey JK, Copelas L, MacKinnon R et al. Abnormal intracellular calcium handling in myocardium from patients with end-stage heart failure. Circ Res 1987;61:70-6.
78. Hunter WC. Role of myofilaments and calcium handling in left ventricular relaxation. Cardiol Clin 2000;18:443-57.
79. Shim CY, Park S, Choi EY et al. The relationship between ventricular-vascular uncoupling during exercise and impaired left ventricular longitudinal functional reserve in hypertensive patients. J Am Soc Hypertens 2013;7:198-205.

80. Gibby C, Wiktor DM, Burgess M, Kusunose K, Marwick TH. Quantitation of the diastolic stress test: filling pressure vs. diastolic reserve. Eur Heart J Cardiovasc Imaging 2013;14:223-7.
81. Sonaglioni A, Lombardo M, Baravelli M, Trotta G, Sommese C, Anza C. Exercise stress echocardiography with tissue Doppler imaging in risk stratification of mild to moderate aortic stenosis. Int J Cardiovasc Imaging 2015;31:1519-27.
82. Christensen NL, Dahl JS, Carter-Storch R et al. Association Between Left Atrial Dilatation and Invasive Hemodynamics at Rest and During Exercise in Asymptomatic Aortic Stenosis. Circ Cardiovasc Imaging 2016;9.
83. Gorter TM, Obokata M, Reddy YNV, Melenovsky V, Borlaug BA. Exercise unmasks distinct pathophysiologic features in heart failure with preserved ejection fraction and pulmonary vascular disease. Eur Heart J 2018.
84. Obokata M, Olson TP, Reddy YNV, Melenovsky V, Kane GC, Borlaug BA. Haemodynamics, dyspnoea, and pulmonary reserve in heart failure with preserved ejection fraction. Eur Heart J 2018.
85. Obokata M, Reddy YNV, Melenovsky V et al. Myocardial Injury and Cardiac Reserve in Patients With Heart Failure and Preserved Ejection Fraction. J Am Coll Cardiol 2018;72:29-40.
86. Obokata M, Nagata Y, Kado Y, Kurabayashi M, Otsuji Y, Takeuchi M. Ventricular-Arterial Coupling and Exercise-Induced Pulmonary Hypertension During Low-Level Exercise in Heart Failure With Preserved or Reduced Ejection Fraction. J Card Fail 2017;23:216-220.
87. Kosmala W, Przewlocka-Kosmala M, Rojek A, Marwick TH. Comparison of the Diastolic Stress Test With a Combined Resting Echocardiography and Biomarker Approach to Patients With Exertional Dyspnea: Diagnostic and Prognostic Implications. JACC Cardiovasc Imaging 2018.
88. Hieda M, Howden E, Shibata S et al. Preload-corrected dynamic Starling mechanism in patients with heart failure with preserved ejection fraction. J Appl Physiol (1985) 2018;124:76-82.
89. Tan YT, Wenzelburger F, Lee E, Heatlie G, Frenneaux M, Sanderson JE. Abnormal left ventricular function occurs on exercise in well-treated hypertensive subjects with normal resting echocardiography. Heart 2010;96:948-55.

Chapter 3

Isometric Handgrip Echocardiography: A Non-invasive Stress Test to Assess Left Ventricular Diastolic Function*

T. Jake Samuel, Rhys Beaudry, Mark J. Haykowsky, Satyam Sarma, Suwon Park, Thomas Dombrowsky, Paul S. Bhella, and Michael D. Nelson (2017). Isometric Handgrip Echocardiography: A Non-invasive Stress Test to Assess Left Ventricular Diastolic Function. *Clin Cardiol*, 40(12): 1247-1255. DOI: 10.1002/clc.22818.

Introduction

Normal left ventricular (LV) diastole requires the coordination of several physiological processes which allow the heart to fill sufficiently under low filling pressures. As systole ends, LV elastic recoil and active relaxation gives rise to an abrupt decline in ventricular pressure until the mitral valve opens, and blood flows along a pressure gradient toward the apex. Upon pressure equilibration between the left atrium and the LV (i.e. diastasis), the final component of ventricular filling occurs when the atrium contracts and systole resumes. Derangement of any one of these components can result in a rise in LV filling pressure that is transmitted to the left atrium and pulmonary veins, and may be associated with pulmonary edema and dyspnea.

Doppler ultrasound has emerged as the clinical standard for measuring diastolic function, attributable to its wide accessibility, high temporal resolution and minimal risk (non-invasive). Indeed, Doppler ultrasound provides clear and useful estimates of early (E) and late (A) transmitral flow, tissue Doppler measurement of mitral annular velocity, (e' and a', respectively), and estimations of LV filling pressure (E/e')(1-3). In overt heart disease (i.e. acute myocardial infarction, cardiomyopathy, and heart failure with preserved and reduced ejection fraction), both E/A and E/e' predict all-cause mortality, cardiovascular death, and heart failure hospitalizations (4,5). However, when disease is less advanced (i.e. subclinical) and/or when the diagnosis remains equivocal, diastolic stress echocardiography may be indicated to differentiate cardiac *vs*. non-cardiac pathology.

Over the last several years, "diastolic stress testing" has emerged as a powerful tool to enhance detection of ischemia and/or document diastolic dysfunction as the etiological feature of exertional dyspnea. Ha *et al*. were among the first to combine supine bicycle exercise with

Doppler ultrasound (6), demonstrating the feasibility of this approach to discriminate cardiac *vs*. non-cardiac related exertional dyspnea. This approach has since been adopted by others (3,7-11). For example, Burgess *et al*. were one of the first to validate the use of cycle echocardiography with invasively measured LV filling pressures (3). Obokata *et al*. demonstrated the prognostic power of supine cycle echocardiography in differentiating heart failure with preserved ejection fraction (HFpEF) *vs.* non-cardiac dyspnea (7). Accordingly, cycle exercise echocardiography is now recommended by both the American and European Societies for Echocardiography for diastolic stress testing (12).

Cycle exercise echocardiography is not without limitation. Indeed, supine cycle exercise increases both respiratory and movement artifact, which are exacerbated by the increased body adiposity and poor acoustic window often found in clinical populations (13,14). In contrast, isometric handgrip exercise is a simple, well established, and highly robust tool that reproducibly increases LV afterload and myocardial oxygen demand (15) without movement or respiratory artifact. Moreover, isometric handgrip exercise has long been used during invasive assessment of LV filling pressures, providing robust differentiation between many patient groups, including those at risk for or with established heart failure (7,15,16).

Accordingly, we hypothesized that isometric handgrip echocardiography could be used to differentiate normal from abnormal diastolic function, while avoiding the limitations associated with dynamic whole-body exercise. To test this hypothesis, we first established the normal diastolic stress response to isometric handgrip in a group of healthy young volunteers. Then, we recruited a group of independently living seniors, with age-related diastolic dysfunction, to

determine if isometric handgrip echocardiography could differentiate normal from abnormal diastolic functional reserve.

Methods

Study Population

In order to establish the normative response to isometric handgrip echocardiography, we recruited a group of healthy young volunteers (20-32 years of age). None had any history of cardiovascular, metabolic or neurological disease, nor were they taking any medications other than oral contraceptives. With the normative response established, we then recruited a group of independently living seniors, with age-related diastolic dysfunction, to determine if isometric handgrip echocardiography could differentiate normal from abnormal diastolic functional reserve. Those with a LV ejection fraction <50%, atrial or ventricular arrhythmia, valvular disease (moderate or greater severity), or history of myocardial infarction were excluded. Some individuals had history of hypertension (n = 9) and hypercholesterolemia (n = 4). All participants were instructed to withdraw from any medication and/or supplements the day before testing. Additionally, all subjects presented to the lab after an overnight fast, having abstained from alcohol and caffeine for at least 24 hours.

Results were also compared to a single patient with clinically diagnosed NYHA Class III heart failure with preserved ejection fraction (HFpEF), recruited from the local Dallas-Fort Worth Community. To differentiate cardiac vs. non-cardiac related exertional dyspnea, this patient underwent invasive pulmonary artery capillary wedge pressure assessment at rest and during

low level upright cycle exercise (20 watts). To evaluate peak aerobic power, cardiopulmonary exercise stress testing was also performed on an upright cycle ergometer.

All subjects provided written informed consent before being enrolled to participate in the present study. The study was approved by the Institutional Review Board at the University of Texas at Arlington, and conformed to the standards set by the latest version of the *Declaration of Helsinki*.

Isometric Handgrip Echocardiography

Prior to data collection all participants' height and weight were measured using a dual functioning stadiometer and weighing scale (Health-O-Meter Professional, 500KL, Illinois, USA). Beat-by-beat arterial blood pressure was measured from a small finger cuff placed around the middle finger of the participants right hand (FinometerPRO, Finapres, Arnhem, The Netherlands), calibrated to an automated brachial artery blood pressure cuff (Welch Allyn, Connex Spot Monitor, 71WX-B, New York, USA). Heart rate was determined from the R-R intervals of a single-lead electrocardiogram (ECG, ADInstruments, MLA0313, Colorado, USA).

Two-dimensional transthoracic echocardiography with Doppler ultrasound was performed by an experienced certified sonographer using a commercially available ultrasound machine (Vivid S6, GE Vingmed Ultrasound, Horten, Norway) and a 2.5-MHz transducer. All subjects were studied in the left lateral position. A minimum of 5 consecutive cardiac cycles were collected and stored for offline analysis. From the apical window, standard 4-chamber volumetric images were obtained (17). Pulsed Doppler images were also obtained with the sample volume placed at the tips of the mitral valve leaflets, along with peak lateral annular tissue velocities

using the pulsed wave Doppler mode. All data were stored digitally, and measurements were made at the completion of each study.

After resting images were obtained, subjects performed three minutes of isometric handgrip exercise at 40% of their maximal voluntary contraction (MVC) determined prior to baseline imaging. Arterial blood pressure, heart rate and echocardiography data were recorded during the final minute of isometric handgrip exercise.

Data Analysis

Heart rate and blood pressure data were sampled at a rate of 1,000 Hz, recorded with a data-acquisition system (Powerlab 16/30, ADInstruments, Colorado, USA), and analyzed offline using associated software (LabChart Pro, ADInstruments, Colorado, USA). Hemodynamic and echocardiography data were time aligned using data markers. The product of heart rate and systolic pressure was used to calculate rate pressure product, and is referred to as myocardial oxygen demand throughout.

Echocardiography and Doppler data were analyzed offline using commercially available software (EchoPAC, version 113, GE Medical Systems). LV volumes were calculated and averaged over three cardiac cycles, according to the Simpsons monoplane method, in accordance with the current recommendations for quantification of LV volumes by two-dimensional echocardiography (17). Left atrial volumes were estimated using the area-length method using the 4-chamber image at end-systole (where the left atria is largest) (17). Stroke volume was determined as the difference between end-diastolic and end-systolic volumes, and used to calculate cardiac output and ejection fraction. Left ventricular wall thickness was calculated from

a mid-ventricular short axis image as previously described (17). Left ventricular mass was calculated according to the area-length method, as previously described (17).

Pulsed Doppler was used to quantify early and late diastolic inflow velocities. Tissue Doppler data were used to assess annular tissue velocities (lateral wall) during systole, early diastole, and late diastole. The ratio between early and late diastolic mitral inflow and LV lateral wall velocities were calculated as E/A and e'/a' ratios, respectively. The ratio between early diastolic mitral valve inflow velocity and early diastolic lateral wall tissue velocity (E/e' ratio) was calculated and used as a surrogate measure of diastolic filling pressure (6,7). All Doppler and two-dimensional data were analyzed and averaged over three cardiac cycles when possible.

Statistical analysis

All dependent variables were assessed for normal distribution and homoscedasticity using the Shapiro-Wilk test. In the young healthy population, changes from rest to isometric handgrip echocardiography were assessed using a paired samples *t*-test when parametric, while a two-way Wilcoxon-Mann-Whitney test was used for non-parametric data. In addition, the same statistical method was adopted to test for changes from rest to exercise in the asymptomatic elderly population as a whole. Non-responders and responders were compared for group and exercise main effects using a repeated measures ANOVA, followed by a Bonferroni *post-hoc* test if significant main effects were present. All statistical analyses were performed using GraphPad Prism (GraphPad Prism for Windows, Version 5.0.1, San Diego, California, USA). All data are expressed as mean ± SD unless otherwise stated, while statistical significance was considered when $P \leq 0.05$.

Results

Normative Data

In total, 19 healthy young volunteers participated in this study (*Table 1*). By design, all had a normal body mass index and were free of cardiovascular, metabolic or neurological disease. All had normal diastolic function at rest, with normal LV morphology and systolic function (*Table 1*).

Isometric handgrip echocardiography caused a significant increase in arterial blood pressure and heart rate (*Figure 1*), which was consistent across all subjects studied (*Table 1*). Despite this significant increase in LV afterload and myocardial oxygen demand, diastolic function was well preserved in these healthy normative subjects. In particular, the ratio of early mitral inflow velocity-to-early annular tissue velocity, a surrogate measure of left ventricular filling pressure, changed minimally from rest to exercise (ΔE/e': 0.56 ± 0.89).

Isometric Handgrip Echocardiography in the elderly

In total, 17 independently living seniors participated in this study (data presented in *Table 2*). As expected, some of the participants had a history of hypertension (*n* = 9) and hypercholesterolemia (*n* = 4). Likewise, we observed age-related impairments in diastolic function at rest; however, none had overt LV hypertrophy, or met clinical criteria for left ventricular diastolic dysfunction beyond that which occurs with healthy aging (18), and all had normal systolic function (*Table 2*).

Table 1. Normative demographic, hemodynamic and echocardiographic data at rest and in response to isometric handgrip echocardiography.

Demographics			
Age (years)	24 ± 4		
% of Female Participants	63		
Height (cm)	169.7 ± 7.2		
Weight (Kg)	70.4 ± 15.6		
BMI	24.3 ± 4.5		
BSA (m^2)	1.80 ± 0.20		
	Rest	**Isometric Handgrip**	**Δ Change**
Hemodynamics			
Heart Rate (bpm)	63 ± 10	88 ± 12	25 ± 12*
SBP (mmHg)	120 ± 8	151 ± 24	32 ± 20*
DBP (mmHg)	75 ± 6	99 ± 16	24 ± 16*
MAP (mmHg)	90 ± 6	116 ± 18	26 ± 17*
RPP (mmHg·bpm)	7553 ± 1170	13266 ± 2423	5713 ± 2514*
Left Ventricular Structure			
Diastolic Wall Thickness (cm)	0.80 ± 0.15	0.80 ± 0.13	0.00 ± 0.07
Systolic Wall Thickness (cm)	1.08 ± 0.14	1.08 ± 0.17	0.00 ± 0.12
LV Mass (g)	191.9 ± 63.4	-	-
LV Mass Index ($g \cdot m^2$)	104.7 ± 26.0	-	-
Left Ventricular and Atrial Volumes			
EDVi ($mL \cdot m^2$)	64.0 ± 13.0	62.1 ± 14.5	-1.8 ± 10.1
ESVi ($mL \cdot m^2$)	23.6 ± 7.1	22.9 ± 7.3	-0.7 ± 5.1
Stroke Index ($mL \cdot m^2$)	40.4 ± 7.1	39.3 ± 8.9	-1.2 ± 7.6
EF (%)	63.7 ± 5.2	63.6 ± 6.2	-0.1 ± 6.2
Cardiac Index ($L \cdot min^{-1} \cdot m^2$)	2.53 ± 0.38	3.41 ± 0.60	0.88 ± 0.61*
LA Volume (mL)	40.0 ± 11.8	-	-
LA Volume Index ($mL \cdot m^2$)	22.0 ± 5.4	-	-
Left Ventricular Doppler			
MV E Velocity ($m \cdot s^{-1}$)	0.83 ± 0.15	0.82 ± 0.16	-0.01 ± 0.09
MV Deceleration Time (ms)	174.3 ± 30.2	148.9 ± 35.7	-25.5 ± 31.8*
MV Deceleration Slope ($m \cdot s^2$)	5.1 ± 1.5	6.1 ± 2.3	1.0 ± 1.5*
MV A Velocity ($m \cdot s^{-1}$)	0.39 ± 0.09	0.62 ± 0.18	0.24 ± 0.14*
MV E/A Ratio	2.21 ± 0.42	1.38 ± 0.37	-0.83 ± 0.39*
LV Lateral s' Velocity ($m \cdot s^{-1}$)	0.10 ± 0.03	0.09 ± 0.03	0.00 ± 0.02
LV Lateral e' Velocity ($m \cdot s^{-1}$)	0.17 ± 0.04	0.15 ± 0.04	-0.02 ± 0.02*
LV Lateral a' Velocity ($m \cdot s^{-1}$)	0.06 ± 0.02	0.09 ± 0.02	0.03 ± 0.02*
LV e'/a' Ratio	3.13 ± 0.93	1.72 ± 0.50	-1.36 ± 0.81*
LV E/e' Ratio	5.18 ± 1.48	5.75 ± 1.67	0.56 ± 0.89*

*within group difference. BMI – body mass index, BSA – body surface area, SBP – systolic blood pressure, DBP – diastolic blood pressure, MAP – mean arterial pressure, RPP – rate pressure product, LA – left atrial, LV – left ventricle, EDVi – end-diastolic volume index, ESVi – end-systolic volume index, EF – ejection fraction, MV – mitral valve.

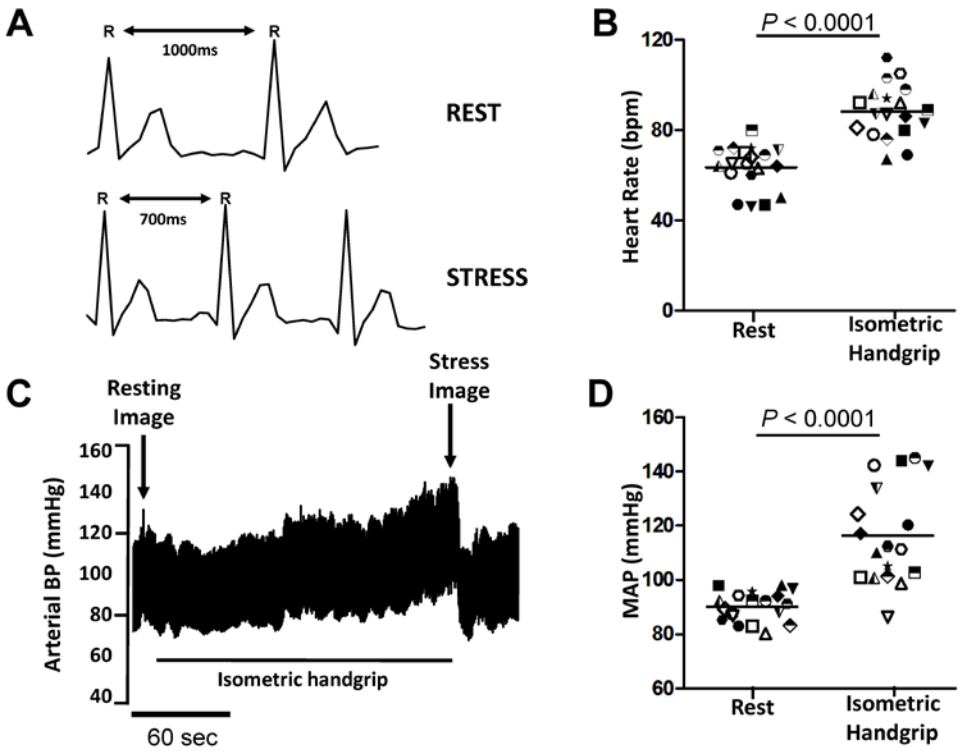

Figure 1. Representative heart rate and arterial blood pressure response to isometric handgrip echocardiography in young healthy individuals. **(A)** Shows a representative electrocardiogram tracing for a healthy young individual at rest and during isometric handgrip exercise stress at 40% MVC. **(B)** Average group heart rate response at rest and during isometric handgrip echocardiography. **(C)** Representative arterial blood pressure tracing at rest and during isometric handgrip echocardiography. **(D)** Average group mean arterial blood pressure response at rest and during isometric handgrip echocardiography. Grouped data shown as mean and 95% confidence intervals.

Similar to our normative data, isometric handgrip echocardiography resulted in a significant increase in arterial blood pressure and heart rate (*Table 2*). In contrast to our normative data however, the ΔE/e' ratio increased significantly from rest to exercise (2.29 ± 1.74, $P < 0.0001$), suggestive of an exercise induced increase in LV filling pressure. However, this response was not universal across all of the aging participants.

Table 2. Elderly demographic, hemodynamic and echocardiographic data at rest and in response to isometric handgrip echocardiography.

Demographics			
Age (years)	72 ± 6		
% of Female Participants	76		
Height (cm)	166.1 ± 9.3		
Weight (Kg)	74.7 ± 11.2		
BMI	27.0 ± 3.3		
BSA (m^2)	1.8 ± 0.2		
	Rest	**Isometric Handgrip**	**Δ Change**
Hemodynamics			
Heart Rate (bpm)	63 ± 7	82 ± 19	19 ± 16*
SBP (mmHg)	139 ± 17	180 ± 25	42 ± 17*
DBP (mmHg)	75 ± 6	91 ± 14	16 ± 14*
MAP (mmHg)	96 ± 8	121 ± 14	25 ± 11*
RPP (mmHg·bpm)	8764 ± 1664	14803 ± 3724	6034 ± 3081*
Left Ventricular Structure			
Diastolic Wall Thickness (cm)	0.86 ± 0.06	0.85 ± 0.07	-0.02 ± 0.06
Systolic Wall Thickness (cm)	1.37 ± 0.13	1.36 ± 0.12	-0.01 ± 0.15
LV Mass (g)	185.9 ± 27.1	-	-
LV Mass Index ($g \cdot m^2$)	101.8 ± 11.6	-	-
Left Ventricular and Atrial Volumes			
EDVi ($mL \cdot m^2$)	53.7 ± 6.5	57.3 ± 7.4	3.6 ± 4.6*
ESVi ($mL \cdot m^2$)	20.6 ± 3.1	24.0 ± 4.4	3.4 ± 2.9*
Stroke Index ($mL \cdot m^2$)	33.2 ± 4.6	33.3 ± 4.6	0.1 ± 3.6
EF (%)	61.6 ± 3.7	58.1 ± 4.2	-3.5 ± 3.6*
Cardiac Index ($L \cdot min^{-1} \cdot m^2$)	2.08 ± 0.34	2.72 ± 0.64	0.64 ± 0.47*
LA Volume (mL)	38.0 ± 9.8	-	-
LA Volume Index ($mL \cdot m^2$)	19.64 ± 7.35	-	-
Left Ventricular Doppler			
MV E Velocity ($m \cdot s^{-1}$)	0.66 ± 0.10	0.75 ± 0.20	0.09 ± 0.17*
MV Deceleration Time (ms)	197 ± 47	159 ± 37	-38 ± 62*
MV Deceleration Slope ($m \cdot s^2$)	3.5 ± 0.9	5.2 ± 2.5	1.7 ± 2.6*
MV A Velocity ($m \cdot s^{-1}$)	0.70 ± 0.26	0.90 ± 0.21	0.20 ± 0.21*
MV E/A Ratio	1.05 ± 0.38	0.82 ± 0.21	-0.23 ± 0.47
LV Lateral s' Velocity ($m \cdot s^{-1}$)	0.09 ± 0.03	0.08 ± 0.02	-0.01 ± 0.02
LV Lateral e' Velocity ($m \cdot s^{-1}$)	0.09 ± 0.03	0.08 ± 0.03	-0.01 ± 0.02*
LV Lateral a' Velocity ($m \cdot s^{-1}$)	0.11 ± 0.03	0.12 ± 0.04	0.01 ± 0.03*
LV e'/a' Ratio	0.94 ± 0.29	0.74 ± 0.31	-0.20 ± 0.30*
LV E/e' Ratio	7.55 ± 2.57	9.84 ± 3.00	2.29 ± 1.74*

*within group difference. BMI – body mass index, BSA – body surface area, SBP – systolic blood pressure, DBP – diastolic blood pressure, MAP – mean arterial pressure, RPP – rate pressure product, LA – left atrial, LV – left ventricle, EDVi – end-diastolic volume index, ESVi – end-systolic volume index, EF – ejection fraction, MV – mitral valve.

To explore this 'responder vs. non-responder' phenomenon further, we divided the elderly participants' according to their diastolic stress response during isometric handgrip echocardiography (*Figure 2*). Specifically, and in line with several recent cycle echocardiography publications (6,7), a "responder" was defined as someone who changed E/e' >1.5 with exercise stress. With this new definition, 6 elderly participants were found to be "non-responders" *versus* 11 elderly participants found to be "responders". Remarkably, both responders and non-responders had similar resting diastolic function (*Table 3*), and a similar rise in both heart rate and blood pressure (myocardial oxygen demand) with isometric handgrip (*Figure 2*). No differences in age were observed between the two groups (*Table 3*). Individual E/E' data are presented in Supplemental Figure 1.

Isometric Handgrip Echocardiography in HFpEF: A Case Study

To begin to establish the clinical significance of this novel diastolic stress test, isometric handgrip echocardiography was also performed in a 78 year-old female with NYHA Class III HFpEF (weight, 110 kg; height, 169 cm; VO_{2peak}, 10.6 $ml \cdot kg^{-1} \cdot min^{-1}$; LV ejection fraction, 58%; left atrial volume index, 30.5 mL/m^2). With mild upright cycle exercise (20 W), pulmonary artery capillary wedge pressure increased dramatically, from 10 mmHg at rest to 29 mmHg during exercise; characteristic of HFpEF exercise hemodynamics (7). With isometric handgrip echocardiography, E/e' changed by 6.7 (from 12.5 at rest to 19.2 with stress), reflecting changes in cardiac filling pressures seen with exercise.

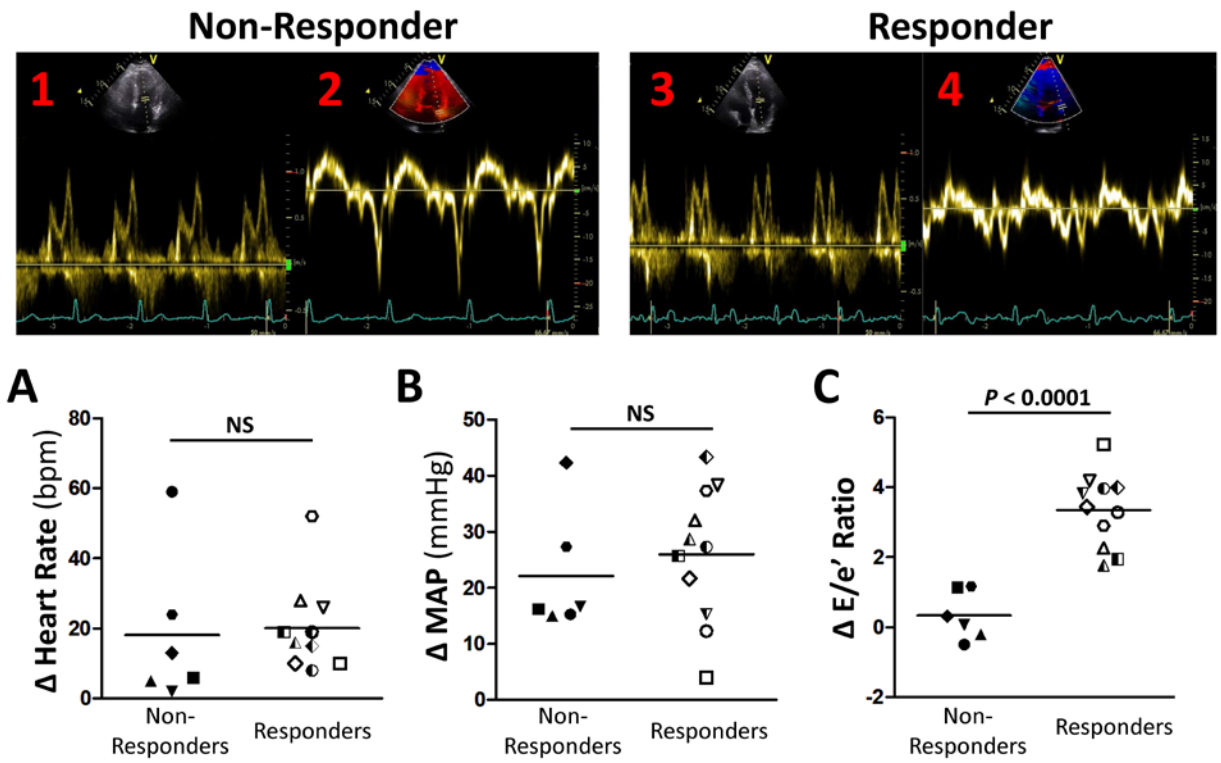

Figure 2. Example of a Doppler mitral inflow velocity tracing for a representative 'responder' at rest (**1**) and during isometric handgrip echocardiography at 40% MVC (**3**), along with tissue Doppler tracing from the lateral wall of the same individual during rest (**2**) and isometric handgrip echocardiography at 40% MVC 'responder' (**4**) during isometric handgrip at 40% MVC. Change in heart rate (**A**), mean arterial blood pressure (**B**) and left ventricular early mitral inflow velocity to

Reproducibility of Measures

To determine the reproducibility of the diastolic stress response, 6 elderly participants (3 non-responders and 3 responders) repeated isometric handgrip echocardiography on a separate visit. Upon re-testing, all 3 responders showed a similar rise in E/e' (3.9 *vs*. 4.0, visit 1 *vs*. visit 2) while E/e' remained <1.5 in the non-responders during the re-test visit (0.2 *vs*. 1.2, visit 1 *vs*. visit 2). The between day co-efficient of variation for the change in E/e', expressed in absolute terms, was 0.97 $\pm$ 0.74. Individual data are illustrated in Supplemental Figure 2.

Table 3. Demographic, hemodynamic, and echocardiographic data comparing 'non-responders' with 'responders' at rest and during isometric handgrip exercise.

	Non-Responders (*n* = 6)		**Responders (*n* = 11)**	
Demographics				
Age (years)	71 ± 7		73 ± 6	
% of Female Participants	100		64	
Height (cm)	158.8 ± 4.6		170.1 ± 8.9†	
Weight (Kg)	68.2 ± 6.6		78.2 ± 11.8	
BMI	27.1 ± 3.3		27.0 ± 3.4	
BSA (m^2)	1.70 ± 0.07		1.90 ± 0.17†	
	Rest	**Isometric Handgrip**	**Rest**	**Isometric Handgrip**
Hemodynamics				
Heart Rate (bpm)	61 ± 7	79 ± 25	64 ± 8	84 ± 16*
SBP (mmHg)	134 ± 22	168 ± 27*	141 ± 14	187 ± 23*
DBP (mmHg)	73 ± 6	90 ± 11*	76 ± 6	92 ± 16*
MAP (mmHg)	94 ± 10	116 ± 14*	98 ± 8	124 ± 13*
RPP (mmHg·bpm)	8229 ± 1779	13090 ± 3688*	9056 ± 1608	15737 ± 3559*
Left Ventricular Structure				
Diastolic Wall Thickness (cm)	0.85 ± 0.07	0.83 ± 0.04	0.87 ± 0.06	0.86 ± 0.08
Systolic Wall Thickness (cm)	1.38 ± 0.08	1.32 ± 0.09	1.36 ± 0.16	1.37 ± 0.13
LV Mass (g)	167.80 ± 20.83	-	195.81 ± 25.58†	-
LV Mass Index ($g \cdot m^2$)	98.54 ± 10.10	-	103.53 ± 12.45	-
LV and LA Volumes				
EDVi ($mL \cdot m^2$)	57.5 ± 7.3	62.2 ± 7.2*	51.7 ± 5.3	54.6 ± 6.3†
ESVi ($mL \cdot m^2$)	22.8 ± 3.6	27.2 ± 5.3*	19.4 ± 2.2†	22.3 ± 2.6*†
Stroke Index ($mL \cdot m^2$)	34.7 ± 5.6	35.0 ± 2.6	32.3 ± 3.9	32.3 ± 5.3
EF (%)	60.2 ± 5.2	56.6 ± 4.1	62.4 ± 2.7	58.9 ± 4.3*
Cardiac Index ($L \cdot min^{-1} \cdot m^2$)	2.11 ± 0.49	2.74 ± 0.79	2.06 ± 0.27	2.71 ± 0.58*
LA Volume (mL)	37.7 ± 14.2	-	38.2 ± 7.0	-
LA Volume Index ($mL \cdot m^2$)	21.93 ± 7.26	-	18.39 ± 7.43	-
LV Doppler				
MV E Velocity ($m \cdot s^{-1}$)	0.67 ± 0.13	0.64 ± 0.21	0.65 ± 0.09	0.82 ± 0.18*
MV Deceleration Time (ms)	192 ± 26	164 ± 35	200 ± 57	157 ± 40
MV Deceleration Slope ($m \cdot s^2$)	3.6 ± 0.8	4.0 ± 1.2	3.5 ± 1.0	5.8 ± 2.9*
MV A Velocity ($m \cdot s^{-1}$)	0.70 ± 0.31	0.86 ± 0.23	0.70 ± 0.23	0.93 ± 0.21*
MV E/A Ratio	1.11 ± 0.49	0.77 ± 0.23	1.01 ± 0.32	0.85 ± 0.21
LV Lateral s' Velocity ($m \cdot s^{-1}$)	0.08 ± 0.02	0.07 ± 0.02*	0.09 ± 0.03	0.08 ± 0.02
LV Lateral e' Velocity ($m \cdot s^{-1}$)	0.08 ± 0.02	0.07 ± 0.02	0.10 ± 0.03	0.09 ± 0.04*
LV Lateral a' Velocity ($m \cdot s^{-1}$)	0.10 ± 0.03	0.12 ± 0.05	0.11 ± 0.03	0.12 ± 0.04
LV e'/a' Ratio	0.85 ± 0.28	0.75 ± 0.38	0.99 ± 0.30	0.73 ± 0.29*
LV E/e' Ratio	8.42 ± 2.31	8.76 ± 2.12	7.08 ± 2.69	10.43 ± 3.33*

*within group difference; †between group differences. BMI – body mass index, BSA – body surface area, SBP – systolic blood pressure, DBP – diastolic blood pressure, MAP – mean arterial pressure, RPP – rate pressure product, LA – left atrial, LV – left ventricle, EDVi – end-diastolic volume index, ESVi – end-systolic volume index, EF – ejection fraction, MV – mitral valve.

Discussion

The data herein introduce a simple but effective diastolic stress test which could be easily implemented clinically as a noninvasive exertional diastolic discriminator. The major novel findings were three-fold: First, isometric handgrip echocardiography is associated with a robust increase in left ventricular afterload and myocardial oxygen demand, while maintaining an optimal acoustic window and limiting respiratory artifact. Second, in young healthy individuals, diastolic function is well-preserved in response to isometric handgrip echocardiography, establishing the normal healthy response. Third, isometric handgrip echocardiography is able to distinguish between a normal and abnormal diastolic stress response, in a group of seniors with age-related resting diastolic impairments, and a clinically stable well-characterized HFpEF patients with severe exercise intolerance (peak VO_2 36% lower than healthy age and sex-matched sedentary control).

Diastolic stress testing is becoming a popular noninvasive alternative to enhance detection of ischemia and/or document diastolic dysfunction. Seminal work by Ha *et al*. (6) were among the first to demonstrate the feasibility of using the change in E/e' in response to supine cycle exercise to discriminate cardiac *vs*. non-cardiac related exertional dyspnea. More recently, Obokata *et al*. demonstrated the prognostic power of supine cycle echocardiography in differentiating heart failure with preserved ejection fraction (HFpEF) *versus* non-cardiac dyspnea (7). Importantly, this study showed a strong relationship between the change in E/e' and invasively measured pulmonary capillary wedge pressures. Of note, the change in E/e' in "non-responders" from each of these studies, was less than 1.5. Despite its growing popularity however, cycle echocardiography has several important limitations which can limit its

application, especially in clinical populations. For example, resting image quality is often compromised by increased body adiposity, poor respiratory function and orthopedic challenges, and cycle exercise only exacerbates these limitations by increase respiratory and movement artifacts even during low intensity exercise.

In contrast to cycle exercise however, isometric handgrip exercise is associated with a marked increase in myocardial oxygen demand while avoiding respiratory and movement artifacts. Indeed, isometric handgrip exercise has been used in the clinical setting to elicit stress for close to a century (19). The sympathetic neural response to this form of exercise is well described (20), and related to local mechanical and chemical afferent stimuli, as well as central sympathetic outflow (21-25). As shown by our own data, these sympathetic stimuli result in formidable increases in both heart rate and arterial blood pressure. Here, we combined this well-established clinical approach with echocardiography in order to create a simple and effective stress echocardiography test. Whereas cycle exercise focuses largely on global oxygen demand (i.e. central and peripheral), we believe the unique afterload challenge caused by isometric handgrip produces a more "isolated" (i.e. central) diastolic stress. Indeed, the increase in end-systolic wall stress observed during isometric handgrip echocardiography in this study was entirely explained by a rise in arterial blood pressure (see *Supplemental Table*). This increase in afterload will result in a large infiltration of calcium in to the myocyte having a positive inotropic and chronotropic effect during systole, as reflected by the increase in heart rate and contractility (end-systolic elastance) in this study. However, the inability of the myocyte to efficiently sequestrate or remove the elevated levels of cytosolic calcium during diastole will result in prolonged actin-myosin cross-bridge formation and subsequently impair LV active relaxation

(26,27). The result of this delayed myocardial relaxation would be a stiffer LV giving rise to increased LV pressures.

To our knowledge, this is the first report using isometric handgrip echocardiography to non-invasively discriminate normal from abnormal diastolic function in healthy older individuals. We first established the "normative" response to this unique approach in a group of young healthy individuals. As expected, diastolic function was preserved in this cohort, despite a significant rise in left ventricular afterload and myocardial oxygen demand. That E/e' changed minimally (< 0.6) with isometric handgrip in this group, suggests that a healthy heart can, and should, compensate by maintaining the intraventricular pressure gradient.

To translate these normative data to a more at risk population, we studied a group of asymptomatic seniors (60 – 83 years of age), and a single patient with well-characterized HFpEF. As expected, the majority of the seniors studied showed evidence of resting grade 1 diastolic dysfunction (impaired relaxation), consistent with healthy aging (28). Despite this age-related change in diastolic function however, there was a heterogeneous response to isometric handgrip echocardiography. Specifically, in nearly two-thirds of seniors studied, E/e' changed > 1.5, suggestive of stress induced increase LV filling pressure (1-3,7,12). In contrast, the remaining subjects showed a minimal change in E/e' during isometric handgrip echocardiography (< 0.4), a finding comparable with our young normative data. That isometric handgrip echocardiography is reproducible, and mirrors the pattern of LV filling pressure changes during exercise in HFpEF, strongly supports the validity of our results. Taken together, these proof-of-concept data establish the clinical utility of this simple stress test for differentiating cardiac *vs*. non-cardiac pathology. Future work is warranted to determine the predictive value of this stress test.

Our ability to differentiate between “normal” and “abnormal” diastolic reserve is entirely consistent with previous invasive (7,15) and non-invasive diastolic stress testing protocols (6). The exact mechanism for this response however, remains to be elucidated. Importantly, these observations do not appear to be related to hemodynamic differences, as heart rate and arterial blood pressure (and thus myocardial oxygen demand) changed similarly in both responders and non-responders. Since isometric handgrip produces an “isolated” afterload challenge (similar to the original A.V Hill experiments (29)), it is interesting to speculate that the group differences observed herein, may be related to impaired intracellular calcium handling. Specifically, in a sick or failing myocardium (even one that is asymptomatic, as described herein), transient increases in intracellular calcium would lead to prolonged actin-myosin cross-bridge formation and increased myocardial stiffness.

Experimental Considerations.

The primary outcome measure in this study was E/e’, which is regarded as a surrogate measure of LV filling pressure (1-3). Gold-standard invasive pressure measurements are indeed warranted to confirm the present results; however, inter-individual changes in E/e’ are considered fairly robust and reflective of a true changes in LV filling pressure (7). In this initial clinical investigation, we chose to study asymptomatic seniors living independently in the community, as opposed to symptomatic patients with dyspnea, limiting the prognostic application of our results. However, the fact that we observed reproducible, within group differences (i.e. ‘responders’ *vs*. ‘non-responders’), supports the hypothesis that isometric handgrip echocardiography is a powerful discriminator of normal/abnormal diastolic dysfunction, even in subclinical populations. In addition, all data were obtained before and during

isometric handgrip exercise. Future studies should consider assessing diastolic function during post-exercise recovery to evaluate the sensitivity of this measurement to acute changes in physiological status. Lastly, this acute proof-of-concept study cannot provide any insight into the predictive potential of this stress test. Future longitudinal studies are therefore warranted to address this specific limitation.

Despite these limitations, these initial proof-of-concept data demonstrate the feasibility of isometric handgrip echocardiography as a simple and effective tool for evaluating diastolic function during simulated activities of daily living. Future studies are warranted to extend these observations to additional patient's further along the heart failure continuum (AHA/ACC class B and D heart failure).

Reference List

1. Nagueh SF, Appleton CP, Gillebert TC et al. Recommendations for the evaluation of left ventricular diastolic function by echocardiography. Eur J Echocardiogr 2009;10:165-93.
2. Nagueh SF, Middleton KJ, Kopelen HA, Zoghbi WA, Quinones MA. Doppler tissue imaging: a noninvasive technique for evaluation of left ventricular relaxation and estimation of filling pressures. J Am Coll Cardiol 1997;30:1527-33.
3. Burgess MI, Jenkins C, Sharman JE, Marwick TH. Diastolic stress echocardiography: hemodynamic validation and clinical significance of estimation of ventricular filling pressure with exercise. J Am Coll Cardiol 2006;47:1891-900.
4. Aljaroudi W, Alraies MC, Halley C et al. Impact of progression of diastolic dysfunction on mortality in patients with normal ejection fraction. Circulation 2012;125:782-8.
5. Okura H, Takada Y, Kubo T et al. Tissue Doppler-derived index of left ventricular filling pressure, E/E', predicts survival of patients with non-valvular atrial fibrillation. Heart 2006;92:1248-52.
6. Ha JW, Oh JK, Pellikka PA et al. Diastolic stress echocardiography: a novel noninvasive diagnostic test for diastolic dysfunction using supine bicycle exercise Doppler echocardiography. J Am Soc Echocardiogr 2005;18:63-8.
7. Obokata M, Kane GC, Reddy YN, Olson TP, Melenovsky V, Borlaug BA. The Role of Diastolic Stress Testing in the Evaluation for HFpEF:A Simultaneous Invasive-Echocardiographic Study. Circulation 2016.
8. Donal E, Lund LH, Oger E et al. Value of exercise echocardiography in heart failure with preserved ejection fraction: a substudy from the KaRen study. Eur Heart J Cardiovasc Imaging 2016;17:106-13.
9. Donal E, Thebault C, Lund LH et al. Heart failure with a preserved ejection fraction additive value of an exercise stress echocardiography. Eur Heart J Cardiovasc Imaging 2012;13:656-65.
10. Tartiere-Kesri L, Tartiere JM, Logeart D, Beauvais F, Cohen Solal A. Increased proximal arterial stiffness and cardiac response with moderate exercise in patients with heart failure and preserved ejection fraction. J Am Coll Cardiol 2012;59:455-61.
11. Talreja DR, Nishimura RA, Oh JK. Estimation of left ventricular filling pressure with exercise by Doppler echocardiography in patients with normal systolic function: a simultaneous echocardiographic-cardiac catheterization study. J Am Soc Echocardiogr 2007;20:477-9.
12. Mitter SS, Shah SJ, Thomas JD. A Test in Context: E/A and E/e' to Assess Diastolic Dysfunction and LV Filling Pressure. J Am Coll Cardiol 2017;69:1451-1464.
13. Haykowsky MJ, Brubaker PH, Morgan TM, Kritchevsky S, Eggebeen J, Kitzman DW. Impaired aerobic capacity and physical functional performance in older heart failure patients with preserved ejection fraction: role of lean body mass. J Gerontol A Biol Sci Med Sci 2013;68:968-75.
14. Upadhya B, Haykowsky MJ, Eggebeen J, Kitzman DW. Exercise intolerance in heart failure with preserved ejection fraction: more than a heart problem. J Geriatr Cardiol 2015;12:294-304.

15. Penicka M, Bartunek J, Trakalova H et al. Heart failure with preserved ejection fraction in outpatients with unexplained dyspnea: a pressure-volume loop analysis. J Am Coll Cardiol 2010;55:1701-10.
16. Yoshikawa T, Miyazaki T, Akaishi M, Ohnishi S, Handa S, Nakamura Y. Diastolic pressure-volume relationship during handgrip exercise in patients with coronary artery disease. Clin Cardiol 1991;14:743-8.
17. Lang RM, Badano LP, Mor-Avi V et al. Recommendations for cardiac chamber quantification by echocardiography in adults: an update from the American Society of Echocardiography and the European Association of Cardiovascular Imaging. J Am Soc Echocardiogr 2015;28:1-39 e14.
18. Redfield MM. Heart Failure with Preserved Ejection Fraction. N Engl J Med 2016;375:1868-1877.
19. Alam M, Smirk FH. Observations in man upon a blood pressure raising reflex arising from the voluntary muscles. J Physiol 1937;89:372-83.
20. Fisher JP, Young CN, Fadel PJ. Autonomic adjustments to exercise in humans. Compr Physiol 2015;5:475-512.
21. Mark AL, Victor RG, Nerhed C, Wallin BG. Microneurographic studies of the mechanisms of sympathetic nerve responses to static exercise in humans. Circ Res 1985;57:461-9.
22. Victor RG, Secher NH, Lyson T, Mitchell JH. Central command increases muscle sympathetic nerve activity during intense intermittent isometric exercise in humans. Circ Res 1995;76:127-31.
23. Victor RG, Vissing SF, Urias L, Scherrer U. Central Motor Command Activates Sympathetic Outflow to Skin during Static Exercise in Humans. Clin Res 1989;37:A524-A524.
24. Delaney EP, Greaney JL, Edwards DG, Rose WC, Fadel PJ, Farquhar WB. Exaggerated sympathetic and pressor responses to handgrip exercise in older hypertensive humans: role of the muscle metaboreflex. Am J Physiol Heart Circ Physiol 2010;299:H1318-27.
25. Ogoh S, Wasmund WL, Keller DM et al. Role of central command in carotid baroreflex resetting in humans during static exercise. J Physiol-London 2002;543:349-364.
26. Gwathmey JK, Copelas L, MacKinnon R et al. Abnormal intracellular calcium handling in myocardium from patients with end-stage heart failure. Circ Res 1987;61:70-6.
27. Hunter WC. Role of myofilaments and calcium handling in left ventricular relaxation. Cardiol Clin 2000;18:443-57.
28. Carrick-Ranson G, Hastings JL, Bhella PS et al. Effect of healthy aging on left ventricular relaxation and diastolic suction. Am J Physiol Heart Circ Physiol 2012;303:H315-22.
29. Hill AV. The Heat of Shortening and the Dynamic Constants of Muscle. Proceedings of the Royal Society B: Biological Sciences 1938;126:136-195.

Chapter 4

Diastolic Stress Testing: Similarities and Differences Between Isometric Handgrip and Cycle Echocardiography*

T. Jake Samuel, Rhys Beaudry, Mark J. Haykowsky, Satyam Sarma, and Michael D. Nelson (2018). Diastolic Stress Testing: Similarities and Differences Between Isometric Handgrip and Cycle Echocardiography. *J Appl Physiol*, 125 (2): 529-535. DOI: 10.1152/japplphysiol.00304.2018.

Introduction

Diastolic stress testing is recommended by the American Society of Echocardiography and the European Association of Cardiovascular Imaging for diagnosis of diastolic dysfunction, and for discriminating between cardiac and non-cardiac symptom-based pathology (1,2). Current guidelines recommend cycle echocardiography with Doppler ultrasound for assessment of early transmitral inflow (E), and early annular tissue velocities (e'), to non-invasively assess left ventricular filling pressures (3-5). Conventional cycle echocardiography has indeed proven to be a strong prognostic indicator in patients with unexplained dyspnea upon exertion (6,7), and for classification of heart failure with preserved ejection fraction (8).

Despite its promise however, diastolic stress testing using cycle echocardiography has several limitations. For example, the respiratory and movement artefacts associated with dynamic exercise will only be compounded by the limited acoustic windows expected in patient populations referred for diastolic stress testing (i.e. obese and elderly). While contrast enhanced echocardiography can improve endocardial border delineation, and systolic wall motion assessment, Doppler imaging is contraindicated in the presence of contrast because of the way the Doppler signal is artificially, and inconsistently, augmented (9). To overcome these limitations, our group recently established isometric handgrip echocardiography—which avoids respiratory and movement artifacts— as a powerful discriminator of subclinical diastolic dysfunction (10). It remains unclear however, how isometric handgrip echocardiography compares to conventional cycle echocardiography, for the purpose of diastolic stress testing.

While cycle echocardiography is a multi-system stressor, which presumably challenges the stiff ventricle by increasing cardiac preload, and elevating myocardial oxygen demand,

isometric handgrip uniquely challenges the heart by increasing cardiac afterload, with minimal changes in skeletal muscle metabolic demand. We hypothesized that, despite clear differences in hemodynamic stress, isometric handgrip echocardiography would similarly discriminate between normal and abnormal diastolic function, compared to cycle echocardiography.

Methods

Study Population

We recruited independently living seniors from the Dallas-Fort-Worth Community (***Table 1***). Those with a LV ejection fraction <50%, atrial or ventricular arrhythmia, valvular disease (moderate or greater severity), or history of myocardial infarction were excluded. All participants were instructed to withhold medications and/or supplements 24 hours prior to testing. All subjects attended the laboratory having fasted overnight and having abstained from alcohol and caffeine for at least 24 hours. All subjects provided written informed consent before being enrolled to participate in the present study, which was approved by the Institutional Review Board at the University of Texas at Arlington, and in accordance with the latest version of the *Declaration of Helsinki*.

Diastolic Stress Testing Protocols

All participants attended the laboratory on one occasion between 9am and 1pm having conformed to the dietary instructions listed above. Prior to data collection all participants' height and weight were measured using a dual functioning stadiometer and weighing scale (Health-O-Meter Professional, 500KL, Illinois, USA). A finger blood pressure cuff was placed around the participants right hand, middle finger for recording of beat-by-beat arterial blood pressure

(FinometerPRO, Finapres, Arnhem, The Netherlands), which was calibrated to an automated brachial artery blood pressure cuff (Welch Allyn, Connex Spot Monitor, 71WX-B, New York, USA). Heart rate was determined from the R-R intervals of a single-lead electrocardiogram (ECG, ADInstruments, MLA0313, Colorado, USA).

An experienced certified sonographer collected conventional two-dimensional and pulsed Doppler transthoracic echocardiography images using a commercially available ultrasound machine (Vivid S6, GE Vingmed Ultrasound, Horten, Norway) and a 2.5-MHz transducer. All subjects were studied in a supine left lateral position. A minimum of 5 consecutive cardiac cycles were collected and stored for *post-hoc* offline analysis. From the apical window, standard 4-chamber volumetric images were obtained (11). The sample volume was placed over the tips of the mitral valve leaflets and the lateral wall annulus of the pulsed Doppler images, for assessment of transmitral blood and lateral tissue velocities, respectively. All data were stored digitally and measurements were made at the completion of each study.

After resting images were obtained, subjects were familiarized with both isometric handgrip and cycle exercise. Once each participant was familiar with the stress protocol, they performed three minutes of isometric handgrip exercise at 40% of their maximal voluntary contraction (MVC, determined prior to baseline imaging), followed by a resting period before the commencement of three minutes of dynamic cycling at 20W. This level of exercise was chosen because it is sufficient to differentiate patients with cardiac and non-cardiac related dyspnea upon exertion (8,12-15). Handgrip exercise was performed using the left hand of every participant and always preceded cycle exercise in all participants to limit systemic carry-over effect of performing cycle exercise prior to handgrip exercise. Arterial blood pressure, heart rate

and echocardiography data were analyzed during the final minute of rest and both diastolic stress test protocols.

Data Analysis

Heart rate and blood pressure data were sampled at a rate of 1,000 Hz, recorded with a data-acquisition system (Powerlab 16/30, ADInstruments, Colorado, USA), and analyzed offline using associated software (LabChart Pro, ADInstruments, Colorado, USA). Hemodynamic and echocardiography data were time aligned using manually inserted data markers. The product of heart rate and systolic pressure was used to calculate rate pressure product, and is referred to as myocardial oxygen demand throughout this manuscript (16).

Conventional and Doppler echocardiography data were analyzed offline using commercially available software (EchoPAC, version 113, GE Medical Systems). LV volumes were calculated and averaged over three cardiac cycles where possible, according to the Simpsons monoplane method, in accordance with the current recommendations for quantification of LV volumes by two-dimensional echocardiography (11). Stroke volume was determined as the difference between end-diastolic and end-systolic volumes (EDV and ESV, respectively), and used to calculate cardiac output and ejection fraction. LV wall thickness was calculated as the average from both the septal and lateral wall from a mid-ventricular short axis image, and LV mass was calculated according to the area-length method, as previously described (11).

Pulsed Doppler was used to quantify early (E) and late (A) diastolic inflow velocities, in addition to the deceleration time and slope. Tissue Doppler data were used to assess annular tissue velocities (lateral wall) during systole (s'), early diastole (e'), and late diastole (a'). The ratio between early and late diastolic mitral inflow and LV lateral wall velocities were calculated as E/A

and e'/a' ratios, respectively. The ratio between early diastolic mitral valve inflow velocity and early diastolic lateral wall tissue velocity (E/e' ratio) was calculated and used as a surrogate measure of LV filling pressure (13,17). All Doppler and two-dimensional data were analyzed and averaged over three cardiac cycles where possible. Individuals who had a change in E/e' from rest to each stress protocol of >1.5 were defined as "responders" while individuals who demonstrated a change in E/e' <1.5 were "non-responders", which has previously been shown to represent a clinically significant elevation in LV filling pressures (13), and in line with our previous publication (10).

Statistical analysis

All dependent variables were tested for normality and homoscedasticity using the Shapiro-Wilk test. Changes from rest to isometric handgrip echocardiography and rest to cycle echocardiography were assessed using a two-way paired Student's *t*-test when normally distributed or the Wilcoxon signed-rank test when non-parametric. Furthermore, differences between the handgrip responses and cycle responses (Δ change during handgrip *vs*. Δ change during cycle) were assessed using a two-way paired Student's *t*-test or Wilcoxon signed-rank tests where appropriate. A *post hoc* power calculation determined that sufficient statistical power was achieved for detecting changes in E/e' from rest to both isometric handgrip and cycle exercise (both > 0.89). All statistical analyses were performed using SPSS (version 24 IBM SPSS Statistics, Armonk, NY). All data are expressed as mean ± SD unless otherwise stated, while statistical significance was considered when $P \leq 0.05$.

Results

Twelve older subjects with evidence of age-related diastolic dysfunction participated in this study (***Table 1***). Seven had history of hypertension and 3 had history of hypercholesterolemia.

Table 1. Demographic data for all study participants.

Subject Characteristics	Mean ± SD	Range
n	12	---
Age, years	71 ± 6	61 – 80
Female Sex, %	67	---
Height, cm	169 ± 9	157 – 187
Weight, Kg	76.8 ± 12.2	62.7 – 96.6
BMI, Kg/m^2	26.9 ± 3.5	20.2 – 33.4
BSA, m^2	1.87 ± 0.18	1.63 – 2.18
LV Diastolic Wall Thickness, cm	0.87 ± 0.06	0.77 – 0.96
LV Mass, g	188 ± 27	152 – 229
LV Mass Index, g/m^2	101 ± 11	86 - 122

BMI – body mass index; BSA – body surface area; LV – left ventricle.

Isometric Handgrip Echocardiography

Compared to rest, heart rate, LV end-diastolic volume, LV end-systolic volume, cardiac index, arterial blood pressure and myocardial oxygen demand were significantly higher, while LV ejection fraction was significantly lower, during isometric handgrip exercise (**Figure 1**). Early mitral inflow velocity (E) remained unchanged, while early diastolic annular tissue velocity (e') was significantly reduced, resulting in a significant increase in E/e' during isometric exercise (2.49 ± 1.46, **Figure 2**). Of note, in the absence of diastolic dysfunction, E/e' should not change with isometric handgrip exercise (10).

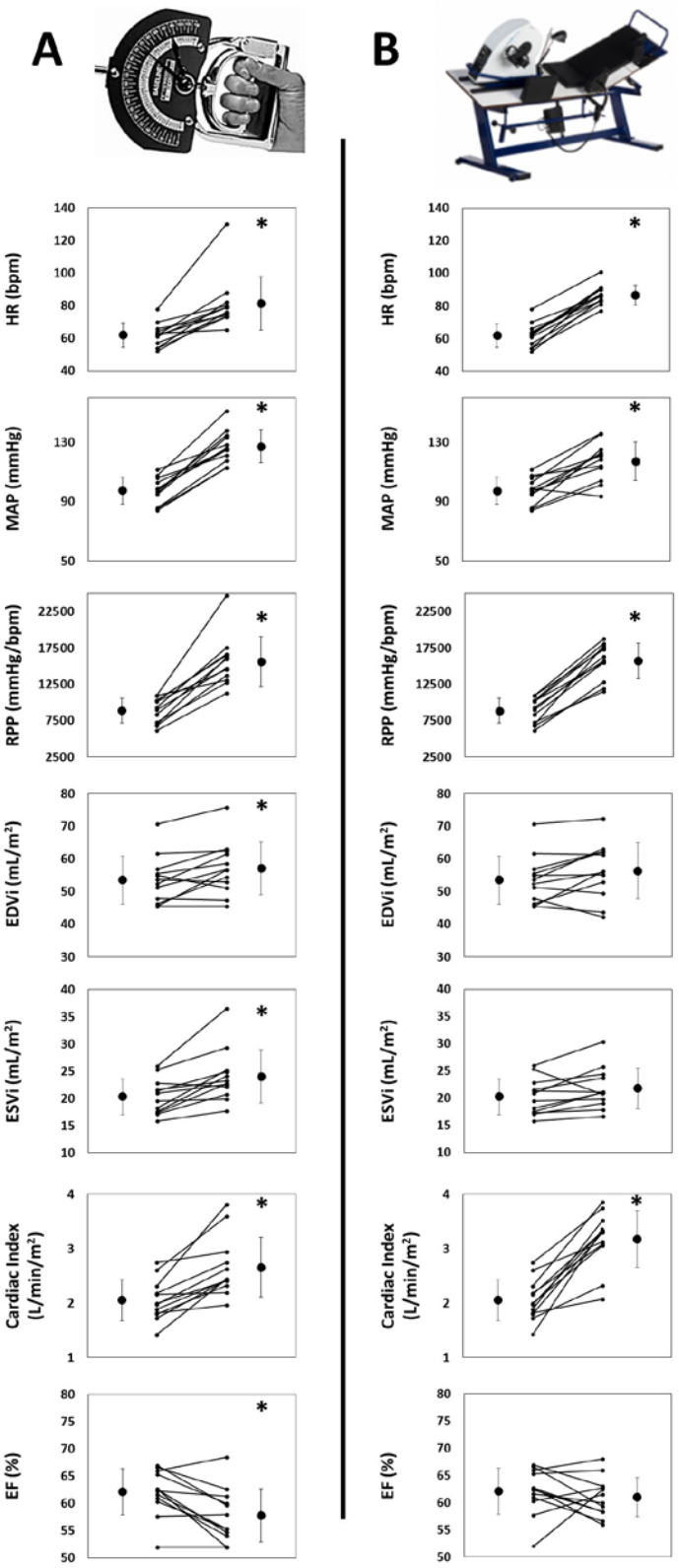

Figure 1. Hemodynamic responses to both isometric handgrip echocardiography **(A)** and conventional cycle echocardiography **(B)** in a population of asymptomatic elderly individuals. Despite, both diastolic stress tests resulting in similar increases in myocardial oxygen demand (rate pressure product; RPP), isometric handgrip echocardiography resulted in a greater increase in afterload stress (mean arterial pressure; MAP) compared to cycle exercise, while cycle exercise led to a greater increase in cardiac index. * - significant difference from rest ($P < 0.05$). HR – heart rate; EDVi – end-diastolic volume index; ESVi – end-systolic volume index; EF – ejection fraction.

Cycle Echocardiography

The hemodynamic response to conventional cycle echocardiography is illustrated in ***Figure 1*** and summarized in ***Table 2***. Compared to rest, neither LV end-diastolic volume nor end-systolic volume changed with cycle exercise (both $P > 0.05$), resulting in a similar stroke index. Accordingly, the large increase in cardiac index observed with cycle exercise (2.06 ± 0.37 L/min/m^2 *vs*. 3.18 ± 0.52 L/min/m^2, rest *vs*. cycle exercise; $P < 0.0001$) was therefore driven entirely by heart rate.

Early mitral inflow velocity (E) was significantly increased in all 12 subjects. The early diastolic annular tissue velocity (e') also rose significantly with cycle exercise, but the response was much more variable (6/12 increased). As a result, E/e' was also elevated with cycle exercise (ΔE/e': 2.09 ± 2.08; $P < 0.0001$). To help put these results into context, when young healthy subjects perform similar cycle exercise, early mitral inflow velocity also increases, but with a similar increase in e', resulting in a preservation of E/e' (data not shown).

Isometric Handgrip versus Cycle Echocardiography

Similarities and differences between isometric handgrip echocardiography and conventional cycle echocardiography are reported in ***Table 2***. Isometric handgrip elicited a greater increase in mean arterial blood pressure (30 *vs*. 20 mmHg, respectively, $P < 0.05$) compared to cycle exercise, resulting in a higher end-systolic volume index and a greater reduction in ejection fraction (both $P < 0.05$). Isometric handgrip also resulted in a marked reduction in e', while cycle exercise had an opposing response (Δe': -0.02 ± 0.02 m/s *vs*. 0.02 ± 0.02 m/s; $P < 0.001$). Despite these diverging diastolic stress responses, both stress tests resulted in similar changes in E/e' (ΔE/e': 2.49 ± 1.46 *vs*. 2.09 ± 2.08, handgrip *vs*. cycle; $P = 0.43$).

Table 2. Hemodynamic and left ventricular functional response of all participants to both isometric handgrip echocardiography and traditional cycle echocardiography.

	Isometric Handgrip Echocardiography			Cycle Echocardiography			
	Rest	**Stress**	**Δ Change**	**Rest**	**Stress**	**Δ Change**	**P-value**
Hemodynamics							
Heart Rate, bpm	62 ± 7	81 ± 16	19 ± 13	62 ± 7	87 ± 6	25 ± 6	0.14
Systolic BP, mmHg	142 ± 17	192 ± 18	50 ± 12	142 ± 17	181 ± 25	39 ± 18	0.06
Diastolic BP, mmHg	75 ± 7	94 ± 15	19 ± 15	75 ± 7	85 ± 10	10 ± 12	0.12
MAP, mmHG	97 ± 9	127 ± 11	30 ± 9	97 ± 9	117 ± 13	20 ± 12	0.046
RPP, mmHg/bpm	8854 ± 1708	15621 ± 3417	6766 ± 2881	8854 ± 1708	15720 ± 2426	6865 ± 1670	0.92
LV Volumes							
EDVi, mL/m^2	54 ± 7	57 ± 8	4 ± 5	54 ± 7	56 ± 9	3 ± 5	0.60
ESVi, mL/m^2	20 ± 3	24 ± 5	4 ± 3	20 ± 3	22 ± 4	2 ± 3	0.04
Stroke Index, mL/m^2	33 ± 5	33 ± 5	0 ± 4	33 ± 5	35 ± 6	1 ± 5	0.13
Cardiac Index, L/min/m^2	2.06 ± 0.37	2.66 ± 0.55	0.60 ± 0.42	2.06 ± 0.37	3.18 ± 0.52	1.12 ± 0.50	0.01
EF, %	62 ± 4	58 ± 5	-4 ± 4	62 ± 4	61 ± 4	-1 ± 5	0.02
LV Doppler							
MV E velocity, m/s	0.66 ± 0.10	0.77 ± 0.19	0.10 ± 0.17	0.66 ± 0.10	1.03 ± 0.15	0.37 ± 0.15	0.001
MV Deceleration Time, ms	204 ± 55	163 ± 42	-41 ± 72	204 ± 55	165 ± 18	-40 ± 61	0.90
MV Deceleration Slope, m/s^2	3.5 ± 1.0	5.3 ± 2.9	1.8 ± 3.0	3.5 ± 1.0	6.3 ± 1.3	2.8 ± 1.5	0.22
MV A velocity, m/s	0.68 ± 0.27	0.93 ± 0.20	0.27 ± 0.23	0.68 ± 0.27	0.94 ± 0.27	0.27 ± 0.21	0.78
MV E/A Ratio	1.12 ± 0.43	0.79 ± 0.22	-0.36 ± 0.56	1.12 ± 0.43	1.16 ± 0.25	0.03 ± 0.47	< 0.001
s' Velocity, m/s	0.09 ± 0.03	0.08 ± 0.02	-0.01 ± 0.02	0.09 ± 0.03	0.10 ± 0.02	0.01 ± 0.02	0.001
e' Velocity, m/s	0.10 ± 0.03	0.08 ± 0.03	-0.02 ± 0.02	0.10 ± 0.03	0.12 ± 0.03	0.02 ± 0.02	< 0.001
a' Velocity, m/s	0.11 ± 0.03	0.14 ± 0.04	0.02 ± 0.03	0.11 ± 0.03	0.14 ± 0.03	-0.01 ± 0.05	0.11
e'/a' Ratio	0.94 ± 0.32	0.68 ± 0.31	-0.18 ± 0.29	0.94 ± 0.32	0.89 ± 0.27	-0.19 ± 0.50	0.94
E/e' Ratio	7.38 ± 3.02	9.87 ± 3.17	2.49 ± 1.46	7.38 ± 3.02	9.47 ± 3.95	2.09 ± 2.08	0.43

P-value indicates significant difference between Δ change during isometric handgrip echocardiography compared to Δ change during cycle echocardiography. BP – blood pressure; MAP – mean arterial pressure; RPP – rate pressure product; EDVi – end-diastolic volume index; ESVi – end-systolic volume index; EF – ejection fraction; E – early mitral inflow velocity; MV – mitral valve; A – late/atrial mitral inflow velocity; E/A – early to late mitral inflow velocity; s' – systolic lateral annular tissue velocity; e' – early diastolic lateral annular tissue velocity; a' – late/atrial diastolic lateral annular tissue velocity; e'/a' – ratio between early and late lateral annular tissue velocity; E/e' – ratio between early diastolic mitral inflow velocity-to-early diastolic lateral annular tissue velocity.

Both stress tests also identified a similar number of "responders" and "non-responders", defined as a change in E/e' of >1.5 (9 *vs*. 8, handgrip *vs*. cycle). All other variables were not significantly different between the two diastolic stress tests (all $P > 0.05$).

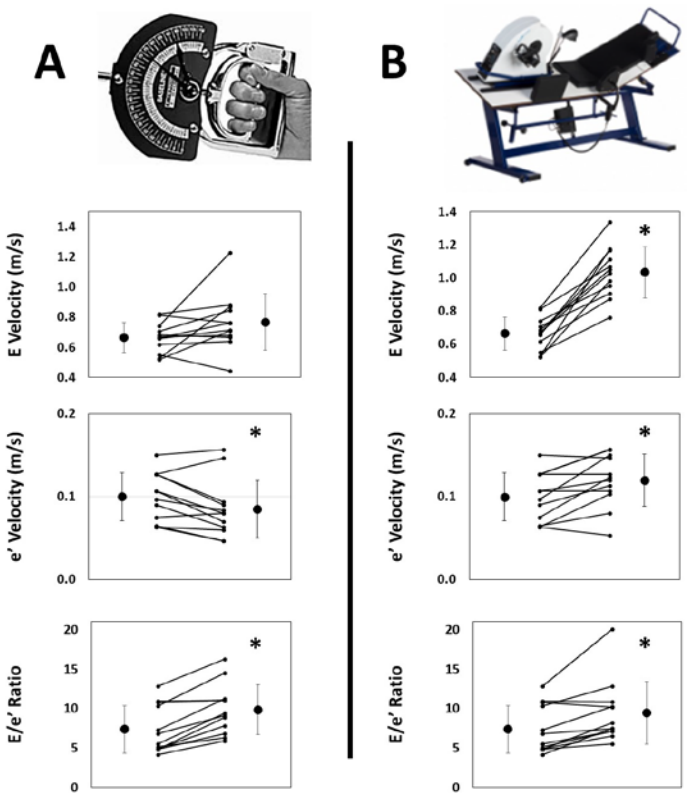

Figure 2. Left ventricular diastolic response to both isometric handgrip echocardiography **(A)** and conventional cycle echocardiography **(B)** in a population of asymptomatic elderly individuals. Both diastolic stress tests were equally as robust at causing an increase in E/e' ratio, however, the mechanism by which each response was achieved was different. Indeed, cycle exercise led to a significantly larger increase in early mitral inflow velocity (E velocity) compared to isometric handgrip echocardiography, while isometric handgrip elucidated a significant impairment in early myocardial tissue relaxation velocity (e' velocity). * - significant difference from rest ($P < 0.05$).

Discussion

The optimal exercise stress test to uncouple diastolic dysfunction remains uncertain. To our knowledge, this is the first study to compare the diastolic stress response between isometric handgrip exercise and conventional cycle exercise. The data suggest that isometric handgrip echocardiography is comparable to conventional cycle echocardiography, both in terms of its hemodynamic challenge and global diastolic stress response. Important differences in the way these two stress tests challenge left ventricular relaxation, particularly the way isometric handgrip preferentially targets early ventricular relaxation (e'), support

isometric handgrip echocardiography for diastolic stress testing. Moreover, that isometric handgrip echocardiography eliminates both respiratory and movement artifact, is low cost, and incredibly portable, support its immediate integration into routine echocardiography exams.

Diastolic stress testing provides valuable information regarding diagnosis of diastolic dysfunction and is able to discriminate between cardiac and non-cardiac heart failure pathology, beyond that of resting images alone (6-8). Indeed, diastolic stress testing is now recommended by both the American Society of Echocardiography and the European Association of Cardiovascular Imaging in individuals complaining of unexplained dyspnea upon exertion (1,2). To date, conventional cycle exercise is the most common method used to illicit exertional dyspnea symptoms and unmask elevated LV filling pressures and its non-invasive surrogate (6-8,13,17). However, this technique has several inherent limitations which are often exacerbated in clinical populations who stand to benefit from diastolic stress testing. Our group and others have previously shown that isometric handgrip exercise significantly elevates LV filling pressures and unmasks clinical (13,18,19) and pre-clinical (10) diastolic dysfunction. This is the first study to compare of the diastolic stress response between isometric handgrip echocardiography and conventional cycle echocardiography. The data suggest that both methods are equally robust at unmasking subclinical diastolic dysfunction, but highlight several key physiological mechanisms which differentiate the two diastolic approaches.

Conventional Cycle Echocardiography

Dynamic exercise is a multi-system stressor leading to increased cardiac output in order to meet whole body metabolic demand. This is often achieved by increasing heart rate and stroke volume (20). Here we found that cardiac index was significantly increased with cycle exercise; however, this response was solely driven by an increase in heart rate. The lack of an increase in stroke volume in response to supine cycle exercise supports some (21,22), but not all (23,24), previous investigations. In the supine position, end-diastolic volume is thought to be near maximum, before venous return is augmented by the respiratory and skeletal muscle pumps during exercise. That end-systolic volume is not reduced during this low-level exercise, may be second to the increase in arterial blood pressure (i.e. cardiac afterload) and/or reflect low sympathetic drive.

The mechanism leading to diastolic dysfunction during cycle exercise is likely multifactorial. That we observed a significant rise in myocardial oxygen demand (estimated by rate pressure product) may suggest an ischemic component. Diastole is indeed an energy dependent (25). It is also possible that the unique preload challenge that supine cycling represents is driving, at least in part, the observed increase in E/e'. In this scenario, a relative imbalance between cardiac preload (supine positioning, increased venous return, and reduced relaxation time) and LV compliance, leads to an increase in LV filling pressure. Interestingly, this phenomenon is not observed in young healthy subjects, but because of their faster LV relaxation rate, is not met with a clinically meaningful increase in E/e'.

Isometric Handgrip Echocardiography

Isometric handgrip stimulates the exercise pressor reflex, causing an increase neural sympathetic activity (26-30) and concomitant increase in arterial blood pressure, above that which is observed during low level cycle exercise. To support the ejection of blood during systole, this increased pressure load is met by an increase in intracellular calcium. The increased in intracellular calcium during systole must be either sequestrated back in to the sarcoplasmic reticulum or extruded from the myocyte during ventricular relaxation (31-33). Dysregulation of this processes, will lead to prolonged actin-myosin cross-bridge formation and impaired active relaxation (34,35); and thus increased LV stiffness and elevated LV filling pressures (36). The impaired early tissue relaxation seen in many of the individuals during isometric handgrip echocardiography in this study may therefore be related to an impairment in calcium handling. While we speculate that this impairment is directly related to myocardial oxygen demand, given the strikingly similar rate pressure products between handgrip and cycle exercise, we also cannot rule out changes in actin-myosin affinity with age/disease (37).

Isometric Handgrip versus Cycle Echocardiography

As hypothesized, both of the diastolic stress tests studied here resulted in a similar rise in E/e'. That the hemodynamic responses were also comparable was somewhat unexpected, but entirely consistent with previous observations (13,18,19). In light of these similarities, and the fact that isometric handgrip echocardiography avoids respiratory and movement artifact, is low cost (relative to a cycle ergometer), time effective, and extremely portable, we believe this stress test should be considered as an alternative to conventional

cycle echocardiography. It is intriguing to note the divergent responses each of the diastolic stress tests produced on early annular tissue relaxation velocity (i.e. e'). While e' remained unchanged with conventional cycle echocardiography, it was markedly reduced with isometric handgrip, highlighting the potential specificity of isometric handgrip echocardiography.

Experimental Considerations

This study is not without limitation. First, invasive LV filling pressures were not directly measured in this investigation, and therefore Doppler derived E/e' was considered as a surrogate measure of LV filling pressure (1,3,4). This assumption is however currently accepted and advocated for diastolic stress testing, making the present results clinically relevant. Second, this cross-sectional proof-of-concept study cannot provide insight into the predictive potential of these diastolic stress tests. Future longitudinal investigations are needed to address this specific limitation. Finally, while the elderly subjects studied in this investigation showed evidence of stress-induced LV diastolic dysfunction, these results will need to be extended to clinical populations suffering from unexplained dyspnea upon exertion and/or to help differentiate cardiac from non-cardiac pathology.

Conclusion

Taken together, the results show that isometric handgrip echocardiography is comparable to conventional cycle echocardiography, both in terms of their cardiac hemodynamic response and diastolic functional response. That isometric handgrip

echocardiography avoids many limitations associated with cycle exercise highlight its diagnostic potential. Future work is needed to translate these proof-of-concept data to clinical populations at risk for or with diagnosed heart failure.

Reference List

1. Nagueh SF, Smiseth OA, Appleton CP et al. Recommendations for the Evaluation of Left Ventricular Diastolic Function by Echocardiography: An Update from the American Society of Echocardiography and the European Association of Cardiovascular Imaging. Eur Heart J Cardiovasc Imaging 2016;17:1321-1360.
2. Nagueh SF, Smiseth OA, Appleton CP et al. Recommendations for the Evaluation of Left Ventricular Diastolic Function by Echocardiography: An Update from the American Society of Echocardiography and the European Association of Cardiovascular Imaging. J Am Soc Echocardiogr 2016;29:277-314.
3. Burgess MI, Jenkins C, Sharman JE, Marwick TH. Diastolic stress echocardiography: hemodynamic validation and clinical significance of estimation of ventricular filling pressure with exercise. J Am Coll Cardiol 2006;47:1891-900.
4. Nagueh SF, Appleton CP, Gillebert TC et al. Recommendations for the evaluation of left ventricular diastolic function by echocardiography. Eur J Echocardiogr 2009;10:165-93.
5. Nagueh SF, Middleton KJ, Kopelen HA, Zoghbi WA, Quinones MA. Doppler tissue imaging: a noninvasive technique for evaluation of left ventricular relaxation and estimation of filling pressures. J Am Coll Cardiol 1997;30:1527-33.
6. Aljaroudi W, Alraies MC, Halley C et al. Impact of progression of diastolic dysfunction on mortality in patients with normal ejection fraction. Circulation 2012;125:782-8.
7. Okura H, Takada Y, Kubo T et al. Tissue Doppler-derived index of left ventricular filling pressure, E/E', predicts survival of patients with non-valvular atrial fibrillation. Heart 2006;92:1248-52.
8. Borlaug BA, Jaber WA, Ommen SR, Lam CS, Redfield MM, Nishimura RA. Diastolic relaxation and compliance reserve during dynamic exercise in heart failure with preserved ejection fraction. Heart 2011;97:964-9.
9. Stewart MJ. Contrast echocardiography. Heart 2003;89:342-8.
10. Samuel TJ, Beaudry R, Haykowsky MJ et al. Isometric handgrip echocardiography: A noninvasive stress test to assess left ventricular diastolic function. Clin Cardiol 2017;40:1247-1255.
11. Lang RM, Badano LP, Mor-Avi V et al. Recommendations for cardiac chamber quantification by echocardiography in adults: an update from the American Society of Echocardiography and the European Association of Cardiovascular Imaging. J Am Soc Echocardiogr 2015;28:1-39 e14.
12. Borlaug BA, Kane GC, Melenovsky V, Olson TP. Abnormal right ventricular-pulmonary artery coupling with exercise in heart failure with preserved ejection fraction. Eur Heart J 2016;37:3293-3302.
13. Obokata M, Kane GC, Reddy YN, Olson TP, Melenovsky V, Borlaug BA. The Role of Diastolic Stress Testing in the Evaluation for HFpEF:A Simultaneous Invasive-Echocardiographic Study. Circulation 2016.

14. Borlaug BA, Nishimura RA, Sorajja P, Lam CS, Redfield MM. Exercise hemodynamics enhance diagnosis of early heart failure with preserved ejection fraction. Circ Heart Fail 2010;3:588-95.
15. Donal E, Thebault C, Lund LH et al. Heart failure with a preserved ejection fraction additive value of an exercise stress echocardiography. Eur Heart J Cardiovasc Imaging 2012;13:656-65.
16. Gobel FL, Norstrom LA, Nelson RR, Jorgensen CR, Wang Y. The rate-pressure product as an index of myocardial oxygen consumption during exercise in patients with angina pectoris. Circulation 1978;57:549-56.
17. Ha JW, Oh JK, Pellikka PA et al. Diastolic stress echocardiography: a novel noninvasive diagnostic test for diastolic dysfunction using supine bicycle exercise Doppler echocardiography. J Am Soc Echocardiogr 2005;18:63-8.
18. Penicka M, Bartunek J, Trakalova H et al. Heart failure with preserved ejection fraction in outpatients with unexplained dyspnea: a pressure-volume loop analysis. J Am Coll Cardiol 2010;55:1701-10.
19. Yoshikawa T, Miyazaki T, Akaishi M, Ohnishi S, Handa S, Nakamura Y. Diastolic pressure-volume relationship during handgrip exercise in patients with coronary artery disease. Clin Cardiol 1991;14:743-8.
20. Blomqvist CG, Saltin B. Cardiovascular adaptations to physical training. Annu Rev Physiol 1983;45:169-89.
21. Loeppky JA, Greene ER, Hoekenga DE, Caprihan A, Luft UC. Beat-by-beat stroke volume assessment by pulsed Doppler in upright and supine exercise. J Appl Physiol Respir Environ Exerc Physiol 1981;50:1173-82.
22. Stein RA, Michielli D, Fox EL, Krasnow N. Continuous ventricular dimensions in man during supine exercise and recovery. An echocardiographic study. Am J Cardiol 1978;41:655-60.
23. Poliner LR, Dehmer GJ, Lewis SE, Parkey RW, Blomqvist CG, Willerson JT. Left ventricular performance in normal subjects: a comparison of the responses to exercise in the upright and supine positions. Circulation 1980;62:528-34.
24. Thadani U, Parker JO. Hemodynamics at rest and during supine and sitting bicycle exercise in normal subjects. Am J Cardiol 1978;41:52-9.
25. Pouleur H. Diastolic dysfunction and myocardial energetics. Eur Heart J 1990;11 Suppl C:30-4.
26. Mark AL, Victor RG, Nerhed C, Wallin BG. Microneurographic studies of the mechanisms of sympathetic nerve responses to static exercise in humans. Circ Res 1985;57:461-9.
27. Victor RG, Secher NH, Lyson T, Mitchell JH. Central command increases muscle sympathetic nerve activity during intense intermittent isometric exercise in humans. Circ Res 1995;76:127-31.
28. Victor RG, Vissing SF, Urias L, Scherrer U. Central Motor Command Activates Sympathetic Outflow to Skin during Static Exercise in Humans. Clin Res 1989;37:A524-A524.

29. Delaney EP, Greaney JL, Edwards DG, Rose WC, Fadel PJ, Farquhar WB. Exaggerated sympathetic and pressor responses to handgrip exercise in older hypertensive humans: role of the muscle metaboreflex. Am J Physiol Heart Circ Physiol 2010;299:H1318-27.
30. Ogoh S, Wasmund WL, Keller DM et al. Role of central command in carotid baroreflex resetting in humans during static exercise. J Physiol-London 2002;543:349-364.
31. Kawase Y, Ly HQ, Prunier F et al. Reversal of cardiac dysfunction after long-term expression of SERCA2a by gene transfer in a pre-clinical model of heart failure. J Am Coll Cardiol 2008;51:1112-9.
32. Balderas-Villalobos J, Molina-Munoz T, Mailloux-Salinas P, Bravo G, Carvajal K, Gomez-Viquez NL. Oxidative stress in cardiomyocytes contributes to decreased SERCA2a activity in rats with metabolic syndrome. Am J Physiol Heart Circ Physiol 2013;305:H1344-53.
33. Berridge MJ, Bootman MD, Roderick HL. Calcium signalling: dynamics, homeostasis and remodelling. Nat Rev Mol Cell Biol 2003;4:517-29.
34. Gwathmey JK, Copelas L, MacKinnon R et al. Abnormal intracellular calcium handling in myocardium from patients with end-stage heart failure. Circ Res 1987;61:70-6.
35. Hunter WC. Role of myofilaments and calcium handling in left ventricular relaxation. Cardiol Clin 2000;18:443-57.
36. Arbab-Zadeh A, Dijk E, Prasad A et al. Effect of aging and physical activity on left ventricular compliance. Circulation 2004;110:1799-805.
37. Flagg TP, Cazorla O, Remedi MS et al. Ca2+-independent alterations in diastolic sarcomere length and relaxation kinetics in a mouse model of lipotoxic diabetic cardiomyopathy. Circ Res 2009;104:95-103.

Chapter 5

Diastolic dysfunction in women with ischemia but no obstructive coronary artery disease: Mechanistic insight from magnetic resonance imaging

Introduction

Ischemia with no obstructive coronary artery disease (INOCA) is prevalent in women, and is associated with increased risk of major adverse cardiovascular events, including heart failure with preserved ejection fraction (HFpEF) (1-5). The exact mechanism driving heart failure progression in INOCA however, remains to be elucidated. One common trait consistently observed in both populations is left ventricular diastolic dysfunction, characterized by impaired early diastolic relaxation and elevated end-diastolic pressures (6-11). Identifying the mechanism(s) causing diastolic dysfunction in INOCA is therefore critically import for understanding disease progression and developing new therapeutic interventions.

Multiple mechanisms have been implicated in the development of left ventricular diastolic dysfunction in INOCA, including: (1) ischemia-mediated impairment in active, energy-dependent, myocardial relaxation, (2) adverse left ventricular remodeling and diffuse myocardial fibrosis (i.e. reduced chamber compliance), and/or (3) impaired ventricular-arterial coupling, challenging calcium handling and compromising coronary blood flow. This study sought to determine which of these proposed mechanisms plays a dominant role in INOCA. To accomplish this goal, we performed comprehensive magnetic resonance imaging (MRI) to evaluate left ventricular diastolic function, myocardial perfusion reserve, left ventricular tissue properties, and aortic stiffness.

Methods

Study Population

Sixty-five women with INOCA from the Women's Ischemia Syndrome Evaluation – Heart Failure with Preserved Ejection Fraction (WISE-HFpEF) study (NCT02582021), enrolled between October 2015 - June 2019, were considered for the current investigation. INOCA was defined as having signs and symptoms of ischemia but <50% coronary artery stenosis confirmed by angiography, as previously described (12). Twelve reference control women were also studied to establish the range of normal. Control women had no symptoms, risk factors for, or evidence of, ischemic heart disease; confirmed by a standardized 12-lead treadmill stress test (13). All study subjects provided written informed consent prior to evaluation, and the study protocol was approved by the Institutional Review Board at Cedars-Sinai Medical Center.

Magnetic resonance imaging protocol

Magnetic resonance imaging was performed on a 3.0T scanner (Siemens Healthineers, Erlangen, Germany), with electrocardiogram-gating and a phase-array surface coil (CP Body Array Flex; Siemens Healthineers). Heart rate and blood pressure were measured and recorded throughout the study.

Left ventricular mass, volume and function were assessed using a series of short-axis steady-state free-precession cine images spanning the entire left ventricle, along with 2- and 4-chamber long-axis images. Typical cine imaging parameters were as follows: 8mm slice

thickness, 40° flip angle, 0mm gap, 1.34mm x 1.34mm x 8mm voxel size, 155mm x 224mm matrix, 25 cardiac phases, 11 segments, 10 heartbeats/slice.

To assess mitral inflow velocities in diastole, a single through-plane phase-contrast image at the level of the mitral valve leaflets was acquired (VENC 150, repetition time 10 ms, echo time 1.9 ms, 20° flip angle, slice thickness 8 mm, 256mm x 256mm matrix, bandwidth 1240 Hz/pixel, 25 images per cardiac cycle).

To assess aortic pulse wave velocity (aPWV), two separate through-plane phase-contrast images were acquired: (1) at the level of the ascending aorta, and (2) ~10 cm distal, along the descending aorta. Typical image parameters include: VENC 150 cm/s, repetition time 10 ms, echo time 1.9 ms, 20° flip angle, slice thickness 8mm, 256mm x 256mm matrix, bandwidth 1240 Hz/pixel, 25 images per cardiac cycle). The distance between the ascending and descending images was manually determined from a sagittal image of the aortic arch.

To challenge the myocardial oxygen supply-demand relationship, participants performed 5-7 minutes of continuous isometric handgrip exercise, at 30% of maximal voluntary contraction, using an MRI compatible handgrip dynamometer (Smedley, Stoelting Company, Wood Dale, Illinois). Left ventricular volume and function during handgrip was assessed by repeating the 2- and 4-chamber long-axis images, together with a mid-ventricular short-axis image. Individuals with an insufficient increase in the hemodynamic stress associated with isometric handgrip (defined as Δ heart rate <10 bpm and Δ mean arterial pressure <10 mmHg) were not considered for rest-stress handgrip comparisons.

Basal, mid and distal short-axis first-pass myocardial perfusion images were acquired under resting conditions and in response to intra-venous adenosine (140 µg/kg/min over ~4 min; Adenoscan, Astellas Pharma US, Inc., Northbrook, IL) infusion, with use of a gadolinium-based contrast agent (0.05 mmol/kg Gadavist, Bayer HealthCare Pharmaceuticals) also administered intravenously (at 4 mL/s) as previously described (14,15). Imaging parameters for first-pass perfusion imaging were as follows: gradient echo–EPI hybrid sequence, relaxation time per slice was 134.8 ms, echo time 0.94 ms, bandwidth 1240 Hz/pixel, readout flip angle 43°, slice thickness 8 mm, image matrix 155mm x 224mm pixels, in-plane resolution 1.34mm x 1.34mm x 8mm^2, parallel imaging (GRAPPA) factor 2, imaging 3 slices every heartbeat. If peak stress heart rate exceeded 120 bpm, 2 slices were obtained during stress first-pass imaging with exclusion of the distal left ventricular slice.

Prior to first-pass perfusion imaging, a mid-ventricular short-axis T1 relaxation image (vendor provided MOLLI 5[3]3) was acquired in mid-diastole for assessment of native myocardial T1 relaxation time (imaging parameters: 35° flip angle, repetition time 2.7 ms, echo time 1.1 ms, slice thickness: 8 mm, in-plane resolution 1.4 mm x 1.8 mm^2, parallel imaging [GRAPPA] factor 2). Following first-pass perfusion imaging, an additional 0.1 mmol/kg of gadolinium contrast was administered (total gadolinium dose 0.2 mmol/kg), and after waiting 12 minutes, post-contrast mid-ventricular short axis T1 imaging was repeated.

Analysis of magnetic resonance images

All image analysis was performed using commercially available software (CVI[42] version 5.6.8; Circle Cardiovascular Imaging Inc., Calgary, AB, Canada). Resting left ventricular mass and volumes were measured using the method of disks by manually tracing the endocardial and epicardial boarders, of the short-axis series, at end-diastole and end-systole. For rest-handgrip comparisons, left ventricular volumes were assessed using the biplane method by manually delineating the endocardial boarder, of the 2- and 4-chamber images, at end-diastole and end-systole. Left ventricular mass and volumes were indexed to body surface area. End-systolic elastance was calculated as (0.9 x peak brachial systolic blood pressure)/end-systolic volume and effective arterial elastance was calculated as (0.9 x peak brachial systolic blood pressure)/stroke volume (16). Rate pressure product was calculated as the product of peak brachial systolic blood pressure and heart rate, and referred to as a surrogate measure of myocardial oxygen demand throughout (17).

Left ventricular circumferential and longitudinal strain and strain rates were assessed by myocardial feature tracking, as previously described (18). Briefly, the endocardial and epicardial boarders were manually traced at end-diastole, on both short-axis and long-axis cine images, before applying the feature tracking algorithm across the remaining cardiac phases. Short-axis slices close to luminal obliteration (lumen diameter <2cm), and slices which included left ventricular outflow tract, were excluded as previously described (18). Patients with insufficient tracking quality were excluded from the final analyses.

The distance between ascending and distal portion of descending aorta were measured between the precise locations where the through-plane phase-contrast images were collected using an oblique sagittal image through the thoracic aorta. The aortic transit time was calculated as the average time difference between the systolic upslope of the ascending and descending aortic flow curves. aPWV was calculated as the distance between the ascending and descending aorta, divided by the transit time between the two aortic locations.

Myocardial perfusion reserve index (MPRI) was calculated as the average relative upslope from the three first-pass perfusion images collected during adenosine stress divided by the average relative upstroke from the three resting images, normalized to the basal slice blood pool upslopes at rest and during stress, respectively (14).

Statistical analyses

All statistical analyses were performed using SPSS (version 25 IBM SPSS Statistics, Armonk, NY). Homoscedasticity and normal distributions were confirmed by the Shapiro-Wilk test. Cross-sectional resting group differences and patient characteristics between women with INOCA and controls were assessed by independent Student's t-test. To test the hypothesis that coronary vascular dysfunction is the primary mechanism driving left ventricular diastolic function in INOCA, women with INOCA were sub-divided by low (<1.84) and high (≥1.84) MPRI, based on previous investigations (14,19). Cross-sectional group differences at rest, and patient characteristics, were assessed by one-way ANOVA for

normally distributed variables and the Kruskal-Wallis test for non-parametric variables. LSD post-hoc corrections were performed for variables with significant group main effects. Assessment of group differences in dependent variables in response to handgrip exercise were performed using repeated-measures ANOVA. To test the hypothesis that ventricular-arterial uncoupling is the primary mechanism driving diastolic dysfunction in INOCA, the INOCA group were sub-divided by the median aPWV, with low aPWV being defined as <7.4 m/s and high aPWV as ≥7.4 m/s. Cross-sectional resting group differences and patient characteristics between controls and INOCA with low and high aPWV were assessed by one-way ANOVA for normally distributed variables and the Kruskal-Wallis test for non-parametric variables, with LSD post-hoc correction. Pearson's and Spearman's correlations were used to assess correlations between parametric and non-parametric dependent variables, respectively. Strong correlations were considered when r ≥0.5, whereas moderate correlations were considered when r ≥0.3. Categorical variables were summarized using counts and percentages and compared using the Chi-squared test. All parametric data are expressed as means ± SD, and non-parametric as median (inter-quartile range). Statistical significance was accepted at $P \leq 0.05$.

Results

A total of 65 women with INOCA, and 12 reference controls, were enrolled in this investigation. Subject characteristics are depicted in ***Table 1***. INOCA subjects were of a similar

age, body mass index and body surface area as reference controls but had a greater number of cardiovascular risk factors. Left ventricular mass, indexed to body surface area, tended to be higher in the INOCA women (40.3 ± 3.5 g/m^2 vs. 44.0 ± 6.4 g/m^2, control vs. INOCA, respectively; P = 0.058); with no other observed difference in LV morphology between groups (***Table 1***).

Consistent with previous reports from our group, early diastolic circumferential strain rate was reduced in women with INOCA (***Figure 1A***), compared to reference controls, as was early diastolic longitudinal strain rate, and the ratio between early mitral inflow-and-early diastolic strain rate (**Table 1**). To explore the determinants of diastolic dysfunction, we then evaluated three potential mechanisms: (a) coronary vascular dysfunction and associated oxygen supply-demand mismatch, (b) adverse left ventricular remodeling and diffuse myocardial fibrosis, and/or (c) impaired ventricular-arterial coupling.

Table 1. Baseline characteristics and left ventricular function in women with INOCA and controls.

	Control (n = 12)	**INOCA (n = 65)**	**P-value**
Anthropometrics and Hemodynamics			
Age (years)	50 ± 5	55 ± 11	0.14
Height (cm)	161 ± 6	161 ± 10	0.82
Weight (kg)	69.2 ± 8.9	71.2 ± 15.2	0.65
BMI (kg/m^2)	26.7 ± 3.7	27.9 ± 6.7	0.54
BSA (m^2)	1.73 ± 0.11	1.74 ± 0.18	0.84
SBP (mmHg)	114 ± 15	120 ± 14	0.20
DBP (mmHg)	64 ± 11	63 ± 10	0.79
MAP (mmHg)	81 ± 10	82 ± 9	0.66
Medical History			
Hypertension n (%)	0 (0)	19 (29)	**0.03**
Diabetes n (%)	0 (0)	2 (3)	0.54
Hypercholesteremia n (%)	1 (8)	8 (12)	0.71
LV Mass & Volumes			
EDVi (mL/m^2)	64 ± 8	68 ± 10	0.18
ESVi (mL/m^2)	23 ± 6	25 ± 6	0.28
SVi (mL/m^2)	41 ± 4	43 ± 6	0.24
EF (%)	64 ± 5	63 ± 5	0.62
E_{es} (mmHg/mL)	2.69 ± 0.74	2.60 ± 0.72	0.69

E_a (mmHg/mL)	1.48 ± 0.35	1.48 ± 0.32	0.98
E_{es}/E_a	0.57 ± 0.13	0.59 ± 0.14	0.65
COi (L/min/m^2)	2.6 ± 0.3	2.70 ± 0.49	0.35
LV Mass Index (g/m^2)	40.3 ± 3.5	44.0 ± 6.4	0.06
Concentricity (g/mL)	0.63 ± 0.06	0.65 ± 0.10	0.59
LA Volume Index (mL/m^2)	36.1 ± 4.2	35.8 ± 6.7	0.89
LV Strain and Strain Rate			
Circumferential Strain (%)	-24.8 ± 1.67	-24.3 ± 2.5	0.51
Circumferential Systolic SR (/s)	-1.14 ± 0.15	-1.13 ± 0.19	0.84
Circumferential Early Diastolic SR (/s)	1.61 ± 0.33	1.36 ± 0.31	**0.02**
Circumferential Late Diastolic SR (/s)	0.70 ± 0.17	0.74 ± 0.21	0.51
Longitudinal Strain (%)	-21.6 ± 2.4	-20.9 ± 2.6	0.42
Longitudinal Systolic SR (/s)	-0.98 ± 0.18	-0.93 ± 0.31	0.57
Longitudinal Early Diastolic SR (/s)	1.23 ± 0.36	1.06 ± 0.25	**0.04**
Longitudinal Late Diastolic SR (/s)	0.88 ± 0.22	0.83 ± 0.23	0.52
Mitral Inflow			
E Velocity (ml/s)	298 ± 66	307 ± 92	0.75
A Velocity (ml/s)	219 ± 40	234 ± 91	0.60
E/A Ratio	1.39 ± 0.35	1.53 ± 0.88	0.60
E/e'sr Ratio (from circumferential)	192 ± 40	228 ± 56	**0.05**
E/e'sr Ratio (from longitudinal)	275 ± 111	302 ± 106	0.44
Myocardial Tissue Characteristics and Perfusion Reserve			
Native T1 (ms)	1246 ± 38	1253 ± 72	0.75
Post-Contrast T1 (ms)	456 ± 24	446 ± 59	0.61
ECV (%)	29.0 ± 1.9	28.0 ± 3.2	0.38
MPRI	1.89 ± 0.29	1.72 ± 0.30	0.08
Aortic Stiffness			
aPWV (m/s)	6.1 ± 1.5	8.1 ± 3.2	**0.05**

INOCA – ischemia but no obstructive coronary artery disease; BMI – body mass index; BSA – body surface area; SBP – systolic blood pressure; DBP – diastolic blood pressure; MAP – mean arterial pressure; LV – left ventricular; EDVi – end-diastolic volume index; ESVi – end-systolic volume index; SVi – stroke index; EF – ejection fraction; E_{es} – end-systolic elastance; E_a – effective arterial elastance; COi – cardiac index; LA – left atrial; SR – strain rate; E Velocity – early mitral inflow velocity; A Velocity – late mitral inflow velocity; E/e'SR – ratio between early mitral inflow velocity and early diastolic strain rate; ECV – extracellular volume; MPRI – myocardial perfusion reserve index; aPWV – aortic pulse wave velocity. Mean ± SD.

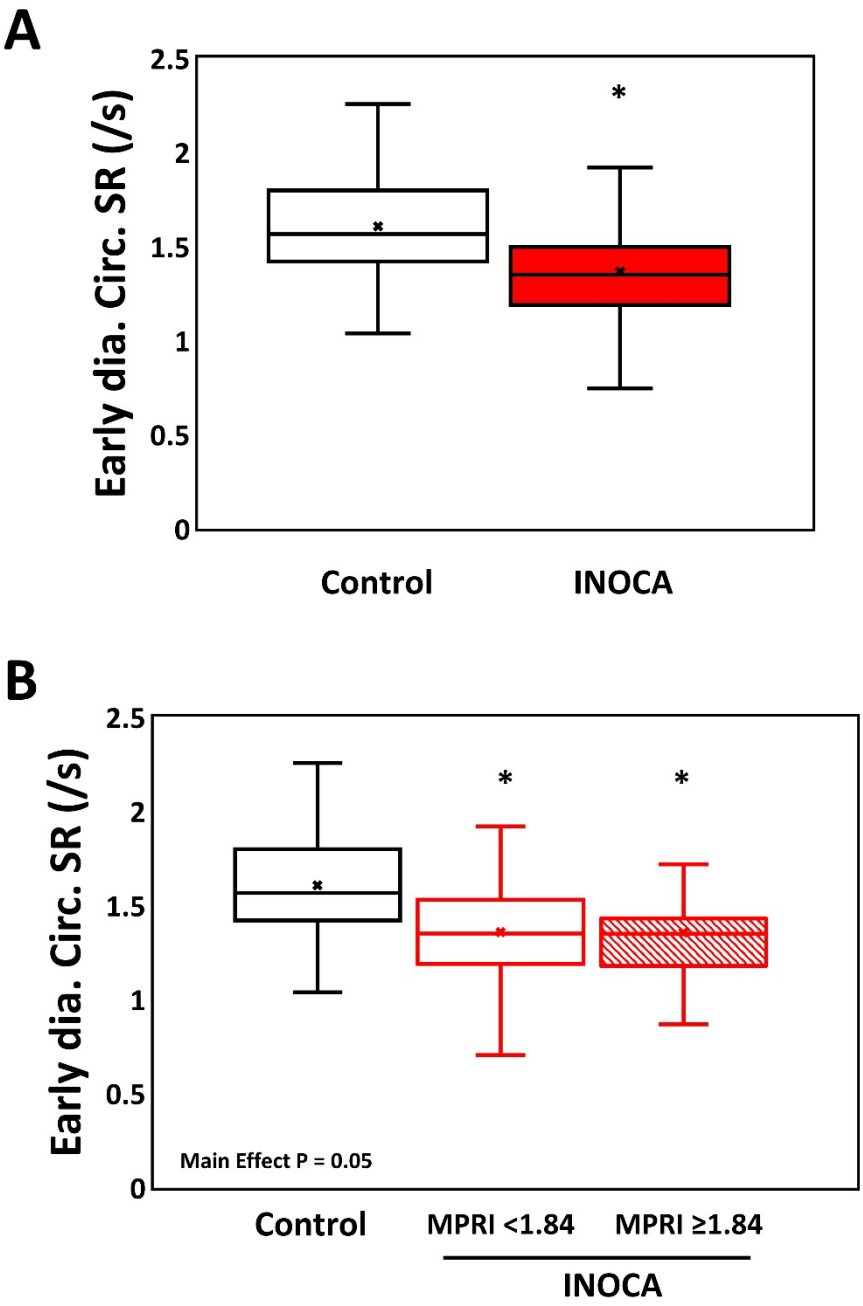

Figure 1. Left ventricular early diastolic circumferential strain rate is reduced in women with INOCA compared to reference controls (**A**). However, this impairment was not exacerbated by splitting the women with INOCA by low and high myocardial perfusion reserve index (MPRI; **B**). * - indicated significantly different from controls ($P < 0.05$).

Coronary vascular dysfunction

To test the coronary vascular dysfunction hypothesis, we first evaluated left ventricular diastolic function in women with INOCA grouped by either low (<1.84; n = 41) or high (≥1.84; n = 22) MPRI, compared to reference controls. Two women with INOCA did not receive adenosine and therefore were not considered for this analysis. Participant characteristics and resting cardiovascular measures did not differ between women with INOCA grouped by MPRI (***Table 2***). While early diastolic circumferential strain rate remained lower in INOCA compared to controls, having a lower MPRI did not exacerbate diastolic dysfunction in INOCA (***Figure 1B***).

To further explore whether coronary vascular dysfunction contributes to diastolic dysfunction in INOCA, a subset of participants performed isometric handgrip exercise. Women with INOCA remained sub-divided by MPRI. The rest-handgrip response is summarized in ***Table 3***. By design, isometric handgrip increased heart rate and arterial blood pressure in all groups (exercise main effect $P < 0.001$), despite a small but significant elevation in resting heart rate (group main effect $P = 0.015$) and blood pressure (group main effect $P < 0.001$) in the INOCA group with low MPRI. Consistent with the physiologic stress response, all three groups shared a similar increase in single point end-systolic elastance, effective arterial elastance, cardiac index, late diastolic circumferential and longitudinal strain rate, and longitudinal systolic strain rate (all $P < 0.001$). In contrast to our hypothesis however, no stress induced group differences were observed in left ventricular early diastolic relaxation, regardless of grouping variable.

Table 2. Left ventricular morphology and resting function in INOCA women with low and high MPRI and reference controls.

	Control (n = 12)	INOCA (n = 63)		P-value
		MPRI < 1.84 (n = 41)	MPRI ≥ 1.84 (n = 22)	
Anthropometrics and Hemodynamics				
Age (years)	50 ± 5	56 ± 11	53 ± 9	0.17
Height (cm)	161 ± 6	160 ± 11	161 ± 8	0.88
Weight (kg)	66.8 (65.0,76.4)	74.4 (64.2,82.4)	61.2 (57.4,75.2)†	**0.04**
BMI (kg/m^2)	27.3 (23.1,29.0)	28.3 (24.2,33.2)	25.1 (21.6,27.9)†	**0.04**
BSA (m^2)	1.73 ± 0.11	1.77 ± 0.20	1.68 ± 0.13	0.14
SBP (mmHg)	114 ± 15	120 ± 14	120 ± 13	0.41
DBP (mmHg)	64 ± 11	65 ± 10	59 ± 10	0.11
MAP (mmHg)	81 ± 10	83 ± 10	80 ± 8	0.28
Medical History				
Hypertension n (%)	0 (0)	11 (27)	6 (27)	**0.02**
Diabetes n (%)	0 (0)	1 (2)	1 (5)	0.23
Hypercholesteremia n (%)	1 (8)	5 (12)	3 (13)	**0.01**
LV Mass & Volumes				
EDVi (mL/m^2)	64 ± 8	67 ± 11	71 ± 9	0.09
ESVi (mL/m^2)	23 ± 6	25 ± 6	27 ± 5	0.16
SVi (mL/m^2)	41 ± 4	42 ± 7	44 ± 6	0.21
EF (%)	64 ± 5	64 ± 5	62 ± 4	0.56
E_{es} (mmHg/mL)	2.69 ± 0.74	2.67 ± 0.77	2.48 ± 0.63	0.57
E_a (mmHg/mL)	1.48 ± 0.35	1.49 ± 0.34	1.47 ± 0.27	0.97
E_{es}/E_a	0.56 (0.44,0.68)	0.56 (0.50,0.65)	0.58 (0.53,0.68)	0.52
COi (L/min/m^2)	2.56 ± 0.32	2.71 ± 0.48	2.69 ± 0.54	0.63
LV mass index (g/m^2)	40 ± 4	43 ± 6	45 ± 4	0.08
Concentricity index (g/mL)	0.63 ± 0.06	0.66 ± 0.10	0.64 ± 0.09	0.56
LA Volume Index (mL/m^2)	36 ± 4	36 ± 7	36 ± 6	0.99
LV Strain and Strain Rate				
Circumferential Strain (%)	-25.0 (-26.2,-23.0)	-24.4 (-26.2,-22.8)	-24.2 (-25.1,-22.6)	0.45
Circumferential Systolic SR (/s)	-1.14 ± 0.15	-1.13 ± 0.20	-1.15 ± 0.17	0.88
Circumferential Early Diastolic SR (/s)	1.61 ± 0.33	1.36 ± 0.33*	1.35 ± 0.27*	**0.05**
Circumferential Late Diastolic SR (/s)	0.70 ± 0.17	0.78 ± 0.20	0.70 ± 0.23	0.24
Longitudinal Strain (%)	-21.5 ± 2.4	-21.0 ± 3.0	-20.8 ± 1.7	0.71
Longitudinal Systolic SR (/s)	-0.93 (-0.99,-0.88)	-0.98 (-1.08,-0.87)	-0.92 (-0.97,-0.85)	0.16
Longitudinal Early Diastolic SR (/s)	1.23 ± 0.36	1.07 ± 0.24	1.03 ± 0.25	0.11
Longitudinal Late Diastolic SR (/s)	0.88 ± 0.22	0.87 ± 0.24	0.79 ± 0.19	0.37
Mitral Inflow				
E Velocity (ml/s)	298 ± 66	303 ± 101	313 ± 79	0.87
A Velocity (ml/s)	222 (186,256)	229 (194,273)	195 (143,267)	0.39
E/A Ratio	1.33 (1.13,1.51)	1.38 (0.81,1.74)	1.45 (1.16,2.38)	0.35
E/e'sr Ratio (from circumferential)	192 ± 40	223 ± 60	234 ± 50	0.13
E/e'sr Ratio (from longitudinal)	238 (202,320)	279 (215,329)	312 (244,410)	0.15
Myocardial Tissue Characteristics and Perfusion Reserve				
Native T1 (ms)	1246 ± 38	1255 ± 53	1257 ± 75	0.76
Post-Contrast T1 (ms)	456 ± 24	443 ± 58	451 ± 53	0.73
ECV (%)	29.0 ± 1.9	28.0 ± 3.1	28.0 ± 3.1	0.67
MPRI	1.89 ± 0.29	1.53 ± 0.17	2.06 ± 0.16	By Design
Aortic Stiffness				

aPWV (m/s)	6.6 (5.2,6.9)	7.7 (5.9,8.8)	6.9 (5.9,8.1)	0.05

INOCA – ischemia but no obstructive coronary artery disease; MPRI – myocardial perfusion reserve index; BMI – body mass index; BSA – body surface area; SBP – systolic blood pressure; DBP – diastolic blood pressure; MAP – mean arterial pressure; LV – left ventricular; EDVi – end-diastolic volume index; ESVi – end-systolic volume index; SVi – stroke index; EF – ejection fraction; E_{es} – end-systolic elastance; E_a – effective arterial elastance; COi – cardiac index; LA – left atrial; SR – strain rate; E Velocity – early mitral inflow velocity; A Velocity – late mitral inflow velocity; E/e'SR – ratio between early mitral inflow velocity and early diastolic strain rate; ECV – extracellular volume; aPWV – aortic pulse wave velocity. Mean ± SD. * - indicates significantly different from control, $P < 0.05$. † - indicates significantly different from INOCA with low MPRI, $P < 0.05$.

To further explore whether coronary vascular dysfunction contributes to diastolic dysfunction in INOCA, a subset of participants performed isometric handgrip exercise. Women with INOCA remained sub-divided by MPRI. The rest-handgrip response is summarized in ***Table 3***. By design, isometric handgrip increased heart rate and arterial blood pressure in all groups (exercise main effect $P < 0.001$), despite a small but significant elevation in resting heart rate (group main effect $P = 0.015$) and blood pressure (group main effect $P < 0.001$) in the INOCA group with low MPRI. Consistent with the physiologic stress response, all three groups shared a similar increase in single point end-systolic elastance, effective arterial elastance, cardiac index, late diastolic circumferential and longitudinal strain rate, and longitudinal systolic strain rate (all $P < 0.001$). In contrast to our hypothesis however, no stress induced group differences were observed in left ventricular early diastolic relaxation, regardless of grouping variable.

Table 3. Cardiovascular response to isometric handgrip stress in INOCA women with low and high MPRI and reference controls.

	Control (n = 7)		INOCA (n = 30)				Group	Time	Group x Time
			MPRI < 1.84 (n = 21)		MPRI ≥ 1.84 (n = 9)				
	Rest	IsoHG	Rest	IsoHG	Rest	IsoHG			
Hemodynamics									
HR (bpm)	56 ± 7	66 ± 9	63 ± 7	79 ± 9	58 ± 7	71 ± 7	**0.02**	**<0.001**	0.07
SBP (mmHg)	106 ± 7	124 ± 7	116 ± 11	136 ± 12	114 ± 11	129 ± 13	**0.001**	**<0.001**	0.26
DBP (mmHg)	62 ± 7	78 ± 10	67 ± 10	83 ± 12	60 ± 10	69 ± 10	**0.008**	**<0.001**	0.08
MAP (mmHg)	77 ± 4	93 ± 6	84 ± 9	101 ± 11	78 ± 8	89 ± 9	**0.001**	**<0.001**	**0.05**
LV Volumes									
EDVi (mL/m^2)	63 ± 10	63 ± 9	61 ± 12	61 ± 13	61 ± 9	59 ± 9	0.72	0.94	0.48
ESVi (mL/m^2)	22 ± 6	23 ± 5	22 ± 7	22 ± 8	21 ± 5	22 ± 5	0.80	0.21	0.76
SVi (mL/m^2)	41 ± 6	40 ± 7	40 ± 9	38 ± 10	40 ± 7	38 ± 6	0.83	0.07	0.82
EF (%)	65 ± 5	64 ± 7	64 ± 8	63 ± 10	65 ± 6	64 ± 4	0.97	0.10	0.99
E_{es} (mmHg/mL)	2.57 ± 0.54	2.88 ± 0.50	2.95 ± 1.15	3.50 ± 1.28	2.92 ± 0.66	3.28 ± 0.77	0.65	**<0.001**	0.63
E_a (mmHg/mL)	1.33 ± 0.18	1.63 ± 0.31	1.58 ± 0.53	2.04 ± 1.05	1.57 ± 0.46	1.82 ± 0.33	0.60	**<0.001**	0.77
E_{es}/E_a	0.54 ± 0.12	0.59 ± 0.16	0.58 ± 0.22	0.65 ± 0.37	0.55 ± 0.15	0.57 ± 0.12	0.89	0.11	0.92
COi (L/min/m^2)	2.30 ± 0.34	2.62 ± 0.48	2.50 ± 0.59	2.84 ± 1.01	2.28 ± 0.38	2.65 ± 0.32	0.27	**<0.001**	0.70
LV Strain and Strain Rate									
CS (%)	-23.1 ± 2.4	-22.2 ± 1.8	-23.2 ± 3.0	-22.4 ± 3.2	-24.2 ± 2.1	-25.1 ± 3.3	0.49	0.30	0.30
CSRs (/s)	-0.97 ± 0.10	-0.95 ± 0.12	-0.97 ± 0.19	-1.06 ± 0.34	-1.20 ± 0.29	-1.09 ± 0.17	0.30	0.70	0.27
CSRe (/s)	1.51 ± 0.28	1.35 ± 0.31	1.42 ± 0.33	1.31 ± 0.57	1.42 ± 0.59	1.47 ± 0.38	0.94	0.73	0.83
CSRa (/s)	0.66 ± 0.21	0.65 ± 0.12	0.66 ± 0.29	0.89 ± 0.28	0.73 ± 0.38	0.92 ± 0.41	0.66	**0.004**	0.13
LS (%)	-21.1 ± 1.9	-20.9 ± 1.7	-19.8 ± 2.9	-20.5 ± 3.4	-21.5 ± 2.4	-20.9 ± 1.9	0.63	0.74	0.39
LSRs (/s)	-0.92 ± 0.11	-0.90 ± 0.11	-0.90 ± 0.14	-0.98 ± 0.19	-0.96 ± 0.09	-1.08 ± 0.17	0.36	**0.003**	0.19
LSRe (/s)	1.20 ± 0.09	1.20 ± 0.27	1.01 ± 0.27	1.01 ± 0.34	0.96 ± 0.27	0.81 ± 0.10	0.15	0.09	0.31
LSRa (/s)	0.81 ± 0.14	0.87 ± 0.22	0.74 ± 0.28	0.96 ± 0.47	0.78 ± 0.21	0.94 ± 0.21	0.98	**0.001**	0.39

INOCA – ischemia but no obstructive coronary artery disease; MPRI – myocardial perfusion reserve index; HR – heart rate; SBP – systolic blood pressure; DBP – diastolic blood pressure; MAP – mean arterial pressure; LV – left ventricular; EDVi – end-diastolic volume index; ESVi – end-systolic volume index; SVi – stroke index; EF – ejection fraction; E_{es} – end-systolic elastance; E_a – effective arterial elastance; COi – cardiac index; CS – circumferential strain; CSRs - circumferential systolic strain rate; CSRe – circumferential early diastolic strain rate; CSRa – circumferential late diastolic strain rate; LS – longitudinal strain; LSRs – longitudinal systolic strain rate; LSRe – longitudinal early diastolic strain rate; LSRa – longitudinal late diastolic strain rate. Mean ± SD.

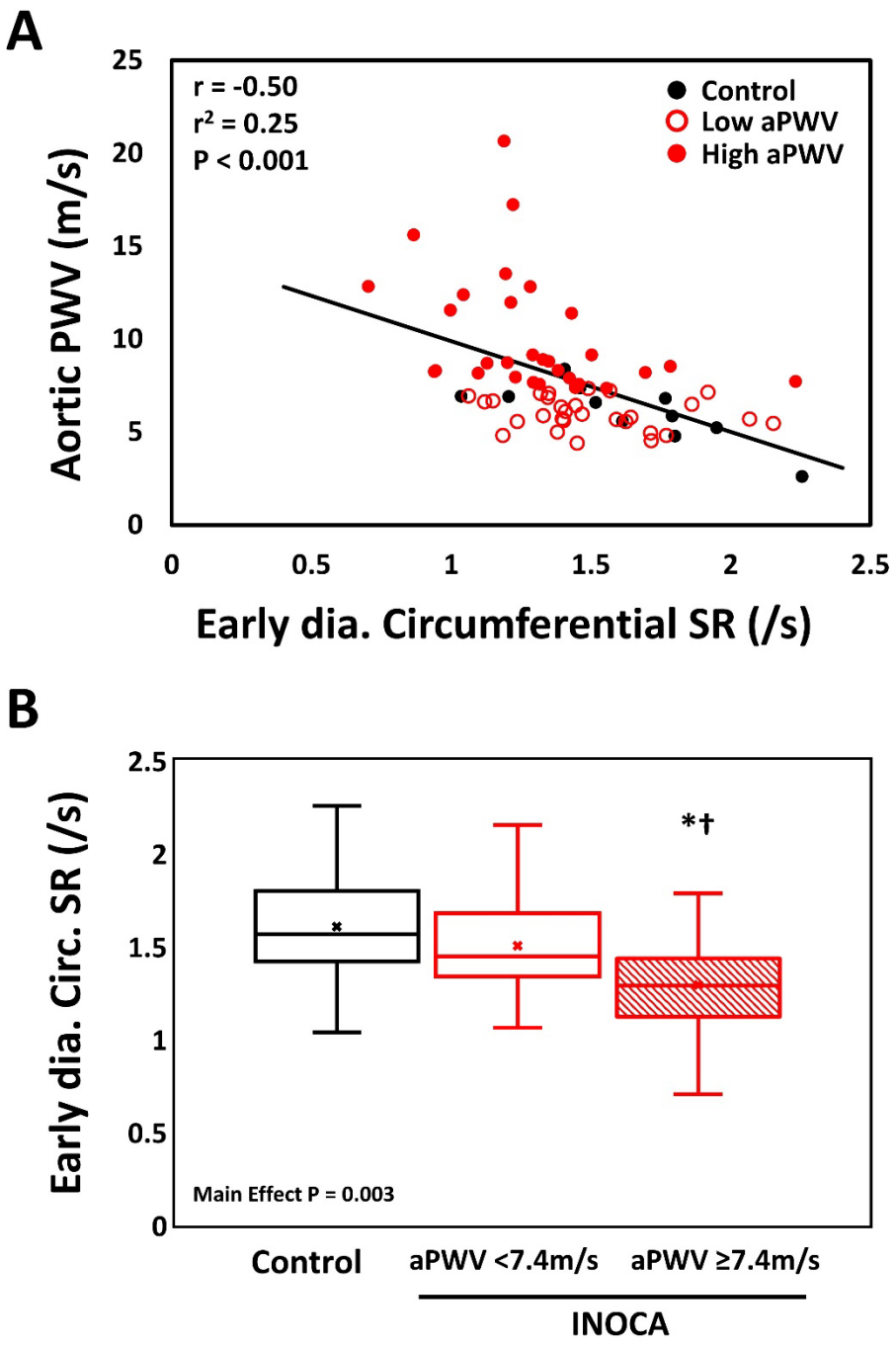

Figure 2. Aortic pulse wave velocity (aPWV) is inversely correlated with left ventricular early diastolic circumferential strain rate in all three groups (**A**). INOCA women with high aPWV have significantly lower left ventricular early diastolic circumferential strain rate compared to INOCA women with low aPWV and reference controls (**B**). * - indicated significantly different from controls ($P < 0.01$); † - indicates significantly different from INOCA women with low aortic pulse wave velocity ($P < 0.05$).

Adverse left ventricular remodeling and diffuse myocardial fibrosis

To test the hypothesis that diastolic dysfunction in INOCA is associated with diffuse myocardial fibrosis, we measured both native T1 and post-contrast T1, in order to assess myocardial tissue properties and calculate ECV. Compared to reference controls, women with INOCA had similar native T1 (1246 ± 38 ms vs. 1253 ± 72 ms, control vs. INOCA, respectively; P = 0.75) and calculated ECV (29.0 ± 1.9% vs. 28.0 ± 3.2%, control vs. INOCA, respectively; P = 0.38). Likewise, we observed no difference in LV concentricity between INOCA and reference controls (P = 0.59), and only a trend towards elevated LV mass index (P = 0.058, ***Table 1***).

Ventricular-arterial uncoupling

To test the hypothesis that ventricular-arterial uncoupling contributes to left ventricular diastolic function in INOCA, we examined the relationship between aPWV and indices of left ventricular diastolic function. Image quality prevented aPWV measurements in 6 women with INOCA. Compared to reference controls, aPWV was higher in women with INOCA (6.1 ± 1.5 m/s vs. 8.1 ± 3.2 m/s, control vs. INOCA, respectively; P = 0.045; ***Table 1***), and was associated with early diastolic left ventricular circumferential strain rate (r = -0.50, r^2 = 0.25, P < 0.001; ***Figure 2A***) and early diastolic left ventricular longitudinal strain rate (r = -0.35, r^2 = 0.12, P = 0.003). To further explore this observation, we sub-divided women with INOCA by either low (<7.4 m/s; n = 29) or high (≥7.4 m/s; n = 30) aPWV (***Table 4***). Consistent with the correlation data, INOCA women with high aPWV had the worst early diastolic circumferential (P = 0.003; ***Figure 2B***), and longitudinal strain rates (P = 0.04) and were over-

reliant on late diastolic strain rates (both $P < 0.001$), compared to either INOCA women with low aPWV and reference controls. INOCA women with high aPWV tended to be older, had elevated systolic blood pressure (114 ± 15 mmHg vs. 113 ± 11 mmHg vs. 124 ± 14 mmHg, controls vs. INOCA low aPWV vs. INOCA high aPWV, respectively; $P = 0.003$), and increased left ventricular mass (41.7 [37.3,43.7] g/m^2 vs. 42.4 [40.3,44.3] g/m^2 vs. 45.2 [39.1,50.4] g/m^2, control vs. INOCA low aPWV vs. INOCA high aPWV, respectively; $P = 0.04$).

Discussion

Using a comprehensive cardiac MRI approach, this study systematically evaluated the three leading hypotheses thought to be responsible for the development of diastolic dysfunction in INOCA. Together, the data show that elevated aortic pulse wave velocity, and associated ventricular-arterial uncoupling, is the strongest determinant of left ventricular diastolic dysfunction in women with INOCA, with no discernible direct contribution from either coronary vascular dysfunction related oxygen supply-demand mismatch or diffuse myocardial fibrosis.

Table 4. Participant characteristics and left ventricular morphology and function for INOCA women with low and high aPWV and reference controls.

	Control (n = 12)	INOCA (n = 59)		P-value
		aPWV < 7.4 (n = 29)	aPWV ≥ 7.4 (n = 30)	
Anthropometrics and Hemodynamics				
Age (years)	50 ± 5	47 ± 10	61 ± 7*†	**< 0.001**
Height (cm)	160 (157,167)	165 (160,168)	160 (149,167)	0.08
Weight (kg)	67.8 (65.0,76.4)	69.4 (59.0,82.8)	67.6 (58.7,77.6)	0.81
BMI (kg/m^2)	26.7 ± 3.7	27.9 ± 7.1	28.5 ± 6.6	0.71
BSA (m^2)	1.73 ± 0.11	1.79 ± 0.20	1.69 ± 0.15	0.12
SBP (mmHg)	114 ± 15	113 ± 11	124 ± 14*†	**0.003**
DBP (mmHg)	64 ± 11	61 ± 11	66 ± 10	0.16
MAP (mmHg)	81 ± 10	78 ± 8	86 ± 9†	**0.01**
Medical History				
Hypertension n (%)	0 (0)	6 (20)	12 (40)*†	**0.02**
Diabetes n (%)	0 (0)	0 (0)	2 (7)	0.23
Hypercholesteremia n (%)	1 (8)	3 (10)	4 (13)	0.88
LV Mass and Volumes				
EDVi (mL/m^2)	64 ± 8	68 ± 9	69 ± 12	0.43
ESVi (mL/m^2)	23 ± 6	25 ± 6	29 ± 15	0.65
SVi (mL/m^2)	51 ± 4	43 ± 6	44 ± 7	0.43
EF (%)	64 ± 6	63 ± 5	64 ± 4	0.96
E_{es} (mmHg/mL)	2.69 ± 0.74	2.41 ± 0.59	2.81 ± 0.75	0.09
E_a (mmHg/mL)	1.48 ± 0.35	1.37 ± 0.27	1.57 ± 0.34	0.06
E_{es}/E_a	0.57 ± 0.14	0.59 ± 0.15	0.57 ± 0.09	0.87
COi (L/min/m^2)	2.57 ± 0.32	2.65 ± 0.43	2.80 ± 0.56	0.29
LV mass index (g/m^2)	41.7 (37.3,43.7)	42.4 (40.3,44.3)	45.2 (39.1,50.4)*	**0.04**
Concentricity index (g/mL)	0.63 ± 0.06	0.63 ± 0.09	0.67 ± 0.11	0.26
LA Volume Index (mL/m^2)	36 ± 4	35 ± 5	37 ± 7	0.49
LV Strain and Strain Rate				
Circumferential Strain (%)	-24.8 ± 1.7	-24.1 ± 2.4	-24.6 ± 2.1	0.57
Circumferential Systolic SR (/s)	-1.14 ± 0.15	-1.15 ± 0.18	-1.14 ± 0.20	0.96
Circumferential Early Diastolic SR (/s)	1.61 ± 0.33	1.50 ± 0.27	1.29 ± 0.30*†	**0.003**
Circumferential Late Diastolic SR (/s)	0.70 ± 0.17	0.64 ± 0.18	0.86 ± 0.19*†	**< 0.001**
Longitudinal Strain (%)	-21.5 ± 2.4	-20.8 ± 2.4	-20.9 ± 2.2	0.64
Longitudinal Systolic SR (/s)	-0.98 ± 0.18	-0.86 ± 0.42	-1.00 ± 0.15	0.15
Longitudinal Early Diastolic SR (/s)	1.23 ± 0.36	1.12 ± 0.24	1.01 ± 0.24*	**0.04**
Longitudinal Late Diastolic SR (/s)	0.88 ± 0.22	0.72 ± 0.20*	0.96 ± 0.20†	**< 0.001**
Mitral Inflow				
E Velocity (ml/s)	298 ± 66	346 ± 82	281 ± 90†	**0.02**
A Velocity (ml/s)	219 ± 40	210 ± 78	259 ± 99	0.09
E/A Ratio	1.33 (1.13,1.51)	1.63 (1.34,2.31)	0.98 (0.77,1.52)†	**0.001**
E/e'sr Ratio (from circumferential)	177 (164,215)	226 (194,258)	198 (175,266)	0.07
E/e'sr Ratio (from longitudinal)	275 ± 111	323 ± 112	291 ± 103	0.37
Myocardial Tissue Characteristics and Perfusion Reserve				
Native T1 (ms)	1246 ± 38	1252 ± 85	1250 ± 63	0.94
Post-Contrast T1 (ms)	456 ± 24	432 ± 56	457 ± 55	0.19
ECV (%)	29.0 ± 1.9	28.8 ± 3.3*	27.1 ± 3.1*	**0.04**
MPRI	1.89 ± 0.29	1.70 ± 0.34	1.73 ± 0.28	0.24
Aortic Stiffness				
aPWV (m/s)	6.7 (5.2,6.9)	5.9 ± (5.6,6.8)	8.8 (8.0,12.1)	By Design

INOCA – ischemia but no obstructive coronary artery disease; aPWV – aortic pulse wave velocity; BMI – body mass index; BSA – body surface area; SBP – systolic blood pressure; DBP – diastolic blood

pressure; MAP – mean arterial pressure; LV – left ventricular; EDVi – end-diastolic volume index; ESVi – end-systolic volume index; SVi – stroke index; EF – ejection fraction; E_{es} – end-systolic elastance; E_a – effective arterial elastance; COi – cardiac index; LA – left atrial; SR – strain rate; E Velocity – early mitral inflow velocity; A Velocity – late mitral inflow velocity; E/e'SR – ratio between early mitral inflow velocity and early diastolic strain rate; ECV – extracellular volume; MPRI – myocardial perfusion reserve index. Mean ± SD or median (inter-quartile range). * - indicates significantly different from control, $P < 0.05$. † - indicates significantly different from INOCA with low aortic PWV, $P < 0.05$.

Women with INOCA are at increased risk of developing HFpEF, yet the mechanism driving disease progression remains incompletely understood. Women with INOCA often have left ventricular diastolic dysfunction (5,7-9); a common trait also frequently observed in HFpEF (10,11). Moreover, women with INOCA often have coronary vascular dysfunction (5,14,20-22), and HFpEF patients with coronary vascular dysfunction have worse diastolic function then HFpEF without (23). Taken together, this has led to the hypothesis that coronary vascular dysfunction both directly (via energy dependent active relaxation) and indirectly (via diffuse myocardial fibrosis) leads to left ventricular diastolic dysfunction, and heart failure progression. Moreover, it is believed that vascular dysfunction seen in the coronary arteries also manifests in the systemic circulation, and therefore may contribute to diastolic dysfunction indirectly through ventricular-arterial uncoupling.

Diastolic function is a highly energy-dependent process, where sufficient ATP synthesis (and therefore oxygen delivery and utilization) is required for three important diastolic processes: (a) uncoupling of actin from myosin, (b) sequestration of calcium into the sarcoplasmic reticulum via sarcoendoplasmic reticulum ATP-ase pumps, and (c) the removal of calcium from troponin-C. Impairment in myocardial perfusion, second to coronary vascular

dysfunction, could therefore challenge diastolic function through any one or combination of these pathways. That grouping women with INOCA according to MPRI did not differentiate between normal and abnormal diastolic function argues against the coronary vascular dysfunction mediated oxygen supply-demand mismatch hypothesis. Because this comparison was performed using magnetic resonance images collected under resting conditions, it is possible that diastolic dysfunction may only be unmasked under conditions of increased oxygen demand (i.e. physiological stress leading to an oxygen supply-demand mismatch). To test this, isometric handgrip was performed in a subset of participants. In contrast to our hypothesis however, isometric handgrip failed to exacerbate diastolic dysfunction in INOCA. While we did not directly assess myocardial ischemia in this investigation, our group has indeed documented isometric handgrip induced myocardial ischemia previously in this patient cohort (24). Moreover, inclusion of participants in this sub-analysis was limited only to those individuals who achieved an optimal hemodynamic stress response (i.e. greatest increase in rate pressure product), with INOCA sub-divided according to coronary vascular function (i.e. low vs. high MPRI).

Our group has also observed frequent episodes of ST segment depression in women with INOCA (25), and increased prevalence of focal scar lesions (26). These observations, together with >2 decades of evidence showing a high prevalence of coronary vascular dysfunction in INOCA, has led to the hypothesis that women with INOCA experience repeat episodes of acute myocardial ischemia, which in turn could lead to the expansion of the extracellular matrix and diffuse/patchy myocardial fibrosis. In contrast to this hypothesis

however, we did not observe any difference in native T1 or post-contrast ECV between INOCA and reference controls. That native T1 was not elevated in INOCA is inconsistent with a previous report from our group (15). Though it remains unclear why these two observations are inconsistent, differences in MRI field strength, sample size, and extent of coronary vascular dysfunction may have contributed. Despite these differences however, both investigations found a remarkably similar reduction in early diastolic function in INOCA compared to controls, suggesting that altered myocardial tissue characteristics are unlikely to be playing a predominant role in the development of diastolic dysfunction in INOCA.

Ventricular-arterial coupling has long been recognized as an important contributor to cardiac mechanics and hemodynamics. Alterations in the stiffness of the central and peripheral vascular system elevate cardiac afterload and compromise cardiac efficiency (27,28). Indeed, ventricular-arterial uncoupling has been implicated in hypertension, diabetes and overt heart failure (29-31). The data herein are the first to show that women with INOCA have elevated aPWV compared to reference controls and that aPWV is inversely related to left ventricular early diastolic strain rate. Furthermore, after sub-dividing the INOCA group by low and high aPWV, we found that those with the highest aPWV had the worst left ventricular diastolic function. It is well recognized that increased conduit artery stiffness is associated with elevated left ventricular pulsatile load, which compromises diastolic function via two primary mechanisms: (a) increased left ventricular afterload, and (b) decreased coronary perfusion (16). Proximal aortic impedance, shorter time to the arrival of the reflected wave, and total compliance of the peripheral arterial tree all contribute to increased aortic stiffness.

These mechanisms challenge left ventricular diastolic function by elevating aortic systolic pressure (28), which attenuates passive recoil of titin during isovolumic relaxation (32) and challenges myocyte calcium handling (33). Moreover, the earlier arrival of the reflected wave also leads to reduced aortic diastolic pressure which compromises left ventricular diastolic function via coronary hypoperfusion (34). These data are the first to suggest that aortic stiffness, and associated ventricular-arterial uncoupling, contribute to left ventricular diastolic dysfunction in INOCA.

This study is not without limitation. Due to the cross-sectional nature of this study, we are unable to establish causality. Future investigations evaluating changes in diastolic function in women with INOCA over time or in response to targeted therapy are therefore needed. Moreover, the study design did not allow for the direct assessment of left ventricular chamber compliance and thus we cannot completely rule out chamber stiffness as a contributing mechanism to diastolic dysfunction in INOCA. However, given that we saw no differences in native T1 or ECV between INOCA and controls, we would not expect this to play a major role in the development of diastolic dysfunction in INOCA.

Conclusion

This is the first study to systematically evaluate several leading hypotheses thought to be responsible for the development of left ventricular diastolic dysfunction in INOCA. Using a comprehensive MRI approach, we identified ventricular-arterial uncoupling to be an important determinant of left ventricular diastolic dysfunction in this population, with no

discernible direct contribution from either coronary vascular dysfunction mediated oxygen supply-demand mismatch or diffuse myocardial fibrosis. Future therapeutic interventions should seek to target the mechanism(s) leading to elevated aortic stiffness in INOCA, in an effort to lower the cardiovascular risk in INOCA and prevent progression to HFpEF.

Reference List

1. Alan S . Go MDM, MD, DrPH, FAHA; Véronique L . Roger, MD, MPH, FAHA; Emelia J . Benjamin, MD, ScM, FAHA; Jarett D . Berry, MD, FAHA; William B . Borden, MD, FAHA; Dawn M . Bravata, MD; Shifan Dai, MD, PhD*; Earl S . Ford, MD, MPH, FAHA*; Caroline S . Fox, MD, MPH; Sheila Franco, MS*; Heather J . Fullerton, MD; Cathleen Gillespie, MS*; Susan M . Hailpern, DPH, MS; John A . Heit, MD, FAHA; Virginia J . Howard, PhD, FAHA; Mark D . Huffman, MD, MPH; Brett M . Kissela, MD, MS; Steven J . Kittner, MD, FAHA; Daniel T . Lackland, DrPH, MSPH, FAHA; Judith H . Lichtman, PhD, MPH; Lynda D . Lisabeth, PhD, MPH, FAHA; David Magid, MD; Gregory M . Marcus, MD, MAS, FAHA; Ariane Marelli, MD, MPH; David B . Matchar, MD, FAHA; Darren K . McGuire, MD, MHSc, FAHA; Emile R . Mohler, MD, FAHA; Claudia S . Moy, PhD, MPH; Michael E . Mussolino, PhD, FAHA; Graham Nichol, MD, MPH, FAHA; Nina P . Paynter, PhD, MHSc; Pamela J . Schreiner, PhD, FAHA; Paul D . Sorlie, PhD; Joel Stein, MD; Tanya N . Turan, MD, MSCR, FAHA; Salim S . Virani, MD, PhD; Nathan D . Wong, PhD, MPH, FAHA; , Daniel Woo M, MS, FAHA; Melanie B . Turner, MPH. Heart Disease and Stroke Statistics—2013 Update A Report From the American Heart Association. 2013.
2. Bairey Merz CN, Shaw LJ, Reis SE et al. Insights from the NHLBI-Sponsored Women's Ischemia Syndrome Evaluation (WISE) Study: Part II: gender differences in presentation, diagnosis, and outcome with regard to gender-based pathophysiology of atherosclerosis and macrovascular and microvascular coronary disease. J Am Coll Cardiol 2006;47:S21-9.
3. Gulati M M, MS; Rhonda M. Cooper-DeHoff, PharmD, MS; Candace McClure, BS; B. Delia Johnson, PhD; Leslee J. Shaw, PhD; Eileen M. Handberg, PhD; Issam Zineh, PharmD; Sheryl F. Kelsey, PhD; Morton F. Arnsdorf, MD; Henry R. Black, MD; Carl J. Pepine, MD; C. Noel Bairey Merz, MD. Adverse Cardiovascular Outcomes in Women With Nonobstructive Coronary Artery Disease: A Report From the Women's Ischemia Syndrome Evaluation Study and the St James Women Take Heart Project. Arch Intern Med 2009.
4. Bakir M, Nelson MD, Jones E et al. Heart failure hospitalization in women with signs and symptoms of ischemia: A report from the women's ischemia syndrome evaluation study. Int J Cardiol 2016;223:936-939.
5. Taqueti VR, Solomon SD, Shah AM et al. Coronary microvascular dysfunction and future risk of heart failure with preserved ejection fraction. Eur Heart J 2018;39:840-849.
6. Bakir M, Wei J, Nelson MD et al. Cardiac magnetic resonance imaging for myocardial perfusion and diastolic function-reference control values for women. Cardiovasc Diagn Ther 2016;6:78-86.
7. Nelson MD. Left ventricular diastolic dysfunction in women with nonobstructive ischemic heart disease: insights from magnetic resonance imaging and spectroscopy.

American journal of physiology Regulatory, integrative and comparative physiology 2017;313:R322-r329.
8. Nelson MD, Szczepaniak LS, Wei J et al. Diastolic dysfunction in women with signs and symptoms of ischemia in the absence of obstructive coronary artery disease: a hypothesis-generating study. Circ Cardiovasc Imaging 2014;7:510-6.
9. Wei J, Mehta PK, Shufelt C et al. Diastolic dysfunction measured by cardiac magnetic resonance imaging in women with signs and symptoms of ischemia but no obstructive coronary artery disease. Int J Cardiol 2016;220:775-80.
10. Zile MR, Baicu CF, Gaasch WH. Diastolic heart failure--abnormalities in active relaxation and passive stiffness of the left ventricle. N Engl J Med 2004;350:1953-9.
11. Borlaug BA, Nishimura RA, Sorajja P, Lam CS, Redfield MM. Exercise hemodynamics enhance diagnosis of early heart failure with preserved ejection fraction. Circ Heart Fail 2010;3:588-95.
12. Quesada O, AlBadri A, Wei J et al. Design, methodology and baseline characteristics of the Women's Ischemia Syndrome Evaluation-Coronary Vascular Dysfunction (WISE-CVD). Am Heart J 2019;220:224-236.
13. Bairey Merz CN, Pepine CJ, Walsh MN, Fleg JL. Ischemia and No Obstructive Coronary Artery Disease (INOCA): Developing Evidence-Based Therapies and Research Agenda for the Next Decade. Circulation 2017;135:1075-1092.
14. Thomson LE, Wei J, Agarwal M et al. Cardiac magnetic resonance myocardial perfusion reserve index is reduced in women with coronary microvascular dysfunction. A National Heart, Lung, and Blood Institute-sponsored study from the Women's Ischemia Syndrome Evaluation. Circ Cardiovasc Imaging 2015;8.
15. Shaw JL, Nelson MD, Wei J et al. Inverse association of MRI-derived native myocardial T1 and perfusion reserve index in women with evidence of ischemia and no obstructive CAD: A pilot study. Int J Cardiol 2018;270:48-53.
16. Ikonomidis I, Aboyans V, Blacher J et al. The role of ventricular-arterial coupling in cardiac disease and heart failure: assessment, clinical implications and therapeutic interventions. A consensus document of the European Society of Cardiology Working Group on Aorta & Peripheral Vascular Diseases, European Association of Cardiovascular Imaging, and Heart Failure Association. Eur J Heart Fail 2019;21:402-424.
17. Gobel FL, Norstrom LA, Nelson RR, Jorgensen CR, Wang Y. The rate-pressure product as an index of myocardial oxygen consumption during exercise in patients with angina pectoris. Circulation 1978;57:549-56.
18. Nelson MD, Sharif B, Shaw JL et al. Myocardial tissue deformation is reduced in subjects with coronary microvascular dysfunction but not rescued by treatment with ranolazine. Clin Cardiol 2017;40:300-306.
19. Shufelt CL, Thomson LE, Goykhman P et al. Cardiac magnetic resonance imaging myocardial perfusion reserve index assessment in women with microvascular coronary dysfunction and reference controls. Cardiovasc Diagn Ther 2013;3:153-60.

20. AlBadri A, Bairey Merz CN, Johnson BD et al. Impact of Abnormal Coronary Reactivity on Long-Term Clinical Outcomes in Women. J Am Coll Cardiol 2019;73:684-693.
21. Pepine CJ, Anderson RD, Sharaf BL et al. Coronary microvascular reactivity to adenosine predicts adverse outcome in women evaluated for suspected ischemia results from the National Heart, Lung and Blood Institute WISE (Women's Ischemia Syndrome Evaluation) study. J Am Coll Cardiol 2010;55:2825-32.
22. Taqueti VR, Shaw LJ, Cook NR et al. Excess Cardiovascular Risk in Women Relative to Men Referred for Coronary Angiography Is Associated With Severely Impaired Coronary Flow Reserve, Not Obstructive Disease. Circulation 2017;135:566-577.
23. Yang JH, Obokata M, Reddy YNV, Redfield MM, Lerman A, Borlaug BA. Endothelium-dependent and independent coronary microvascular dysfunction in patients with heart failure with preserved ejection fraction. Eur J Heart Fail 2019.
24. Buchthal SD, den Hollander JA, Merz CN et al. Abnormal myocardial phosphorus-31 nuclear magnetic resonance spectroscopy in women with chest pain but normal coronary angiograms. N Engl J Med 2000;342:829-35.
25. Darouian N, Agrawal S, Wei J et al. PREVALENCE OF SILENT MYOCARDIAL ISCHEMIA ON AMBULATORY MONITORING IN WOMEN WITH CORONARY MICROVASCULAR DYSFUNCTION. J Am Coll Cardiol 2016;67:2096.
26. Wei J, Bakir M, Darounian N et al. Myocardial Scar Is Prevalent and Associated With Subclinical Myocardial Dysfunction in Women With Suspected Ischemia But No Obstructive Coronary Artery Disease: From the Women's Ischemia Syndrome Evaluation-Coronary Vascular Dysfunction Study. Circulation 2018;137:874-876.
27. Chantler PD, Lakatta EG, Najjar SS. Arterial-ventricular coupling: mechanistic insights into cardiovascular performance at rest and during exercise. J Appl Physiol (1985) 2008;105:1342-51.
28. Borlaug BA, Melenovsky V, Redfield MM et al. Impact of arterial load and loading sequence on left ventricular tissue velocities in humans. J Am Coll Cardiol 2007;50:1570-7.
29. Ikonomidis I, Lekakis J, Papadopoulos C et al. Incremental value of pulse wave velocity in the determination of coronary microcirculatory dysfunction in never-treated patients with essential hypertension. Am J Hypertens 2008;21:806-13.
30. van Schinkel LD, Auger D, van Elderen SG et al. Aortic stiffness is related to left ventricular diastolic function in patients with diabetes mellitus type 1: assessment with MRI and speckle tracking strain analysis. Int J Cardiovasc Imaging 2013;29:633-41.
31. Pandey A, Khan H, Newman AB et al. Arterial Stiffness and Risk of Overall Heart Failure, Heart Failure With Preserved Ejection Fraction, and Heart Failure With Reduced Ejection Fraction: The Health ABC Study (Health, Aging, and Body Composition). Hypertension 2017;69:267-274.
32. Ikonomidis I, Katsanos S, Triantafyllidi H et al. Pulse wave velocity to global longitudinal strain ratio in hypertension. Eur J Clin Invest 2019;49:e13049.

33. Gorski PA, Ceholski DK, Hajjar RJ. Altered myocardial calcium cycling and energetics in heart failure--a rational approach for disease treatment. Cell Metab 2015;21:183-94.
34. Tritakis V, Tzortzis S, Ikonomidis I et al. Association of arterial stiffness with coronary flow reserve in revascularized coronary artery disease patients. World J Cardiol 2016;8:231-9.

Chapter 6

Dissertation Summary and Concluding Remarks

Left ventricular diastolic stress testing is now recommended by both the American Society of Echocardiography and the European Association of Cardiovascular Imaging for clinical diagnosis of diastolic dysfunction (1,2). Over the past several decades numerous investigations have highlighted the clinical significance of cycle exercise based diastolic stress testing, particularly in well-compensated patients where resting diastolic function can often appear normal (3-6). However, orthopedic restrictions, respiratory and motion artifact, and limited acoustic windows for imaging often seen in patients, all compromise the application of dynamic exercise-based diastolic stress testing. The series of investigations presented in this dissertation establish isometric handgrip diastolic stress testing as a robust alternative that avoids many of the limitations associated with cycle exercise.

In Chapter 3 we showed that isometric handgrip elicits a reproducible increase in left ventricular afterload and myocardial oxygen which can successfully differentiate between normal and abnormal diastolic function. We speculate that the major underlying mechanism contributing to this impaired response is likely related to an oxygen supply-demand mismatch. Indeed, isometric handgrip increases myocardial oxygen demand via an elevated rate of oxidative ATP synthesis, which if not met, could lead to prolonged actin-myosin formation and impaired sarco/endoplasmic reticulum calcium ATP-ase (SERCA) function, both of which would result in delayed and slowed active relaxation (7).

Despite our enthusiasm for isometric handgrip, up to this point cycle exercise based diastolic stress testing was the most common clinically used tool, and thus a direct head-to-head comparison was warranted. In Chapter 4, we directly compared the diastolic stress

response to both isometric handgrip and conventional cycle exercise. The data suggest that both methods have comparable utility and are equally as robust at unmasking diastolic dysfunction not seen at rest. However, we found that while cycle exercise provided a preload mediated increase in early mitral inflow velocity, isometric handgrip provided a unique afterload challenge that resulted in a reduction in early myocardial relaxation. From these first two investigations we can conclude that isometric handgrip is a simple but robust alternative to conventional cycle exercise-based diastolic stress tests, and that isometric handgrip can unmask diastolic dysfunction by increasing left ventricular afterload and myocardial oxygen demand. Therefore, isometric handgrip diastolic stress testing provides a unique perspective into the pathophysiologic mechanism leading to diastolic dysfunction.

Then, in Chapter 5 we applied our established isometric handgrip protocol in women with ischemia but no obstructive coronary artery disease (INOCA) to identify individuals with stress-induced diastolic dysfunction. Indeed, my mentor has consistently shown that women with INOCA have resting diastolic function (8-10), however, until now the pathophysiological mechanism causing this phenomenon remained unknown. While our original hypothesis that isometric handgrip would exacerbate diastolic dysfunction in women with INOCA by challenging the relationship between oxygen supply and demand did not hold true, we were able to identify that ventricular-arterial uncoupling, second to elevated aortic stiffness is the predominant mechanism leading to diastolic dysfunction in INOCA women. The ability to transfer isometric handgrip from the echocardiography laboratory to an MRI, a modality where dynamic exercise is particularly challenging due to the physical constraints of the MRI

bore, allowed us to systematically evaluate the leading hypothesized mechanisms contributing to diastolic dysfunction in INOCA.

Throughout the completion of this series of investigations I have acquired skills in both echocardiography and MRI. Moreover, my theoretical and mechanistic understanding of cardiac mechanics and hemodynamics has substantially improved, and this experience has helped me develop new hypotheses that I would like to address in the future. For example, I would like to further explore the role of impaired calcium handling in diastolic dysfunction. Indeed, in pre-clinical heart failure models there is evidence to suggest that excessive calcium entry through L-type calcium channels (11), a compensatory leak of sarcoplasmic reticulum calcium through ryanodine receptors (12), and extrusion of calcium from the cytosol is ineffective due to a reduced transmembrane sodium gradient (13), all of which could contribute to diastolic dysfunction. Whether these mechanisms are involved in the development of diastolic dysfunction in human patients remains unknown and is a hypothesis I would like to explore further. Furthermore, I would also like to fully explore the role of impaired oxidative metabolism and associated ATP synthesis in the development of diastolic dysfunction. Phosphorous magnetic resonance spectroscopy provides direct in vivo evidence of myocardial creatine kinase flux, and thus ATP synthesis and metabolism (14,15). Addition of this skill will also help me fully test the ischemia-mediated diastolic dysfunction hypothesis. Finally, longitudinal study designs are needed to confirm the prognostic significance of an abnormal diastolic stress test response to isometric handgrip.

Taken together, the collection of work presented in this PhD dissertation supports the use of isometric handgrip as a robust diastolic discriminator that avoids many of the limitations associated with dynamic exercise. That isometric handgrip is easy to perform, requires limited specialized resources, and can be easily adopted into both echocardiography and MRI-based investigations, holds great promise for its widespread adoption into cardiology clinics and laboratories worldwide.

Reference List

1. Nagueh SF, Smiseth OA, Appleton CP et al. Recommendations for the Evaluation of Left Ventricular Diastolic Function by Echocardiography: An Update from the American Society of Echocardiography and the European Association of Cardiovascular Imaging. Eur Heart J Cardiovasc Imaging 2016;17:1321-1360.
2. Nagueh SF, Smiseth OA, Appleton CP et al. Recommendations for the Evaluation of Left Ventricular Diastolic Function by Echocardiography: An Update from the American Society of Echocardiography and the European Association of Cardiovascular Imaging. J Am Soc Echocardiogr 2016;29:277-314.
3. Ha JW, Oh JK, Pellikka PA et al. Diastolic stress echocardiography: a novel noninvasive diagnostic test for diastolic dysfunction using supine bicycle exercise Doppler echocardiography. J Am Soc Echocardiogr 2005;18:63-8.
4. Borlaug BA, Jaber WA, Ommen SR, Lam CS, Redfield MM, Nishimura RA. Diastolic relaxation and compliance reserve during dynamic exercise in heart failure with preserved ejection fraction. Heart 2011;97:964-9.
5. Borlaug BA, Nishimura RA, Sorajja P, Lam CS, Redfield MM. Exercise hemodynamics enhance diagnosis of early heart failure with preserved ejection fraction. Circ Heart Fail 2010;3:588-95.
6. Obokata M, Kane GC, Reddy YN, Olson TP, Melenovsky V, Borlaug BA. Role of Diastolic Stress Testing in the Evaluation for Heart Failure With Preserved Ejection Fraction: A Simultaneous Invasive-Echocardiographic Study. Circulation 2017;135:825-838.
7. Gorski PA, Ceholski DK, Hajjar RJ. Altered myocardial calcium cycling and energetics in heart failure--a rational approach for disease treatment. Cell Metab 2015;21:183-94.
8. Nelson MD, Sharif B, Shaw JL et al. Myocardial tissue deformation is reduced in subjects with coronary microvascular dysfunction but not rescued by treatment with ranolazine. Clin Cardiol 2017;40:300-306.
9. Nelson MD, Szczepaniak LS, Wei J et al. Diastolic dysfunction in women with signs and symptoms of ischemia in the absence of obstructive coronary artery disease: a hypothesis-generating study. Circ Cardiovasc Imaging 2014;7:510-6.
10. Wei J, Mehta PK, Shufelt C et al. Diastolic dysfunction measured by cardiac magnetic resonance imaging in women with signs and symptoms of ischemia but no obstructive coronary artery disease. Int J Cardiol 2016;220:775-80.
11. Schroder F, Handrock R, Beuckelmann DJ et al. Increased availability and open probability of single L-type calcium channels from failing compared with nonfailing human ventricle. Circulation 1998;98:969-76.
12. Goonasekera SA, Hammer K, Auger-Messier M et al. Decreased cardiac L-type Ca(2)(+) channel activity induces hypertrophy and heart failure in mice. J Clin Invest 2012;122:280-90.

13. Sipido KR, Volders PG, Vos MA, Verdonck F. Altered Na/Ca exchange activity in cardiac hypertrophy and heart failure: a new target for therapy? Cardiovasc Res 2002;53:782-805.
14. Schar M, Gabr RE, El-Sharkawy AM, Steinberg A, Bottomley PA, Weiss RG. Two repetition time saturation transfer (TwiST) with spill-over correction to measure creatine kinase reaction rates in human hearts. J Cardiovasc Magn Reson 2015;17:70.
15. Bottomley PA, Panjrath GS, Lai S et al. Metabolic rates of ATP transfer through creatine kinase (CK Flux) predict clinical heart failure events and death. Sci Transl Med 2013;5:215re3.

Appendix A

Diastolic Stress Testing: Have you considered Isometric Handgrip Echocardiography? *

T. Jake Samuel, Mark J. Haykowsky, Satyam Sarma, and Michael D. Nelson (2019). Diastolic Stress Testing: Have you considered Isometric Handgrip Echocardiography? *JACC Cardiovasc Imaging*, 12 (10): 2095-2097. DOI: 10.1016/j.jcmg.2019.07.023.

We read with great interest two recent state-of-the-art review articles by *Ha et al.* (1) and *Obokata et al.* (2) published in *JACC: Cardiovascular Imaging*. Both reviews advocate for the use of cycle exercise in patients with unexplained dyspnea for optimal diagnosis of diastolic dysfunction, particularly when resting assessments remain equivocal. The first review by *Ha et al.* (1) highlight the clinical application of both invasive and non-invasive diastolic stress testing, while the review by *Obokata and coworkers (2)* provides a comprehensive summary of the pathophysiology and phenotyping of heart failure with preserved ejection fraction (HFpEF), with particular emphasis on utilizing cycle exercise echocardiography. Thanks to their seminal work, and important contributions from others, sub-maximal, cycle exercise is now recommended by both the American Society of Echocardiography and the European Association of Cardiovascular Imaging (ASE/EACI) for optimal diagnosis of diastolic dysfunction.

One important limitation raised by both reviews, is the technical challenges often associated with cycle exercise, particularly in patient populations with limited acoustic windows, even at rest. As expected, dynamic lower body exercise increases both respiratory and movement artifact, which is exacerbated in patients with increased body adiposity and/or poor acoustic windows. This is further compounded by orthopedic limitations that often accompany patients. Moreover, as discussed by *Ha and colleagues* (1), there are also technical challenges associated with assessing diastolic function at high heart rates.

In light of these limitations, our group has advocated using isometric handgrip echocardiography (IHE) as an alternative diastolic stress testing modality, as it avoids the above mentioned limitations, while reproducibly increasing left ventricular afterload and myocardial oxygen demand (3,4). We of course are not the first to suggest this, with investigators adopting this approach decades ago, to invasively study stress induced changes in diastolic hemodynamics. In our hands, using a similar non-invasive imaging approach described by *Ha et al.* (1) and *Obokata et al.* (2), IHE at 40% of maximal voluntary contraction (MVC) for 3-5 minutes is able to differentiate between normal and abnormal diastolic function in a group of asymptomatic elderly individuals; a response which parallels that observed in HFpEF (***Figure***) (4). We have also shown that IHE has a similar myocardial oxygen demand as low level cycle exercise (20W), as defined by rate pressure product, and evokes a comparable rise in E/e' (3).

The mechanism(s) by which diastolic dysfunction is unmasked by IHE and cycle exercise are likely different, and is worth consideration (5). Specifically, IHE causes a greater rise in systolic pressure that is expected to pose greater challenge on calcium handling and associated actin-myosin cross-bridge cycling. When ventricular-arterial stiffness is increased, as occurs in HFpEF, the IHE-mediated increase in systolic pressure is associated with delayed cardiac relaxation and increased end-diastolic pressure.

While cycle exercise echocardiography offers significant value in identifying many patients with diastolic dysfunction— that is otherwise hidden at rest— IHE is a convenient

alternative that avoids many of the technical limitations of cycle exercise, while still serving as a robust diastolic discriminator. We therefore reason that IHE should be considered when planning diastolic stress testing in the laboratory and the clinic.

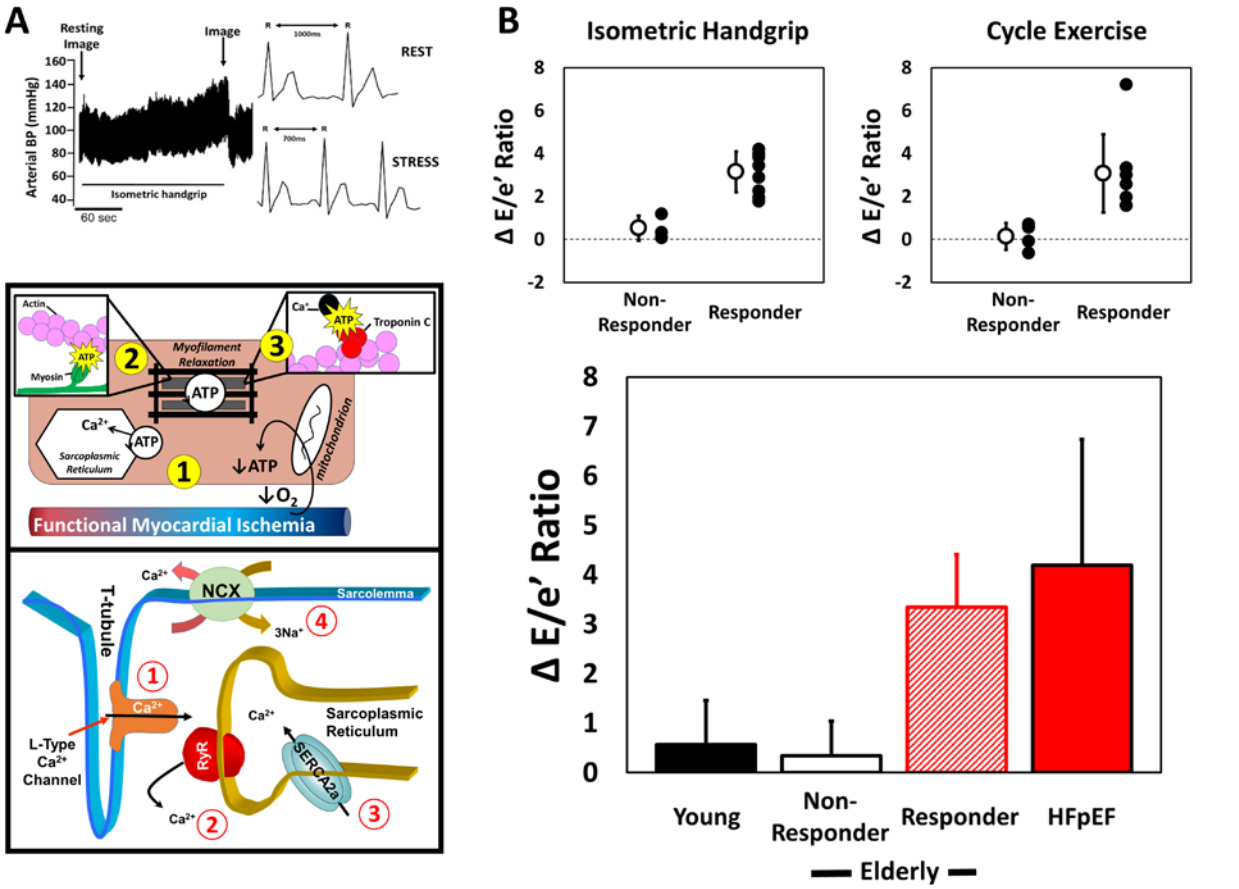

Figure. Central illustration highlighting potential mechanisms and early evidence promoting isometric handgrip echocardiography as a diastolic discriminator. (A) IHE performed at 40% of MVC for 3-5 minutes reproducibly leads to an increase in arterial blood pressure and heart rate by stimulating the exercise pressor reflex (*top*), which acts as a diastolic stressor via two dominant mechanism (*below*): First, the increase in heart rate and blood pressure challenges the myocardial oxygen supply-demand balance, which can compromise ATP production. Second, the elevated afterload stress can lead to impaired calcium handling, leading to delayed and prolonged myocardial relaxation. **(B)** Similar to 20W cycle exercise, IHE leads to a rise in the ratio between Doppler-derived early mitral inflow velocity and early annular tissue velocity (E/e') in a subset of elderly asymptomatic individuals, termed *responders* (*top*). This rise in E/e', induced by IHE, mirrors the response observed in clinically diagnosed HFpEF patients (n=3), which is not seen in young healthy individuals (*below*). Data expressed as mean ± SD. Figures adapted from Samuel et al. (3-5).

Reference List

1. Ha JW, Andersen OS, Smiseth OA. Diastolic Stress Test: Invasive and Noninvasive Testing. JACC Cardiovasc Imaging 2019.
2. Obokata M, Reddy YNV, Borlaug BA. Diastolic Dysfunction and Heart Failure With Preserved Ejection Fraction: Understanding Mechanisms by Using Noninvasive Methods. JACC Cardiovasc Imaging 2019.
3. Samuel TJ, Beaudry R, Haykowsky MJ, Sarma S, Nelson MD. Diastolic stress testing: similarities and differences between isometric handgrip and cycle echocardiography. J Appl Physiol (1985) 2018;125:529-535.
4. Samuel TJ, Beaudry R, Haykowsky MJ et al. Isometric handgrip echocardiography: A noninvasive stress test to assess left ventricular diastolic function. Clin Cardiol 2017;40:1247-1255.
5. Samuel TJ, Beaudry R, Sarma S, Zaha V, Haykowsky MJ, Nelson MD. Diastolic Stress Testing Along the Heart Failure Continuum. Curr Heart Fail Rep 2018;15:332-339.

Appendix B

Correcting Calcium Dysregulation in Chronic Heart Failure Using SERCA2a Gene Therapy*

T. Jake Samuel, Ryan P. Rosenberry, Seungyong Lee, and Zui Pan (2018). Correcting Calcium Dysregulation in Chronic Heart Failure using SERCA2a Gene Therapy. *Int J Mol Sci*, 19, 1086. DOI: 10.3390/ijms19041086.

Introduction

Chronic heart failure (CHF) is a major form of cardiovascular disease and is the leading cause of hospitalization for those over the age of 65 (1). It is expected to account for almost seventy billion dollars in healthcare costs by 2030 in the US alone (2). The current pharmacological therapies for CHF merely target symptom management, with limited success in treating the underlying etiology of the disease. The late stage CHF patients eventually need expensive and hard-to-obtain heart transplantation or mechanical assist devices. Therefore, successful therapies for preventing and reversing CHF progression are urgently required.

Understanding the basic mechanisms involved in the development of CHF has been an active field of research in the quest to identify abnormalities that could potentially be targeted by gene transfer. It has been well established that myocardial calcium (Ca^{2+}) dysregulation is a hallmark of CHF. Tight control of cardiac intracellular Ca^{2+} handling plays an integral role in synchronous actin-myosin cross-bridge cycling and the resulting systolic contraction and diastolic relaxation. Many proteins either at the cell surface or intracellular organelles form the warp and woof of the regulatory network for intracellular Ca^{2+} signals in cardiomyocytes (Figure 1). During systole, Ca^{2+} enters the sarcolemma through L-type Ca^{2+} channels, i.e., dihydropyrodine receptor (DHPR) located on the transverse-tubules (T-tubules), before diffusing across the short distance to the ryanodine receptors (RyRs) located to the sarcoplasmic reticulum (SR). This small amount of Ca^{2+} influx triggers RyRs to generate further Ca^{2+}-induced-Ca^{2+}-release (CICR) from the SR to form magnified Ca^{2+} transient (3). Ca^{2+} then binds to troponin-C in the sarcomere and stimulates actin-myosin cross-bridge linking, i.e., systolic contraction (4). During diastole, in order to reduce the likelihood of Ca^{2+} binding to troponin-C and causing prolonged myocardial systolic contraction, Ca^{2+} is actively sequestrated back into the SR via a sarco/endoplasmic reticulum Ca^{2+} ATPase, SERCA2a in

cardiomyocyte (5,6), or expelled from the sarcolemma by sodium-Ca^{2+} exchanger pumps (NCX) (3). As such, SERCA2a is undoubtedly essential for complete myocyte Ca^{2+} homeostasis.

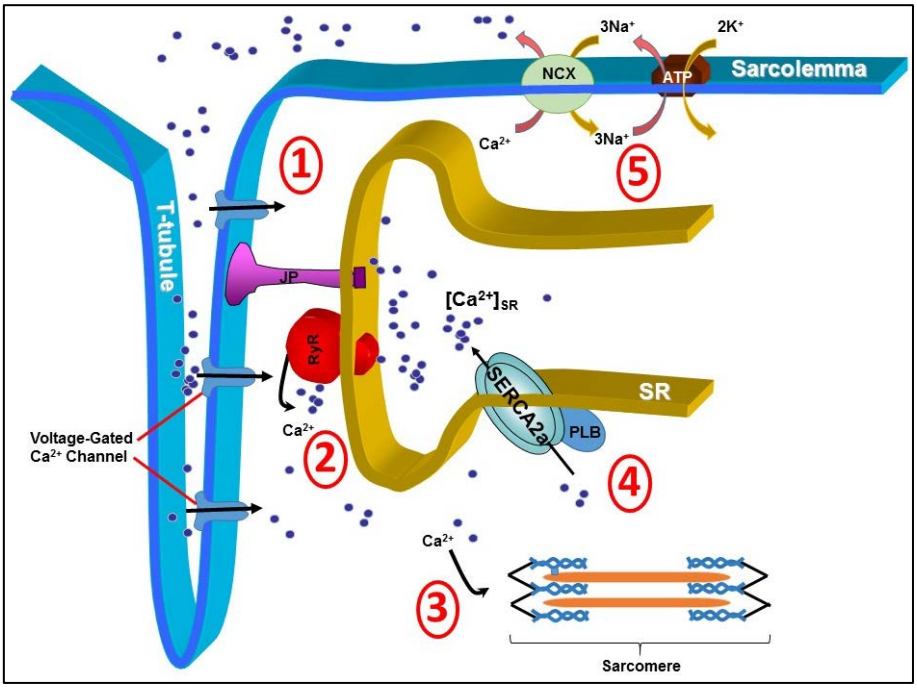

Figure 1. Cardiac intracellular Ca^{2+} is tightly regulated by several proteins. Efficient systolic contraction and diastolic relaxation is reliant on efficient Ca^{2+} handling through 5 main processes. (1) Diffusion of Ca^{2+} in to the cytosol via voltage-gated Ca^{2+} channels (DHPRs) located on the surface of the transverse-tubule (T-tubule); (2) Ca^{2+}-induced-Ca^{2+}-release from the ryanodine receptors (RyRs); (3) Binding of Ca^{2+} to troponin-C in the sarcomere, stimulating actin-myosin cross-linking; (4) Sequestration of Ca^{2+} back in to the sarcoplasmic reticulum via the important Ca^{2+} pump sarco/endoplasmic reticulum Ca^{2+} ATPase (SERCA2a); and (5) Expulsion of Ca^{2+} from the cell via sodium-calcium exchanger pumps (NCX). JP, junctophilins; PLB, phopholamban; ATP, ATP pump; $3Na^{+}$, sodium; K^{+}, potassium.

Dysregulation of any of the above Ca^{2+} handling processes will result in impaired ventricular contractility and impaired myocyte relaxation, leading to cardiac dysfunction (4,7,8). While efforts have been devoted to investigating the therapeutic value of many Ca^{2+} channels and proteins in regulating cytosolic Ca^{2+} concentrations, SERCA2a has received the most interest in recent years.

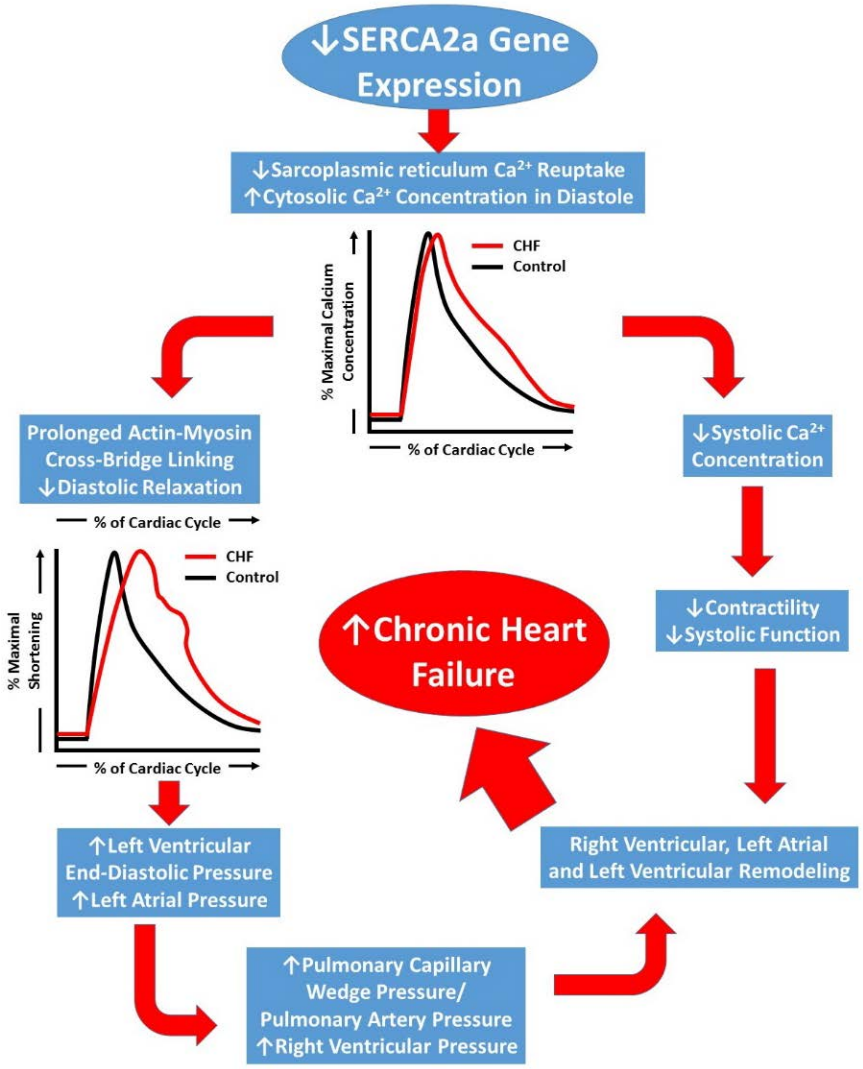

Figure 2. Schematic representation of the progression of chronic heart failure. Initial downregulation of SERCA2a function leads to increased cytosolic Ca^{2+}, which ultimately compromises left ventricular contractility (systolic function) and leads to prolonged left ventricular relaxation. Prolonged relaxation leads to increased filling pressures and a backlog of pressure in to the pulmonary circulation and right heart, the result of which leads to severe right and left heart remodeling and chronic heart failure development.

Reduction in SERCA2a levels in the SR has been reported in failing heart tissues (9,10). Impaired Ca^{2+}-ATPase pump function and decreased SERCA2a gene transcription has recently been attributed to delayed left ventricular relaxation and increased left ventricular filling pressures (11) which may lead to pulmonary edema, a common symptom in CHF (Figure 2). Biotechnological advances over the past two decades have led to gene therapy becoming a

viable option for treating many pathologic conditions—including CHF (12-14). Matter of fact, SERCA2a had been identified as a possible gene therapy target as early as 1978 (15). This review will focus on SERCA2a gene therapy in CHF and attempt to highlight the seminal investigations using early gene delivery techniques in animals that contributed to the early promise for its use in humans. It will also provide a summary of the major human clinical trials which identified several limitations to these methods for treating human CHF. Finally, recent novel developments in gene delivery and targeting will be discussed and future directions for this field of research will be proposed.

Early Techniques of SERCA2a Gene Manipulation in Animals

The role of cytosolic Ca^{2+} in cardiac myocyte contraction has been intensely studied for decades. As far back as 40 years ago, investigators were purifying SERCA proteins to better understand the molecular mechanisms through which Ca^{2+} is transported from the cytosol into the sarcoplasmic reticulum (SR) (15). Shortly following the identification of Ca^{2+} channels as key mediators of cardiac function, they became therapeutic targets in the treatment of various cardiac ailments (16-18). With the rise of interest in genomics and gene editing techniques, the direct manipulation of Ca^{2+} channels or pumps, and thus manipulation of Ca^{2+} handling in cardiac myocytes, became possible.

Plasmid and Direct DNA Injection

The earliest successful approaches of manipulating SERCA2a gene expression in animal models were performed using direct insertion of plasmids into developing mouse oocytes. The rat SERCA2a cDNA was cloned into plasmids containing mouse cardiac α-MHC

promoter. While certain repetitive and unnecessary exons were removed, an additional human growth hormone polyadenylation site was included to promote both polyadenylation and termination (9). Once these sequences are successfully cloned into the plasmid, restriction endonucleases are applied to cleave the gene from the plasmid. The linear DNA fragment can then be purified for direct injection into oocytes. The resulting transgenic mice possessed extra copies of the SERCA2a gene and exhibited increased expression of the protein (9,19,20).

Initial studies applying this transgenic technique sought to characterize and measure the effects of the increased SERCA2a expression in otherwise unaltered mice. Early investigations found that overexpression of the SERCA2a gene in a transgenic mouse model resulted in improved Ca^{2+} handling which translated to augmented myocyte contraction and relaxation (9,10,20). Of note, the transgenic mice had a significantly shorter relaxation time indicating improved relaxation kinetics, consistent with improved Ca^{2+} sequestration via SERCA2a (20). With these positive proof-of-concept results, investigators next sought to determine whether SERCA2a could improve cardiac functionality in disease stages. To test this potential treatment, an aortic stenosis-induced CHF model was employed in transgenic mice. The increased afterload from the artificial stenosis caused left ventricular hypertrophy, mimicking the conditions of early CHF. In this investigation, the transgenic expression of SERCA2a provided chronic protective effects against the progression of CHF (19).

Although these early studies demonstrated positive and profound effects from direct injection of DNA fragment containing SERCA2a gene, there are substantial limitations inherent to this technique. First, this laboratory procedure requires a significant time commitment and many uncontrollable steps before the success of the transfection can be determined. In the case of He et al. super-ovulated eggs were treated with purified SERCA2a

DNA, gestated for 20 days, and the newborn mice were allowed to develop for three weeks before testing tail samples for SERCA2a expression by Southern blotting (20). This process relies on integration of the gene into the embryonic genome, normal gestation and delivery, and inerrant expression in the developed animal. Even if each step is performed to perfection, the imprecision introduces excessive error and contributes to study failure. In fact, only three mice out of nine integrated the SERCA2a plasmid. Of these three mice, the single male was sterile, leaving only two female transgenic mice that successfully passed the gene on to their offspring (20).

A second limitation of this technique is that for additional copies of SERCA2a to be expressed, all biological machinery in the transcription/translation/post-translational modification pathway must also function in a normal and healthy manner. Direct injection of the DNA into oocytes carries the potential risk for improper integration of the gene into the genome. As evidenced by the low number of successfully reared transgenic mice, the possibility for lethality or sterility is considerable. Furthermore, this approach cannot be applied to developed organisms, hindering its expansion and/or adaptation into other animal models. To further investigate SERCA2a as an intervention, it was necessary to explore more advanced and versatile gene modifying techniques.

Last and foremost, direct manipulation of human oocytes raises serious ethical issues, which disqualify this approach from developing into a useful human gene therapy for CHF. Rather, these transgenic animal studies laid the theoretical understanding that prompted improvements in biotechnological techniques to tackle this problem. Alternative ethical and safer approaches have been called upon.

Adenoviral (Ad)-Based Vectors

Ad are double-strand DNA vectors that bind to and enter the cell membrane before being transported to the nucleus, allowing transfection of genes into a variety of cells such as cardiomyocytes, skeletal muscle and smooth muscle myocytes (21). Delivery of Ad-based vectors to cardiomyocytes through intracoronary infusion and direct myocardial injection has showed some success in transduction of the target gene (22). Although Ad-based vectors attain a high level of cellular transduction, the various Ad serotypes result in varied efficiency (21), leading to mixed success in modulating target gene expression.

Ad mediated SERCA2a gene delivery (Ad/SERCA2a) was reported to present improvements in cardiac function in CHF due to the upregulation of SERCA2a genes. Ad/SERCA2a gene transfer in mice with CHF enhances contractile function (23) and restores phosphocreatine and ATP level in the heart, which represents the recovery of heart energetic state and removal of myocardial ischemia (24). Furthermore, there is a dose response to Ad/SERCA2a transfer as overexpression of the SERCA2a gene promotes an additive increase in SERCA2a activity which further influences improved ventricular contractility (25) but has no effect on the atrium (26). In addition to improvements in left ventricular contractility, Ad/SERCA2a gene transfer has also been shown to promote reverse myocardial remodeling by reducing left ventricular anterior wall thickening in Wistar rats with CHF, which reduced arrhythmic events and caused the restoration of left ventricular function similar to the observation in control animals (27).

The benefits of SERCA2a gene transfer via Ad-based vectors were not only limited to the myocardial tissue, however, as it also showed benefits on the vascular smooth muscle cells by preventing vascular remodeling and inhibition of neointimal thickening in a human ex vivo model of the coronary artery (28) and augmented coronary blood flow (29). Although

the Ad-based vector technique was successful overall, there were some inherent limitations to this gene delivery method, such as the presence of neutralizing antibodies and the severe immune response against Ad vector and/or the gene-modified cells (21). Therefore, the development of more sophisticated viral vectors techniques was explored to overcome these limitations.

Adeno-Associated Virus (AAV)-Based Vectors

The AAV-based vector has significant advantage over Ad-based vector in gene delivery. To date, several generations of AAV systems have been adapted and adopted in the SERCA2a gene delivery with each generation improving delivery efficiency and safety over the previous one. AAV-based vector has been shown to safely and successfully alter gene expression in cardiac tissue (21), with much less inflammation than that associated with the Ad-based vector technique (21). AAVs comprise more than 100 serotypes and each serotype presents distinct transduction efficiency in different tissues (21). Among these AAVs, the AAV-1 was the best studied and AAV1-based vector is most commonly used. Indeed, several earlier trials were conducted using the AAV1/SERCA2a intra-coronary injection method in animal CHF models with good success. Hadri and colleagues demonstrated that long-term SERCA2a overexpression via in vivo AAV1-mediated gene transfer improves left ventricular ejection fraction, coronary artery blood flow, and expression of endothelial nitric oxide synthase in a swine model of CHF (30). Similarly, AAV1/SERCA2a gene delivery improves echocardiography derived myocardial function and decreases myocardial apoptosis in pigs (31), as well as restores SERCA2a activity and protein expression following atrial fibrillation-related declines in SERCA2a activity and expression (32). Finally, SERCA2a gene transfer not only effects cardiac tissue but also directly influences vascular endothelial and smooth muscle cell

function by improving Ca^{2+} signaling (33) which highlights SERCA2a as an important therapeutic target for treating cardiovascular disease—including CHF.

Overall, AAV1 and AAV6 mediated-SERCA2a gene delivery methods have provided beneficial improvements in myocardial and coronary artery Ca^{2+} handling, contributing to improved cardiac function and reverse remodeling in animal models of CHF. This initial success in improving cardiac function in animal models led to large-scale clinical trials in humans which will be discussed in the following section.

Human Trials

Over the past decade several large-scale clinical trials have been performed using AAV1/SERCA2a in the treatment of human CHF (Table 1) and are discussed below.

The Calcium Upregulation by Percutaneous Administration of Gene Therapy in Cardiac Disease (CUPID) Trial

In response to the promising preclinical models in animals that demonstrated AAV1/SERCA2a were well tolerated and improved cardiac function, CUPID was the first-in-human clinical trial to evaluate the efficacy of recombinant AAV1/SERCA2a in human CHF (12,13). The initial CUPID multicenter trial included two phases, wherein phase 1 was an open-label dose escalation protocol and phase 2, a randomized, double-blind, placebo-controlled trial. The overall primary outcome of the CUPID trials was to monitor safety, while secondary outcomes included improvements in physical activity and efficacy.

Table 1. Current and previous clinical trials to test the efficacy of AAV1/SERCA2a on the Heart Failure.

National Clinical Trial Code	Status	Study Title	Conditions	Interventions	Study Results	References
NCT02772068	Recruiting	Hemodynamic Response to Exercise in HFpEF Patients After Upregulation of SERCA2a	Congestive Heart Failure	Drug: Istaroxime Other: Exercise	No Published Results	-
NCT01966887	Terminated	AAV1-CMV-Serca2a GENe Therapy Trial in Heart Failure (AGENT-HF)	Congestive Heart Failure Ischemic and non-ischemic Cardiomyopathies	Genetic: AAV1/SERCA2a (MYDICAR)-single intracoronary infusion Genetic: Placebo; single intracoronary infusion	No Positive or Negative Effects	(38)
NCT00534703	Terminated	Investigation of the Safety and Feasibility of AAV1/SERCA2a Gene Transfer in Patients with Chronic Heart Failure (SERCA-LVAD)	Chronic Heart Failure Left Ventricular Assist Device	Genetic: AAV1/SERCA2a Drug: Placebo	Terminated Early—No Results	-
NCT01643330	Completed	A Study of Genetically Targeted Enzyme Replacement Therapy for Advanced Heart Failure (CUPID-2b)	Ischemic and non-ischemic Cardiomyopathies Heart Failure	Genetic: AAV1/SERCA2a (MYDICAR) Genetic: Placebo	No Positive or Negative Effects	(12-14,37,39-41)
NCT00454818	Completed	Efficacy and Safety Study of Genetically Targeted Enzyme Replacement Therapy for Advanced Heart Failure (CUPID)	Heart Failure, Congestive Dilated Cardiomyopathy	Genetic: MYDICAR Phase 1 (Open-label, Serial Dose-Escalation Study) Procedure: Placebo Infusion Genetic: MYDICAR Phase 2 (Placebo-controlled, Randomized Study)	Positive Results	(12,13,40-42)
NCT02346422	Terminated	A Phase 1/2 Study of High-Dose Genetically Targeted Enzyme Replacement Therapy for Advanced Heart Failure	Heart Failure Cardiomyopathy	Genetic: MYICAR Phase 1/2 (Dose 2.5×10^{13} DRP)	Terminated Early—No Results	(12,13,40)

In CUPID phase 1, 12 patients were administered single intracoronary infusions, comparing 3 dose levels of AAV1/SERCA2a (AAV1 capsid with human SERCA2a cDNA flanked with inverted terminal repeats) with placebo, and primary outcomes were measured at 6 and 12 months post-infusion. Patients were enrolled independent of CHF etiology, were NYHA class III/IV, and had exhausted all current pharmacologic therapy. The results of phase 1 suggested that intracoronary infusion of AAV1/SERCA2a demonstrated an acceptable safety profile given the advanced CHF population. Several of the patients exhibited improvements in CHF symptoms and left ventricular structure and function at 6 months follow-up (12). Of note, two of the patients who did not respond to therapy already had pre-existing neutralizing antibodies (NAb) for the viral capsid proteins. Pre-existing natural exposure to NAb, which are known to inhibit vector uptake, limit the efficacy of AAV1 treatment in CHF (34-36). Discussion of the impact of NAb on vector uptake are beyond the scope of the current review and have been comprehensively described elsewhere (37).

The relative success of phase 1 led to initiation of phase 2, including 39 advanced CHF patients randomized to 3 doses of viral vector; low (6×10^{11} DNase resistant particles; DRP), medium (3×10^{12} DRP), and high doses (1×10^{13} DRP). Endpoints included patients' symptomatic (NYHA functional class, Minnesota Living with Heart Failure Questionnaire; MLWHFQ) and functional (maximal oxygen uptake, 6-minute Walk Test) status, blood biomarker levels (N-Terminal-pro Brain Natriuretic Peptide, NT-proBNP), and left ventricular function and remodeling (Ejection fraction and End-systolic volume). One-year follow-up suggested the patients randomized to the "high" treatment dose of AAV1/SERCA2a improved in functional class (Mean reduction in MLWHFQ: −10.3 ± 12.21), blood biomarker (NT-proBNP mean reduction: 12.4 ±

47.83%) and left ventricular function (end-systolic volume mean reduction: −9.6 ± 27.55 mL; −4 ± 13.76%). Importantly, there was a significant increase in the time to cardiac event in all AAV1/SERCA2a groups in the CUPID trial, suggesting that perhaps even the lower doses of viral vector had beneficial effects on patient outcome, independent of physiological changes that are not appreciable at smaller sample sizes (13).

Post-CUPID

Since the conclusion of CUPID, three clinical trials utilizing AAV1 have targeted SERCA2a in human CHF (14,38,39,43). CUPID2, a continuation of the CUPID clinical trials, was the first to recruit patients from outside the United States, enrolling a total of 250 patients with CHF. Patients were randomized to 10-minute intracoronary infusion of either placebo or “high” dose of AAV1/SERCA2a. In contrast to the results of the original CUPID trial, CUPID2 did not reduce either recurrent heart failure events, or terminal events in the study population (14,39).

The other two post-CUPID trails began in the United Kingdom, known as SERCA-LVAD and AGENT-HF. SERCA-LVAD aimed to take tissue biopsies at the time of left ventricular assist device implantation (pre-infusion of AAV1/SERCA2a) and at the time of transplant or LVAD removal (post-infusion) in order to correlate changes in clinical outcome with SERCA2a expression levels (43). AGENT-HF utilized AAV1/SERCA2a with left ventricular structure and function as the primary outcome variables assessed at 6 months post-treatment (38). Unfortunately, due to the negative results of the CUPID2 trial and lack of preliminary success, both studies were terminated prematurely. The studies showed no improvement in ventricular remodeling but were underpowered to demonstrate any effect of AAV1/SERCA2a gene therapy (38). Taken together, the human trials utilizing AAV1/SERCA2a to treat HF have been widely unsuccessful to date.

The early clinical trial CUPID provided the basis for several more aggressive clinical trials (CUPID2, Agent-HF, SERCA-LVAD), all of which failed to demonstrate improvement in survival and/or were terminated prior to sufficient data collection. The reason for the failure of CUPID2 remains largely unknown. One possible reason is attributable to the insufficient delivery of SERCA2a DNA using intracoronary infusion of AAV1 (44), as intracoronary infusion may result in inadequate uptake of the viral vector into cardiomyocytes. In addition, work by Mingozzi and colleagues suggests that viral loads which include empty viral capsid particles enhance the gene delivery as they act as "decoys" and may block the inhibitory activity of antibodies (45). Thus, SERCA2a gene therapy may not be at a dead end yet and there is some light through the tunnel to show it still as a valuable approach for HF patients. The challenge is rather how to effectively deliver the gene to cardiomyocytes. Are there better, more potent viral vectors and more advanced gene editing techniques for gene delivery and expression in human heart?

The Promise of Novel Gene Delivery Techniques in Animals

Among more than 100 wild-type AAV serotypes, some serotypes have been demonstrated to have distinct features on cardiomyocyte transduction (21). Compared to AAV1, AAV8 showed 20-fold higher gene expression in the myocardium in mice. Systemic venous infusion of AAV9 triggers robust level (>200-fold) of gene expression in the cardiomyocytes when compared to AAV1 (46). To date, AAV9-based vectors are by far the most efficient methods for delivering genes to cardiac tissue in mice (46-48). However, AAV6 was also reported to mediate the most efficient transduction in mouse cardiac tissue (49).

Based on these findings, many recent studies have adopted the AAV9 method to transfer SERCA2a genes for treating CHF in animal models. Lyon et al. showed that SERCA2a gene transfer with AAV9 restored SERCA2a proteins in the rat heart and improved left ventricular function by reducing Ca^{2+} leakage from sarcoplasmic reticulum (50). In addition, AAV9/SERCA2a therapy recovers the electrical signal constancy by improving ventricular arrhythmias (50,51) and the treatment rectifies ECG abnormalities such as tachycardia, shortened P-R interval, and prolonged Q-T intervals (52). Similarly, SERCA2a gene therapy overexpressed SERCA2a protein and repressed atrial fibrillation induced by rapid pacing of the atrium in rabbit model (53). Toward clinical application, this line of study has been moved forward to large animals as well. AAV9/SERCA2a gene therapies were performed in German pigs and ovine with ischemic CHF models (54). AAV9 targeting the *S100A1* gene, which augments the activity of SERCA2a proteins so that Ca^{2+} signaling is improved, prevents left ventricular remodeling, and restores SERCA2a protein expression (54). Likewise, injection of AAV9/SERCA2a into the coronary arteries significantly increased SERCA2a gene expression in the walls of the left ventricle in sheep (55). This successful overexpression of SERCA2a triggered improvements in left ventricular systolic and diastolic function and subsequent left ventricular remodeling (55). These positive outcomes provide the basis for future clinical trials in humans utilizing AAV9-based vectors. Current investigations in humans using AAV9-based vectors include Pompe disease (NCT02240407) and Batten disease (NCT02725580). Taken together, these data suggest that the AAV9/SERCA2a gene delivery is an appealing therapeutic method for targeting CHF due to its effects on the ventricular contractile function and restoration of electrical complications associated with the failing heart.

Besides AAVs, gene delivery method using other viral vectors is emerging. For example, lentiviral vectors have been demonstrated to be effective for SERCA2 gene transfer in rat ischemic HF model (56). Since lentivirus can integrate the gene of interest into the host chromosome, this approach can achieve long-term effect of gene expression (57-59). Many research groups have begun to examine safety and efficacy of this gene therapy approach in CHF animal models (56,60-62).

Concluding Remarks and Future Directions

The beneficial left ventricular functional and structural adaptations associated with AAV9/SERCA2a gene therapy provide solid preclinical evidence for future work to focus on translating these findings from animal work to human clinical applications. Compared to AAV1 which used in failed CUPID2 and other earlier trials, AAV9 presents superior efficiency and safety. Therefore, the improved Ca^{2+} handling in cardiac tissues in response to AAV9/SERCA2a would have significant benefits for patients suffering from CHF—particularly CHF of ischemic origin.

In addition to the focus on SERCA2a gene expression, there are a host of other molecules that both indirectly and directly modify SERCA2a function that are worthwhile investigating using modern gene therapy techniques. These molecules include, but are not limited to, small ubiquitin-related modifier-1 (SUMO-1) (63,64). SUMO-1 is a post-transcriptional protein, which plays an important role in modifying other proteins involved in the preservation and stabilization of SERCA2a proteins. In porcine and human cardiac tissue, AAV1/SUMO-1 improved cardiac function. Concurrent transfection of both SUMO-1 and SERCA2a increased both expression and function of SERCA2a (63,64). As such, this approach may represent a possible dual therapy in humans. Indeed, combined gene therapy has recently shown significant promise in the treatment

of animal models of heart failure, with combined transfer of apelin, fibroblast growth factor-2, and SERCA2a demonstrating increased gene expression in ischemic heart failure model (61). Therefore, future work should seek to translate the use of combined gene therapy in humans.

Moreover, novel pharmaceutical therapies targeting activation of SERCA2a have been developed. Istaroxime, a drug developed by Italian pharmaceutical company Sigma-Tau (Pomezia, Italy), is a lusitropic-inotropic drug recently approved for use in CHF (65). In fact, currently a Phase 1 clinical trial at the University of Texas Southwestern is utilizing Istaroxime during exercise (NCT02772068), with primary outcome measure changes in cardiac filling pressures, and secondary outcome measure change in cardiac relaxation time. The study hopes to investigate the effect of SERCA2a activation on exercise-dependent changes in cardiac function (NCT02772068). At the same time, many other altered regulatory proteins involving in cardiomyocyte Ca^{2+} homeostasis could be potential targets for gene therapy in CHF as well, such as phospholamban, junctophilin-2 (JP2), RyRs and NCXs. For example, JP2 downregulation has been reported in human failing heart and restoring JP2 by AAV9-mediated gene therapy could rescue heart failure in mice (66-69).

In conclusion, the development of gene therapy and gene delivery methods have received significant progress over the past few decades, contributing to a novel therapeutic approach for treating CHF. Although the early promising AAV1/SERCA2a method in animal models failed to replicate the same results in humans, recent advancements in gene delivery techniques, especially AAV9/SERCA2a have provided compelling results for beneficial outcome of the upregulation of SERCA2a gene expression. Targeting SERCA2a for treatment of CHF in human patients should be still an option deserving further investigation. Future work should focus on

translating the recent findings using AAV9/SERCA2a techniques into large-scale clinical trials in humans.

Reference List

1. Azad N, Lemay G. Management of chronic heart failure in the older population. Journal of geriatric cardiology : JGC 2014;11:329-37.

2. Heidenreich PA, Albert NM, Allen LA et al. Forecasting the impact of heart failure in the United States: a policy statement from the American Heart Association. Circ Heart Fail 2013;6:606-19.

3. Berridge MJ, Bootman MD, Roderick HL. Calcium signalling: dynamics, homeostasis and remodelling. Nat Rev Mol Cell Biol 2003;4:517-29.

4. Hasenfuss G, Pieske B, Holubarsch C, Alpert NR, Just H. Excitation-contraction coupling and contractile protein function in failing and nonfailing human myocardium. Adv Exp Med Biol 1993;346:91-100.

5. Balderas-Villalobos J, Molina-Munoz T, Mailloux-Salinas P, Bravo G, Carvajal K, Gomez-Viquez NL. Oxidative stress in cardiomyocytes contributes to decreased SERCA2a activity in rats with metabolic syndrome. Am J Physiol Heart Circ Physiol 2013;305:H1344-53.

6. Kawase Y, Ly HQ, Prunier F et al. Reversal of cardiac dysfunction after long-term expression of SERCA2a by gene transfer in a pre-clinical model of heart failure. J Am Coll Cardiol 2008;51:1112-9.

7. Morgan JP. Abnormal intracellular modulation of calcium as a major cause of cardiac contractile dysfunction. N Engl J Med 1991;325:625-32.

8. Schwarzl M, Ojeda F, Zeller T et al. Risk factors for heart failure are associated with alterations of the LV end-diastolic pressure-volume relationship in non-heart failure individuals: data from a large-scale, population-based cohort. Eur Heart J 2016;37:1807-14.

9. Baker DL, Hashimoto K, Grupp IL et al. Targeted overexpression of the sarcoplasmic reticulum Ca2+-ATPase increases cardiac contractility in transgenic mouse hearts. Circ Res 1998;83:1205-14.

10. del Monte F, Harding SE, Schmidt U et al. Restoration of contractile function in isolated cardiomyocytes from failing human hearts by gene transfer of SERCA2a. Circulation 1999;100:2308-11.

11. Studeli R, Jung S, Mohacsi P et al. Diastolic dysfunction in human cardiac allografts is related with reduced SERCA2a gene expression. Am J Transplant 2006;6:775-82.

12. Jaski BE, Jessup ML, Mancini DM et al. Calcium upregulation by percutaneous administration of gene therapy in cardiac disease (CUPID Trial), a first-in-human phase 1/2 clinical trial. J Card Fail 2009;15:171-81.

13. Jessup M, Greenberg B, Mancini D et al. Calcium Upregulation by Percutaneous Administration of Gene Therapy in Cardiac Disease (CUPID): a phase 2 trial of

intracoronary gene therapy of sarcoplasmic reticulum Ca2+-ATPase in patients with advanced heart failure. Circulation 2011;124:304-13.

14. Greenberg B, Butler J, Felker GM et al. Calcium upregulation by percutaneous administration of gene therapy in patients with cardiac disease (CUPID 2): a randomised, multinational, double-blind, placebo-controlled, phase 2b trial. Lancet 2016;387:1178-86.

15. Tada M, Yamamoto T, Tonomura Y. Molecular mechanism of active calcium transport by sarcoplasmic reticulum. Physiol Rev 1978;58:1-79.

16. Leon MB, Rosing DR, Bonow RO, Epstein SE. Combination Therapy with Calcium-Channel Blockers and Beta-Blockers for Chronic Stable Angina-Pectoris. American Journal of Cardiology 1985;55:B69-B80.

17. Cannon RO, 3rd, Watson RM, Rosing DR, Epstein SE. Efficacy of calcium channel blocker therapy for angina pectoris resulting from small-vessel coronary artery disease and abnormal vasodilator reserve. Am J Cardiol 1985;56:242-6.

18. Antman EM, Stone PH, Muller JE, Braunwald E. Calcium channel blocking agents in the treatment of cardiovascular disorders. Part I: Basic and clinical electrophysiologic effects. Ann Intern Med 1980;93:875-85.

19. Ito K, Yan XH, Feng X, Manning WJ, Dillmann WH, Lorell BH. Transgenic expression of sarcoplasmic reticulum Ca2+ ATPase modifies the transition from hypertrophy to early heart failure. Circulation Research 2001;89:422-429.

20. He HP, Giordano FJ, HilalDandan R et al. Overexpression of the rat sarcoplasmic reticulum Ca2+ ATPase gene in the heart of transgenic mice accelerates calcium transients and cardiac relaxation. Journal of Clinical Investigation 1997;100:380-389.

21. Rincon MY, VandenDriessche T, Chuah MK. Gene therapy for cardiovascular disease: advances in vector development, targeting, and delivery for clinical translation. Cardiovasc Res 2015;108:4-20.

22. Williams PD, Ranjzad P, Kakar SJ, Kingston PA. Development of viral vectors for use in cardiovascular gene therapy. Viruses 2010;2:334-71.

23. del Monte F, Lebeche D, Guerrero JL et al. Abrogation of ventricular arrhythmias in a model of ischemia and reperfusion by targeting myocardial calcium cycling. Proc Natl Acad Sci U S A 2004;101:5622-7.

24. del Monte F, Williams E, Lebeche D et al. Improvement in survival and cardiac metabolism after gene transfer of sarcoplasmic reticulum Ca(2+)-ATPase in a rat model of heart failure. Circulation 2001;104:1424-9.

25. Chaudhri B, del Monte F, Hajjar RJ, Harding SE. Contractile effects of adenovirally-mediated increases in SERCA2a activity: a comparison between adult rat and rabbit ventricular myocytes. Mol Cell Biochem 2003;251:103-9.

26. Nassal MM, Wan X, Laurita KR, Cutler MJ. Atrial SERCA2a Overexpression Has No Affect on Cardiac Alternans but Promotes Arrhythmogenic SR Ca2+ Triggers. PLoS One 2015;10:e0137359.

27. Miyamoto MI, del Monte F, Schmidt U et al. Adenoviral gene transfer of SERCA2a improves left-ventricular function in aortic-banded rats in transition to heart failure. Proc Natl Acad Sci U S A 2000;97:793-8.

28. Lipskaia L, Hadri L, Le Prince P et al. SERCA2a gene transfer prevents intimal proliferation in an organ culture of human internal mammary artery. Gene Ther 2013;20:396-406.

29. Sakata S, Lebeche D, Sakata Y et al. Transcoronary gene transfer of SERCA2a increases coronary blood flow and decreases cardiomyocyte size in a type 2 diabetic rat model. Am J Physiol Heart Circ Physiol 2007;292:H1204-7.

30. Hadri L, Bobe R, Kawase Y et al. SERCA2a gene transfer enhances eNOS expression and activity in endothelial cells. Mol Ther 2010;18:1284-92.

31. Xin W, Lu X, Li X, Niu K, Cai J. Attenuation of endoplasmic reticulum stress-related myocardial apoptosis by SERCA2a gene delivery in ischemic heart disease. Mol Med 2011;17:201-10.

32. Kuken BN, Aikemu AN, Xiang SY, Wulasihan MH. Effect of SERCA2a overexpression in the pericardium mediated by the AAV1 gene transfer on rapid atrial pacing in rabbits. Genet Mol Res 2015;14:13625-32.

33. Lipskaia L, Hadri L, Lopez JJ, Hajjar RJ, Bobe R. Benefit of SERCA2a gene transfer to vascular endothelial and smooth muscle cells: a new aspect in therapy of cardiovascular diseases. Curr Vasc Pharmacol 2013;11:465-79.

34. Wobus CE, Hugle-Dorr B, Girod A, Petersen G, Hallek M, Kleinschmidt JA. Monoclonal antibodies against the adeno-associated virus type 2 (AAV-2) capsid: epitope mapping and identification of capsid domains involved in AAV-2-cell interaction and neutralization of AAV-2 infection. J Virol 2000;74:9281-93.

35. Scallan CD, Jiang H, Liu T et al. Human immunoglobulin inhibits liver transduction by AAV vectors at low AAV2 neutralizing titers in SCID mice. Blood 2006;107:1810-7.

36. Moskalenko M, Chen L, van Roey M et al. Epitope mapping of human anti-adeno-associated virus type 2 neutralizing antibodies: implications for gene therapy and virus structure. J Virol 2000;74:1761-6.

37. Greenberg B, Butler J, Felker GM et al. Prevalence of AAV1 neutralizing antibodies and consequences for a clinical trial of gene transfer for advanced heart failure. Gene Ther 2016;23:313-9.

38. Hulot JS, Salem JE, Redheuil A et al. Effect of intracoronary administration of AAV1/SERCA2a on ventricular remodelling in patients with advanced systolic heart

failure: results from the AGENT-HF randomized phase 2 trial. Eur J Heart Fail 2017;19:1534-1541.

39. Greenberg B, Yaroshinsky A, Zsebo KM et al. Design of a phase 2b trial of intracoronary administration of AAV1/SERCA2a in patients with advanced heart failure: the CUPID 2 trial (calcium up-regulation by percutaneous administration of gene therapy in cardiac disease phase 2b). JACC Heart Fail 2014;2:84-92.

40. Zsebo K, Yaroshinsky A, Rudy JJ et al. Long-term effects of AAV1/SERCA2a gene transfer in patients with severe heart failure: analysis of recurrent cardiovascular events and mortality. Circ Res 2014;114:101-8.

41. Horowitz JD, Rosenson RS, McMurray JJ, Marx N, Remme WJ. Clinical Trials Update AHA Congress 2010. Cardiovasc Drugs Ther 2011;25:69-76.

42. Hajjar RJ, Zsebo K, Deckelbaum L et al. Design of a phase 1/2 trial of intracoronary administration of AAV1/SERCA2a in patients with heart failure. J Card Fail 2008;14:355-67.

43. Hulot JS, Ishikawa K, Hajjar RJ. Gene therapy for the treatment of heart failure: promise postponed. Eur Heart J 2016;37:1651-8.

44. Yla-Herttuala S. Gene Therapy for Heart Failure: Back to the Bench. Mol Ther 2015;23:1551-2.

45. Mingozzi F, Anguela XM, Pavani G et al. Overcoming preexisting humoral immunity to AAV using capsid decoys. Sci Transl Med 2013;5:194ra92.

46. Pacak CA, Mah CS, Thattaliyath BD et al. Recombinant adeno-associated virus serotype 9 leads to preferential cardiac transduction in vivo. Circ Res 2006;99:e3-9.

47. Vandendriessche T, Thorrez L, Acosta-Sanchez A et al. Efficacy and safety of adeno-associated viral vectors based on serotype 8 and 9 vs. lentiviral vectors for hemophilia B gene therapy. J Thromb Haemost 2007;5:16-24.

48. Inagaki K, Fuess S, Storm TA et al. Robust systemic transduction with AAV9 vectors in mice: efficient global cardiac gene transfer superior to that of AAV8. Mol Ther 2006;14:45-53.

49. Zincarelli C, Soltys S, Rengo G, Koch WJ, Rabinowitz JE. Comparative cardiac gene delivery of adeno-associated virus serotypes 1-9 reveals that AAV6 mediates the most efficient transduction in mouse heart. Clin Transl Sci 2010;3:81-9.

50. Lyon AR, Bannister ML, Collins T et al. SERCA2a gene transfer decreases sarcoplasmic reticulum calcium leak and reduces ventricular arrhythmias in a model of chronic heart failure. Circ Arrhythm Electrophysiol 2011;4:362-72.

51. Cutler MJ, Wan X, Plummer BN et al. Targeted sarcoplasmic reticulum Ca2+ ATPase 2a gene delivery to restore electrical stability in the failing heart. Circulation 2012;126:2095-104.

52. Shin JH, Bostick B, Yue Y, Hajjar R, Duan D. SERCA2a gene transfer improves electrocardiographic performance in aged mdx mice. J Transl Med 2011;9:132.

53. Wang HL, Zhou XH, Li ZQ et al. Prevention of Atrial Fibrillation by Using Sarcoplasmic Reticulum Calcium ATPase Pump Overexpression in a Rabbit Model of Rapid Atrial Pacing. Med Sci Monit 2017;23:3952-3960.

54. Pleger ST, Shan C, Ksienzyk J et al. Cardiac AAV9-S100A1 gene therapy rescues post-ischemic heart failure in a preclinical large animal model. Sci Transl Med 2011;3:92ra64.

55. Katz MG, Fargnoli AS, Williams RD et al. Safety and efficacy of high-dose adeno-associated virus 9 encoding sarcoplasmic reticulum Ca(2+) adenosine triphosphatase delivered by molecular cardiac surgery with recirculating delivery in ovine ischemic cardiomyopathy. J Thorac Cardiovasc Surg 2014;148:1065-72, 1073e1-2; discussion1072-3.

56. Niwano K, Arai M, Koitabashi N et al. Lentiviral vector-mediated SERCA2 gene transfer protects against heart failure and left ventricular remodeling after myocardial infarction in rats. Molecular therapy : the journal of the American Society of Gene Therapy 2008;16:1026-32.

57. Fleury S, Simeoni E, Zuppinger C et al. Multiply attenuated, self-inactivating lentiviral vectors efficiently deliver and express genes for extended periods of time in adult rat cardiomyocytes in vivo. Circulation 2003;107:2375-82.

58. Miyoshi H, Takahashi M, Gage FH, Verma IM. Stable and efficient gene transfer into the retina using an HIV-based lentiviral vector. Proc Natl Acad Sci U S A 1997;94:10319-23.

59. Naldini L, Blomer U, Gallay P et al. In vivo gene delivery and stable transduction of nondividing cells by a lentiviral vector. Science 1996;272:263-7.

60. Merentie M, Lottonen-Raikaslehto L, Parviainen V et al. Efficacy and safety of myocardial gene transfer of adenovirus, adeno-associated virus and lentivirus vectors in the mouse heart. Gene Ther 2016;23:296-305.

61. Renaud-Gabardos E, Tatin F, Hantelys F et al. Therapeutic Benefit and Gene Network Regulation by Combined Gene Transfer of Apelin, FGF2, and SERCA2a into Ischemic Heart. Mol Ther 2018;26:902-916.

62. Merentie M, Rissanen R, Lottonen-Raikaslehto L et al. Doxycycline modulates VEGF-A expression: Failure of doxycycline-inducible lentivirus shRNA vector to knockdown VEGF-A expression in transgenic mice. PLoS One 2018;13:e0190981.

63. Tilemann L, Lee A, Ishikawa K et al. SUMO-1 gene transfer improves cardiac function in a large-animal model of heart failure. Sci Transl Med 2013;5:211ra159.

64. Kho C, Lee A, Jeong D et al. SUMO1-dependent modulation of SERCA2a in heart failure. Nature 2011;477:601-5.

65. Ferrandi M, Barassi P, Tadini-Buoninsegni F et al. Istaroxime stimulates SERCA2a and accelerates calcium cycling in heart failure by relieving phospholamban inhibition. Br J Pharmacol 2013;169:1849-61.

66. Reynolds JO, Quick AP, Wang Q et al. Junctophilin-2 gene therapy rescues heart failure by normalizing RyR2-mediated Ca(2+) release. International journal of cardiology 2016;225:371-380.

67. Beavers DL, Landstrom AP, Chiang DY, Wehrens XH. Emerging roles of junctophilin-2 in the heart and implications for cardiac diseases. Cardiovascular research 2014;103:198-205.

68. Guo A, Zhang X, Iyer VR et al. Overexpression of junctophilin-2 does not enhance baseline function but attenuates heart failure development after cardiac stress. Proceedings of the National Academy of Sciences of the United States of America 2014;111:12240-5.

69. Zhang C, Chen B, Guo A et al. Microtubule-mediated defects in junctophilin-2 trafficking contribute to myocyte transverse-tubule remodeling and Ca2+ handling dysfunction in heart failure. Circulation 2014;129:1742-50.